# THE WAKSMAN FOUNDATION OF JAPAN INC.

## Honorary President

**Prince Takahito Mikasa**

## Board of Directors

Chairman : Ichiro Kitasato, Chief Corporate Advisor, Meiji Seika Kaisha, Ltd.

Shogo Sasaki, Prof. Emeritus, Keio Univ.

Kazuhisa Saito, Prof. Emeritus, Keio Univ.

Teruhiko Beppu, Prof. Emeritus, Tokyo Univ.

Takeshi Ishikawa, Director, 150th Anniversary Commemorative Project Office of Keio

Shigeo Koyasu, Prof., Keio Univ. Sch. Med.

Kazumine Kobari, Prof. Emeritus, Ryukyu Univ.

Shogo Kuwahara, Prof. Emeritus, Toho Univ.

Rinji Kawana, Prof. Emeritus, Iwate Med. Univ.

Tadakatsu Shimamura, Prof., Showa Univ. Sch. Med.

Toshiro Sato, Adviser, Kitasato Gakuen

Managing Director : Takeji Nishikawa, Prof. Emeritus, Keio Univ.

Comptroller : Yoshiharu Wakiyama, Senior Adviser, Kaken Pharmaceutical Co., Ltd.

Tadashi Hirata, Senior Adviser, Kyowa Hakko Kogyo Co., Ltd.

## Councilors

Susumu Sato, Chairman, Sato Pharmaceutical Co., Ltd.

Ryoichi Mori, Prof. Emeritus, Kyushu Univ.

Yuichiro Anzai, President, Keio Univ.

Keizo Takemi, Member, The House of Councilors

Kiyoshi Morita, President & CEO, Daiichi Pharmaceutical Co., Ltd.

Tetsuo Takato, Corporate Adviser, Sankyo Co., Ltd.

Akira Uehara, President & CEO, Taisho Pharmaceutical Co., Ltd.

Koichi Yamanishi, Director General, National Institute of Biomedical Innovation

Masamichi Fujii, Prof. Emeritus, St. Marianna Univ.

Osamu Sato, Prof. Emeritus, Tokai Univ.

Sachiko Goto, Prof. Emeritus, Toho Univ.

Yoshihiro Miwa, President & CEO, Kowa Co., Ltd.

Yasuo Ikeda, Prof., Keio Univ. Sch. Med.

Osamu Nagayama, President & CEO, Chugai Pharmaceutical Co., Ltd.

Haruo Naito, President & CEO, Eisai Pharmaceutical Co., Ltd.

2006

Edited and Published by

THE WAKSMAN FOUNDATION OF JAPAN INC.

30-8 Daikyo-cho, Shinjuku-ku,
Tokyo 160-0015, Japan
http : //www.waksman.or.jp/
E-mail: toshihisa-sato@waksman.or.jp

Printed by

FUKOKU PRINTING CO., LTD.

Tokyo, Japan

# PREFACE (2000)

Since the Waksman Foundation published its first cinqueannual report in 1962, annual report followed regularly until 1986 without changing its style, i.e. yellow cover in B5 size. The royalties of patent of streptomycin expired in 1970 and the Foundation was forced to change the way of running. Fortunately, it manages to continue its activity by supporting the research activities of Japanese investigators and by encouraging them to take part in an international meeting and also by hosting scientific meetings with professional societies. The total number of support counts 628 research projects and costs approximately 4,500,000 U.S. dollars. The Foundation is administered by the Board of Directors consisting of 5-9 representatives of professional societies and Prince Takahito Mikasa as the honorary President.

At our recent business meeting it was decided unanimously to publish the reports of the researchers who recieved research grant from the Foundation for the past 15 years to commemorate the year 2000. To meet with the current style of a scientific journal the Foundation has adopted an international size and totally renewed the cover as you are aware of. From the new millennium on it is expected that the report from the awardees of the research grants will be distributed regularly each year.

Shozo Yokogawa
*Chairman, Board of Directors,*
*The Waksman Foundation of Japan, Inc.*

# Preface to the First Report (1962)

It is indeed a privilege to take this opportunity to write a few words of introduction to the first report of the Waksman Foundation of Japan Inc., covering five years of its activities and comprising the results of the work of the first two years of research carried out by various scholars in Japan in the fields of microbiology and medical science, supported by this Foundation.

In 1952, I accepted the invitation from Keio University and the Kitasato Institute, to deliver the centennial lecture in honor of the great Japanese bacteriologist, Shibasaburo Kitasato. Before departing for Japan, I proposed to the trustees of the Rutgers Research and Educational Foundation which owned the patents on streptomycin, to share the royalties under the patent in Japan, for the support of research in microbiology and allied fields in that country. The trustees heartily approved my recommendation that I make such announcement to that effect.

Soon upon my arrival in Japan (December 17, 1952), I invited a group of eminent microbiologists, biochemists, and clinical investigators to meet with me in order to discuss the plan. Everyone present was very enthusiastic about the proposal. It was decided that a proper committee be selected to work out the plan of a Foundation under which the royalties were to be received and distributed for the support of Japanese investigators working in different universities in Japan and elsewhere, in the fields of microbiology and medical research. The committee recommended that a Board of Directors be selected and the proposed Foundation be named THE WAKSMAN FOUNDATION OF JAPAN INCORPORATION.

The Rutgers Research and Educational Foundation approved at once the above recommendations and issued a statement, signed by Dr. Lewis Webster Jones, President of the Foundation, to the effect that

"The Rutgers Research and Educational Foundation desires to emphasize that its principal concern is the advancement of scientific knowledge in the public interest and that it confidently expects that the Waksman Foundation for Microbiology and Medical Research in Japan will be similarly motivated, thereby serving the peoples of both countries."

This announcement was received with enthusiasm both by the scientific world and the popular press in Japan and in the United States. It took several years before the Waksman Foundation of Japan Inc. was properly organized, and before applications were received and approved. In 1958, I had the privilege of participating in the first official meetings of the Board of Directors of the Japanese Foundation and to greet personally the first group of scholars to whom grants had been made.

In summarizing these brief remarks in connection with the first cinqueannual report of the Waksman Foundation of Japan Inc., I would like to enphasize that this example of collaboration between universities and scientists of the United States and Japan may serve to encourage collaboration between scientific workers throughout the world towards a better understanding between men and women and towards a happier and healthier human race, so that all the nations on this earth can live in peace and that man may finally "break

his swords and build out of them plowshares" for the betterment of mankind as a whole.

Selman A. Waksman
*Professor Emeritus*
*Rutgers-State University N. J., U. S. A.*

The "Waksman Foundation of Japan Inc." was established in 1957 with the spirit of humanity by Dr. S.A. Waksman, Professor of Microbiology, Rutgers University, U.S.A. The Foundation's operations are possible only because Dr. S.A. Waksman and the Rutgers Research and Educational Foundation donated patent royalties he received from the production in Japan of the discovery, Streptomycin.

Because of these royalties, each year many Japanese scholars and research workers in the fields of Microbiology and medical science are encouraged and find it possible to continue their work. Especially, in accordance with Dr. Waksman's suggestion, the funds are distributed to scholars in local and economically hampered schools and laboratories and to those developing research workers who are endeavoring to expand in their fields. This thought of Dr. Waksman's is most appreciated, as it matches our Oriental phylosophy, and results in the search for a jewel among ordinary stones, which is the highest work of the science-leader.

Some five years have now passed since the start of this Foundation, and many persons have received aid through this period.

The reports which are presented herein cover the first and second group of research workers who received financial assistance from the Foundation.

Toshio Katow, M. D.
*Executive Director*

# Contents

—— Report of Researches in 2005 ——

Haruo Ikeda:

Chromosome Engineering for Efficient Production of Secondary Metabolites in *Streptomyces* ····· 1

Masaaki Iwanaga:

Fluctuation of Drug Susceptibility of *Vibrio cholerae* O1 and Analysis of the Drug Resistance Genes ·····17

Keizo Yamaguchi:

Development of Novel Approach for Treatment of Infectious Diseases Targeting Bacterial Cell-to-Cell Signaling: Focusing on an Opportunistic Pathogen *Pseudomonas aeruginosa* ·····27

Tetsuo Kato:

Effects of Synthetic *N*-Acyl Homoserine Lactones and Eel Lectin on Oral Pathogens ·····37

Hidero Kitasato:

Role of Prostaglandin $D_2$ in Remodeling of Pulmonary Artery Affected by Pulmonary Hypertension ·····45

Susumu Ishida:

Immunotherapy Targeting VEGFR-2 for Prevention from Pathological Retinal Angiogenesis ·····55

# Chromosome Engineering for Efficient Production of Secondary Metabolites in *Streptomyces*

**Haruo Ikeda**

*Kitasato Institute for Life Sciences, Kitasato University, 1-15-1 Kitasato, Sagamihara, Kanagawa 228-8555, Japan*

## Introduction

*Streptomyces avermitilis* (1) is a Gram-positive bacterium of the family Streptomycetaceae in the class Actinobacteria and a member of the diverse *Streptomyces* genus. Streptomycetes are unique bacteria in consideration of the following properties. They grow in soil and form filamentous mycelium, aerial hyphae and conidial spores during their life cycle (2). Although *Streptomyces* belongs to eubacteria, its chromosome forms a linear structure and both ends, containing unique terminal-inverted repeats, bind terminal proteins (3). Linear chromosomes, the predominant genetic element in eukaryotes, have been identified in *Borrelia burgdorferi* (4) and *Agrobacterium tumefaciens* (5, 6), but terminal-inverted repeats or terminal proteins have not been identified in these chromosomes. One of the most interesting and industrially important properties of the genus *Streptomyces* is the diversity of secondary metabolite production, including antibiotics. Streptomycetes are therefore of great use for the commercial production of a variety of antibiotics that are applied in human and veterinary medicine, and agriculture, as well as anti-parasitic agents, herbicides, pharmacologically active metabolites and several enzymes important in the food and other industries (7). Seven complete genomic sequences in the class Actinobacteria are now available from two *Mycobacterium tuberculosis* strains, H37Rv (8) and CDC1551 (9), *M. leprae* TN (10), *Corynebacterium diphtheriae* (11), which are mammalian pathogens with circular chromosome, *C. glutamicum* (12), *Nocardia farcinica* IFO10152 (13), and *S. coelicolor* A3(2) (14). Comparative analysis with these genomes will allow comparison of the sequences of pathogens and secondary metabolite producers within the Actinobacteria and provide us new insights for application of these microbes to industrial fields including drug discovery.

We have determined the complete nucleotide sequences of the linear chromosome and the 94-kilobase linear plasmid SAP1 of *S. avermitilis* (15, 16), which produces antiparasitic agent avermectins used in human and veterinary medicine. *S. avermitilis* has the highest proportion of predicted secondary metabolite gene clusters of all bacterial genomes sequenced. Analysis using FramePlot, BLATP and hmmerpfam showed at least 32 clusters involving the biosynthesis of melanin, terpene, siderophore, polyketide, and peptide compounds (16). We started to investigate two major projects for post-genome analysis in *S. avermitilis* as follows; (i) confirmation and characterization of predicted biosynthetic genes and secondary metabolites synthesized by their gene products, (ii) design the minimum genome for secondary metabolite production.

## Materials and Methods

*Materials*.

*Streptomyces avermitilis* cosmids CL_90_H01, CL_216_D07, CL_225_G12, and CL_228_H03, from the *S. avermitilis* genomic DNA library (http://avermitilis.ls.kitasato-u.ac.jp/), were used as templates for polymerase chain reaction (PCR). Plasmid vectors,

pET21d(+), pET28e and pET31b were used for expression in *E. coli* BL21(DE3) derivatives. pET28e was prepared from pET28a by replacing the *Xba*I site with an *Eco*RI site.

*Methods.*

Electrocompetent cells for electroporation were prepared from *E. coli* BL21(DE3) derivatives by standard methods. Polymerase chain reactions were carried out using Pfu Turbo polymerase as recommended by the manufacturer. For generation of *Streptomyces* exoconjugants and homologous recombination, standard methodology was utilized.

*Isolation of pentalenolactone F.*

A mutant of *S. avermitilis* (*⊿aveR ⊿olmA5*), blocked in the production of both avermectins and oligomycins, was used to examine the production of pentalenolactones. The spores of the mutant were transferred to a 250-ml flask containing 20 ml of vegetative medium [glucose (0.5 g), soy flour (1.5 g), and yeast extract (0.5 g) per 100 ml, pH 7.2] and allowed to grow while shaking at 30ºC for 2 days. A 1-ml portion was removed and used to inoculate into 20 x 500-ml flasks containing 100 ml of production medium [soluble starch (40 g), soy flour (20 g), $FeSO_4 \bullet 7H_2O$ (0.5 g), $K_2HPO_4$ (1 g) and KCl (0.3 g) per liter, pH 6.5]. After incubation by shaking at 28ºC for 4 days, the culture was filtered. The mycelium was washed with tap water and extracted with 500 ml of methanol. The concentrated supernatant was diluted with an equal volume of water and acidified with 2 N $H_2SO_4$ to pH 2.5. The products were then extracted twice with a half volume of chloroform. The organic fraction was concentrated under reduced pressure and subjected to flash silica gel chromatography (30:1=chloroform:methanol). Pentalenolactone-rich fractions were pooled and concentrated to an oil. This residue was dissolved in THF/diethyl ether (1:1) and treated with a solution of diazomethane in diethyl ether and 50% KOH for 10 min at 0ºC. After quenching by addition of ethereal acetic acid, the ether layer was washed with saturated bicarbonate solution. Methyl ester metabolites were further purified by preparative silica TLC and final purification was performed by ODS-HPLC using *n*-hexane/ethyl acetate (1:1).

*Construction of deletion mutants.*

About 2-kb segments both upstream and downstream of the deletion region designated were amplified by PCR from cosmid clone. A resistance gene (*aph* or *aad3"*) was inserted between these two PCR products. The segment carrying PCR products and a resistance gene was ligated together into unique-cut pKU250. The plasmid pKU250::upstream-resistance gene-downstream construct in *E. coli recA dcm*/pUB307*aph*::Tn7 was introduced into *S. avermitilis* by conjugation. After exoconjugants were selected by vector marker (thiostreptone resistance), deletion mutants generated by double homologous recombination upstream of and downstream were obtained by selection for thiostreptone-sensitivity and neomycin (*aph*)- or streptomycin/spectinomycin (*aad3"*)-resistance. A large deletion was performed using two segments, 2,959-bp *Bsp*HI/*Bgl*II (nt 5,847 to 8,806) and 2,593-bp *Bam*HI (nt 1,494,519 to 1,497,112), purified from cosmid CL090_H01 and CL_225_G12, respectively.

*Expression and purification of recombinant proteins.*

Transforms of *E. coli* BL21(DE3) was grown at 37ºC in LB media (1 liter) supplemented with kanamycin (80 mg/l) to an $OD_{600}$ ~ 0.6, then induced by the addition of IPTG (0.5 mM). After a further 5 h at 30ºC, the cells were harvested by centrifugation. The cell pellet was resuspended in lysis buffer [30 ml, 20 mM imidazole, 500 mM NaCl, 50 mM Tris, 5 mM $MgCl_2$, 2.7 mM $\beta$-mercaptoethanol, 10% glycerol (v/v), pH 8.0] and disrupted by sonication. After removal of the cellular debris by centrifugation (20 min, 30,000×*g*, 4ºC), the recombinant protein was purified by HiTrap Ni affinity column chromatography using a linear gradient of imidazole (10-400 mM) in lysis buffer. Fractions were analyzed by SDS-PAGE and those containing the desired protein were concentrated by ultrafiltration (10 kDa NMWL).

*GC-MS analysis of products.*

The spores of wild-type and mutants of *S. avermitilis* were inoculated into 100-ml flask containing 10 ml of vegetative medium [glucose (0.5 g), soy flour (1.5 g), and yeast extract (0.5 g) per 100 ml, pH 7.2] and allowed to grow while shaking at 30ºC for 2 days. The geosmin production was observed in several media but synthetic medium was suitable for the GC-MS analysis because many peaks were detected from the complex medium. A 0.1 ml of portion of the culture was used to inoculate into 100 ml-flask containing 10 ml of synthetic medium [glucose (60 g), $(NH_4)SO_4$ (2 g), $MgSO_4 \cdot 7H_2O$ (0.1 g), $K_2HPO_4$ (0.5 g), NaCl (2 g), $FeSO_4 \cdot 7H_2O$ (0.05 g), $ZnSO_4 \cdot 7H_2O$ (0.05 g), $MnSO_4 \cdot 4H_2O$ (0.05 g), CaCO3 (5 g), yeast extract (2 g) per liter, pH 7.0]. After incubation while shaking at 28ºC for 4 days, the culture was filtered. The supernatant was extracted with 1 ml of n-hexane or n-pentane and the organic layer was dried over $Na_2SO_4$, and filtered through a 1-cm column of $Na_2SO_4$ in a Pasteur pipette. A 1 to 5-$\mu$l portion of the extract was analyzed by GC-MS [Shimadzu GC-17A, 70 eV, EI, positive ion mode; 30 m × 0.25 mm neutral bond-5 capillary column (5% phenylmethylsilicon), using a temperature program of 50-280°C, temperature gradient of 20ºC/min]. The compound was identified by comparison with the spectra of the corresponding reference compounds in the NIST/EPA/NIH MS Library (2002 version). Enzymatic products were also analyzed by the same conditions.

*Analysis of sequence data.*

Clustering profiles of the putative 7,577 genes of *S. avermitilis* was explored by BLASTCLUST (NCBI tool; ftp://ncbi.nlm.nih.gov/) under the conditions; minimum 30% identity, minimum 80% length coverage. The deduced amino acid sequences of the putative secondary metabolite biosynthetic genes of *S. avermitilis* identified and their homologues from public databases were aligned using ClustalX and subjected to phylogenetic analysis by both the maximum parsimony and distance with neighbour-joining methods. Analyses were subjected to 1,000 bootstrap replicates.

## Results

*Characterization of predicted gene clusters for secondary metabolite biosynthesis.*

1. *Pentalenolactone.*

Pentalenolactone is a sesquiterpenoid antibiotic, first isolated in 1957 from *Streptomyces roseogriseus* (17), and subsequently found in the extracts of numerous *Streptomyces* species, including *Streptomyces* UC5319 (18), *S. arenae* (19), *S. chromofuscus*, *S. griseochromogenes*, *S. baarnensis*, *S. omiyaensis*, *S. albofaciens*, and *S. viridifaciens* (20, 21). Pentalenolactone has been shown to be active against both Gram-positive and Gram-negative bacteria as well as a variety of fungi and protozoa (22), and to inhibit the replication of DNA viruses such as HSV-1 and HSV-2 (23). Pentalenolactone also inhibits vascular smooth muscle cell proliferation (24). The antibiotic inhibits selectively the glycolytic enzyme glyceraldehyde-3-phosphate dehydrogenase (GAPDH) (25, 26). Incubation of rabbit muscle GAPDH with pentalenolactone results in time-dependent, irreversible inactivation of GAPDH as a result of alkylation of the active site Cys-149 residue, apparently by reaction with the electrophilic epoxide moiety of the antibiotic (27, 28). Self-resistance in the pentalenolactone-producer *S. arenae* is due to the presence of two GAPDH isozymes, an inducible pentalenolactone-insensitive form, and a constitutive pentalenolactone-sensitive form (29-31).

Thirty-two gene clusters related to secondary metabolites were recognized in *S. avermitilis*, corresponding to nearly 7% of the genome. Among these gene clusters, at least six were encoding putative terpenoid biosynthetic pathways. Centered at 3.75 Mb in the *S. avermitilis* chromosome is a ~13.4-kb cluster containing 13 unidirectionally-transcribed ORFs, among which is the 1,011-bp *ptlA* (SAV2998), encoding a protein of 336 aa with 76% identity and 85% similarity to the pentalenene synthase of *Streptomyces* UC5319 (Fig. 1 and Table 1; proposed biosynthetic pathway is shown in Fig. 2). Just upstream of *ptlA* is *ptlB* (SAV2997), which encodes a typical farnesyl di-

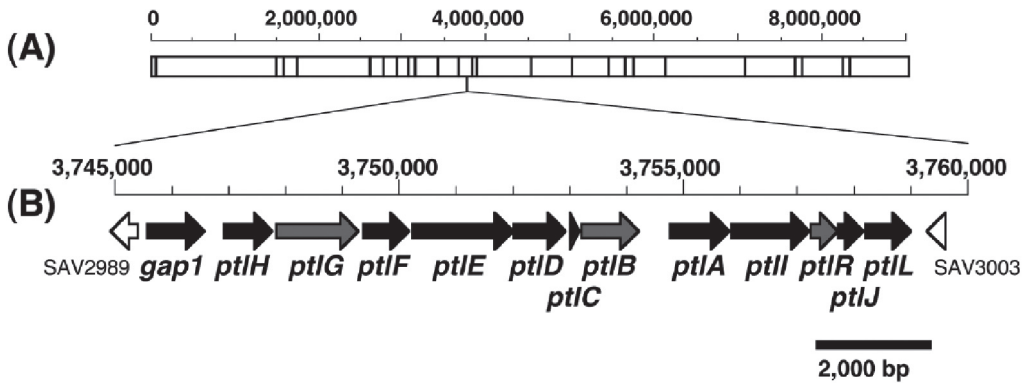


**Fig. 1.** Gene cluster for pentalenolactone biosynthesis in *S. avermitilis*. *Ase*I-physical map of a linear chromosome of *S. avermitilis* (A) and a region involving pentalenolactone biosynthesis (B). Gene names and definitions are given in Table 1.

**Table 1.** Pentalenolactone (*ptl*) gene cluster of *Streptomyces avermitilis*

| Gene | ID | Start nt | End nt | Definition | Best match[a] |
|---|---|---|---|---|---|
| *gap1* | SAV2990 | 3,745,497 | 3,746,501 | glyceraldehyde-3-phosphate dehydrogenase | *ptlK*, pentalenolactone resistance gene |
| *ptlH* | SAV2991 | 3,746,862 | 3,747,719 | putative hydroxylase | PF05721: Phytanoyl-CoA dioxygenase (PhyH) |
| *ptlG* | SAV2992 | 3,747,777 | 3,749,231 | putative transmembrane efflux protein | PF07690: Major Facilitator Superfamily |
| *ptlF* | SAV2993 | 3,749,307 | 3,750,119 | putative oxidoreductase | PF00106: short chain dehydrogenase |
| *ptlE* | SAV2994 | 3,750,177 | 3,751,961 | putative monooxygenase | PF00743: Flavin-binding monooxygenase-like |
| *ptlD* | SAV2995 | 3,751,962 | 3,752,882 | putative dioxygenase | PF02668: Taurine catabolism dioxygenase TauD, TfdA family |
| *ptlC* | SAV2996 | 3,752,934 | 3,753,110 | hypothetical protein | |
| *ptlB* | SAV2997 | 3,753,107 | 3,754,120 | polyprenyl diphosphate synthase | probable farnesyl diphosphate synthase (idsA2) |
| *ptlA* | SAV2998 | 3,754,725 | 3,755,735 | pentalenene synthase | PF03936: Terpene synthase family, metal binding domain |
| *ptlI* | SAV2999 | 3,755,792 | 3,757,141 | cytochrome P450 | CYP183A1 |
| *ptlR* | SAV3000 | 3,757,201 | 3,757,662 | putative AraC-family transcriptional regulator | PF00165: Bacterial regulatory helix-turn-helix proteins, AraC family |
| *ptlJ* | SAV3001 | 3,757,659 | 3,758,093 | putative lyase | PF00903: Glyoxalase/Bleomycin resistance protein, Dioxygenase superfamily |
| *ptlL* | SAV3002 | 3,758,163 | 3,758,933 | hypothetical protein | Nfa37730 of *Nocardia farcinica* IFM 10152 |

[a] PF number is the NCBI PFAM reference.

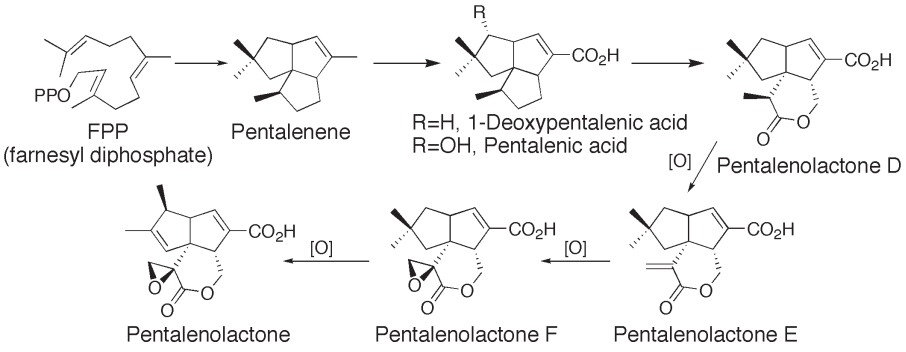


**Fig. 2.** Proposed steps in biosynthesis of pentalenolactone from farnesyl diphosphate (FPP) and known metabolite in each step.

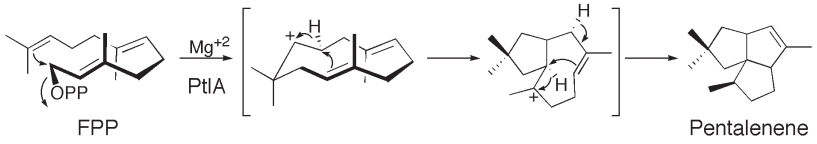


**Fig. 3.** Mechanism of cyclization of FPP to pentalenene catalyzed by pentalenene synthase (PtlA).

phosphate synthase. Of the remaining 11 ORFs, 8 encode putative redox enzymes, including mono- or dioxygenases and a dehydrogenase, while *ptlR* (SAV3000) corresponds to a typical transcriptional regulator. Significantly, the most upstream gene in the cluster, *gap1* (SAV2990), encodes a 335-aa protein with 88% identity and 92% similarity to the previously identified pentalenolactone-resistant GAPDH of *S. arenae*. Since many bacterial antibiotics are co-expressed with the corresponding genes for self-resistance, the 13 ORFs were proposed to make up an operon for the biosynthesis of pentalenolactone. Although pentalenolactones occur widely in *Streptomyces*, there have been no prior reports of their isolation from *S. avermitilis*. A 4-liter culture of *S. avermitilis* (*ΔaveR ΔolmA5*), blocked in the formation of both avermectins and oligomycins, was grown for 4 days at 28ºC. Extraction of the harvested mycelium with methanol followed by chromatographic fractionation of the methylated extract gave 8 mg of purified pentalenolactone F methyl ester whose $^{1}$H NMR, IR, and mass spectra were identical in all respects with those previously reported for pentalenolactone F methyl ester (32). The microorganisms also produced the shunt metabolite, pentalenic acid. Pentalenolactone itself was not detected in the organic extract of *S. avermitilis*. An engineered *S. avermitilis ptl*-deletion mutant, lacking the 13.4-kb segment containing the entire *ptl* cluster (*gap1* to *ptlL*; SAV2990-3002), produced neither pentalenolactone F nor pentalenic acid. In a complementary experiment, when a 14.9-kb *Avr*II-*Sna*BI-segment (nt 3,744,874 to 3,759,745) containing the *ptl* cluster was introduced by conjugation into *S. lividans* 1326, which normally does not produce pentalenolactones, the resultant exoconjugants were found to produce mainly pentalenic acid, accompanied by very small amounts of pentalenolactone metabolites. Using DNA from *S. avermitilis* cosmid CL_216_D07 as template, the 1011-bp presumptive coding region for pentalenene synthase was amplified by PCR while introducing *Nde*I and *Hind*III restriction sites at the 5'- and 3'-termini of the ORF, respectively. The amplified DNA was ligated into the expression vector pET28a. The resultant plasmid, pET28a/SAV2998 was used to transform the T7 RNA polymerase-based expression host *E. coli* BL21(DE3). The resulting soluble protein was subjected to $Ni^{2+}$-affinity purification. The recovered recombinant SAV2998 (9.4 mg from 1 liter of culture) was judged to be >90% pure by SDS-PAGE. Incubation of the purified SAV2998 protein with 80 $\mu$M FPP and analysis of the pentane-soluble extract by capillary chiral GC-MS, revealed the formation of a single sesquiterpene product identical to pentalenene by direct comparison with an authentic sample, thereby confirming the predicted pentalenene synthase activity of PtlA (SAV2998; Fig. 3).

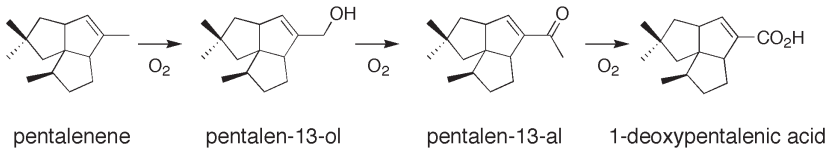


**Fig. 4.** Proposed allylic oxidation of pentalenene to 1-deoxypentalenic acid by cytochrome P450.

According to the proposed biosynthetic pathway (Fig. 2), the enzymes responsible for the conversion of pentalenene to pentalenolactone must first oxidize pentalenene to the corresponding unsaturated carboxylic acid (1-deoxypentaleneic acid). Cytochrome P450s are known to catalyze numerous oxygenation reactions of nonactivated hydrocarbons. The three-step oxidation of a methyl group to a carboxylic acid is amongst these reactions (33-35). We therefore speculated that PtlI might be responsible for the allylic oxidation of pentalenene to 1-deoxypentalenic acid (Fig. 4). PtlI was amplified by polymerase chain reaction (PCR) from DNA of *S. avermitilis* cosmid CL_216_D07 and cloned between the *Nde*I and *Xho*I sites of the vector pET31b. The resulting construct pET31b-*Ptl*I was introduced into *Escherichia coli* BL21(DE3). After induction with IPTG, the expressed PtlI protein, carrying a C-terminal $His_6$-tag, was purified to homogeneity by Ni-NTA chromatography. The purified protein showed subunit peaks $M_D$ by MALDI-TOF MS of *m/z* 51667±50 (calc. 51723 for apo-protein) and *m/z* 52078±50 (calc. 52339 for holo-protein). Treatment of the sodium dithionite-reduced protein with carbon monoxide gave the characteristic P450 UV difference spectrum. Numerous attempts to observe PtlI-catalyzed oxidation of pentalenene using purified P450 in the presence of NADPH and typical redox pairs such as spinach ferredoxin and NADPH: ferredoxin oxidoreductase or putidaredoxin and putidaredoxin reductase (36, 37) were uniformly unsuccessful. Interestingly, when pentalenene and NADPH were incubated with unpurified cell-free extracts of *E. coli* PtlI expression cultures, GC-MS analysis of the resulting organic extracts indicated that trace amounts of pentalen-13-ol had been formed. We speculated that the endogenous *E. coli* flavodoxin (*fld*) and flavodoxin reductase (*fdr*) might support the activity of PtlI, as reported for other P450s. A mixture of recombinant PtlI (0.57 $\mu$M), flavodoxin (3.9 $\mu$M) (38, 39), flavodoxin

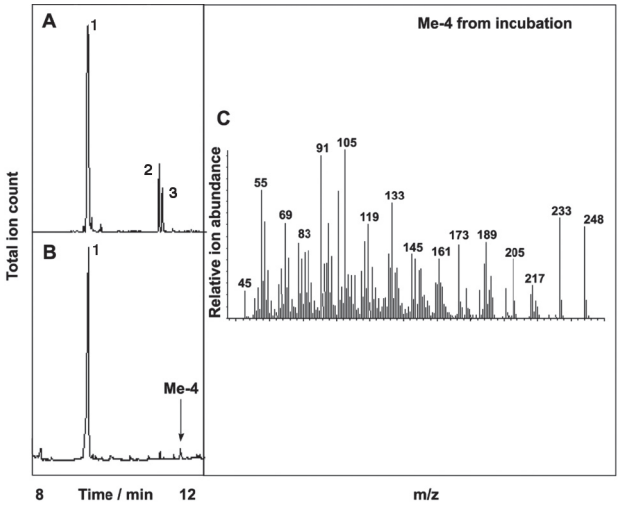


**Fig. 5.** GC-MS analysis of incubation of PtlI with (±)-pentalenene. (A), neutral extract. (B), acidic extract. (C), Mass spectra of Me-4 (methylated compound) from enzymatic oxidation. The peaks 1, 2, 3 and Me-4 indicate pentalenene, pentalen-13-ol, pentalen-13-al and 1-deoxylpentalenic acid methyl ester, respectively.

reductase (6.3 $\mu$M) (38, 39), NADPH (0.45 mM), and a NADPH-regeneration system [glucose-6-phosphate (3.1 mM) and glucose-6-phosphate dehydrogenase (10 units)] in 3.0 ml of 50 mM phosphate buffer, 10% glycerol (v/v), pH 7.4, was incubated with (±)-pentalenene (1.1 mM) plus 0.8% DMSO for 16 h at room temperature. After extraction with pentane, the aqueous phase was acidified to pH 2 and extracted with diethyl ether. The ether extract was treated with TMS-$CHN_2$. GC-MS analysis of the neutral pentane extracts revealed two new peaks with *m/z* 218 (retention time 10.96 min) and 220 (retention time 11.03 min), corresponding to authentic pentalen-13-al and pentalen-13-ol, respectively (Figure 5A). The methylated acidic extract showed a new peak with *m/z* 248 (retention time 11.42 min) with identical properties to authentic methyl ester of 1-deoxypentalenic acid (Figure 5B-5C).

Chiral GC-MS analysis, under conditions in which the enantiomers of (±)-pentalen-13-ol were well resolved, confirmed that the enzymatically-produced pentalen-13-ol was a single enantiomer. A preparative-scale incubation was carried out with PtlI, electron transport proteins Fld and Fdr, the NADPH regeneration system and (±)-pentalenene. The resulting organic extracts were dissolved in methanol and treated with sodium borohydride to give alcohol (pentalen-13-ol), which was shown by $^{1}$H NMR to be identical to chemically synthesized pentalen-13-ol. Control incubations with alcohol and aldehyde, respectively, showed that each of these intermediates was oxidized to 1-deoxypentalenic acid by PtlI.

BLAST searching indicates that *ptlH* has 26% amino acid sequence identity and 44% similarity over 244 residues to phytanoyl-CoA dioxygenase of *Agrobacterium tumefaciens* (Table 1; PhyH, Genbank Accession No. YP_086787). PhyH, which catalyzes the $\alpha$-hydroxylation of phytanoyl-CoA, belongs to the sub-family of Fe(II)/$\alpha$-ketoglutarate-dependent hydroxylases (40). We therefore hypothesized that PtlH might be responsible for hydroxylation of the methylcyclopentane ring of 1-deoxypentalenic acid in the oxidative conversion of 1-deoxypentalenic acid to pentalenolactone D (Fig. 2). A gene *ptlH* was amplified by polymerase chain reaction (PCR) from DNA of *S. avermitilis* cosmid CL_216_D07 and cloned into the vector pET28e. The resulting construct pET28e-*PtlH* was introduced into *Escherichia coli* BL21(DE3). After induction with IPTG, the expressed PtlH protein, carrying an N-terminal $His_6$-tag, was purified to homogeneity by Ni-NTA chromatography. The purified protein had a subunit $M_D$ by MALDI-TOF MS of *m/z* 37139±19 (calc. 37121). The presence of a second peak at *m/z* 73965 suggested that PtlH may be a homodimer. A mixture (1.5 ml) of recombinant PtlH (1.66 $\mu$M), $\alpha$-ketoglutarate (2 mM), L-ascorbic acid (2 mM), $FeSO_4$ (1 mM), DTT (1.5 mM), and bovine catalase (1 mg/ml) in 100 mM Tris-HCl buffer (pH 7.3) was incubated with (±)-1-deoxypentalenic acid (0.64 mM) overnight at room temperature. After acidification with HCl, the mixture was extracted with diethyl ether and the organic extract was treated with TMS-$CHN_2$ to generate the methyl ester. GC-MS analysis

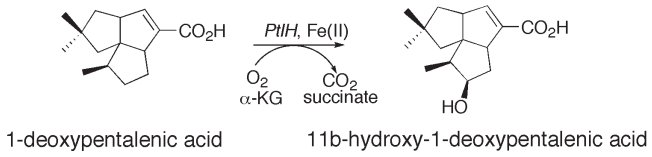


**Fig. 6.** Fe(II)- and $\alpha$-ketoglutarate-dependent hydroxylation of 1-deoxypentalenic acid to 11$\beta$-hydroxy-1-deoxypentalenic acid by PtlH.

revealed a single new peak with *m/z* 264, indicating the formation of the hydroxylated product. Chiral GC-MS analysis, under conditions in which the methyl esters of (±)-deoxypentalenic acid were well resolved, confirmed that the enzymatic reaction product was a single enantiomer. Control incubations that omitted $\alpha$-ketoglutarate or Fe(II) showed no turnover of 1-deoxypentalenic acid. Neither (±)-pentalenene (0.5 mM) nor (±)-pentalen-13-ol (0.1 mM) underwent PtlH-catalyzed hydroxylation. Ultimately, the experimental results firmly establish the biochemical function of the *ptlH* gene product, which is shown to catalyze the Fe(II)- and $\alpha$-ketoglutarate-dependent hydroxylation of 1-deoxypentalenic acid to 11$\beta$-hydroxy-1-deoxypentalenic acid (Fig. 6).

2. *Geosmin.*

Geosmin is a well-known, odoriferous metabolite produced by a wide variety of microorganisms, including *Streptomyces*, cyanobacteria, myxobacteria, and various fungi, as well as by higher plants such as liverworts and sugar beets (41-47). Geosmin, with an especially low detection threshold of 10-100 parts per trillion, is responsible for the characteristic odor of freshly turned earth and is associated with unpleasant off-flavors in water, wine, and fish (48, 49). The *S. avermitilis* open-reading frame, *geoA* (SAV2163), encodes a protein with 77% identity and 87% similarity over 713 aa to the *S. coelicolor* A3(2) germacradienol/geosmin synthase (50; SCO6073p). Interestingly, the level of identity between the catalytically functional N-terminal domains of the *S. avermitilis* and *S. coelicolor* A3(2) proteins is even greater: 89% identity and 98% similarity over 327 aa. Both proteins harbor an aspartate-rich $^{84}$DDHFLE motif and a downstream NSE triad $^{224}$NDLFSYQRE, the universally conserved $Mg^{2+}$-binding domains that are found in all known ses-

quiterpene synthases. *S. avermitilis* produces the typical strong odor of moist soil when grown in several different media. GC-MS analysis of the *n*-hexane or pentane extract of a liquid culture revealed two main peaks (Fig. 7B), rt 9.89 min [$M^+$] *m/z* 182 and 11.42 min [$M^+$+1] *m/z* 223, that were identical to geosmin and germacradienol, respectively, by comparison with authentic samples of each compound. We constructed a *geoA*-deletion mutant by homologous recombination in order to confirm the involvement of the GeoA in geosmin biosynthesis. Two 1.8-kb segments corresponding to both upstream and downstream regions of *geoA* were amplified by PCR and ligated together into *E. coli/Streptomyces* conjugative vector. A resistance gene (*aad3"*) was inserted between these two amplified segments. After introducing the recombinant plas-

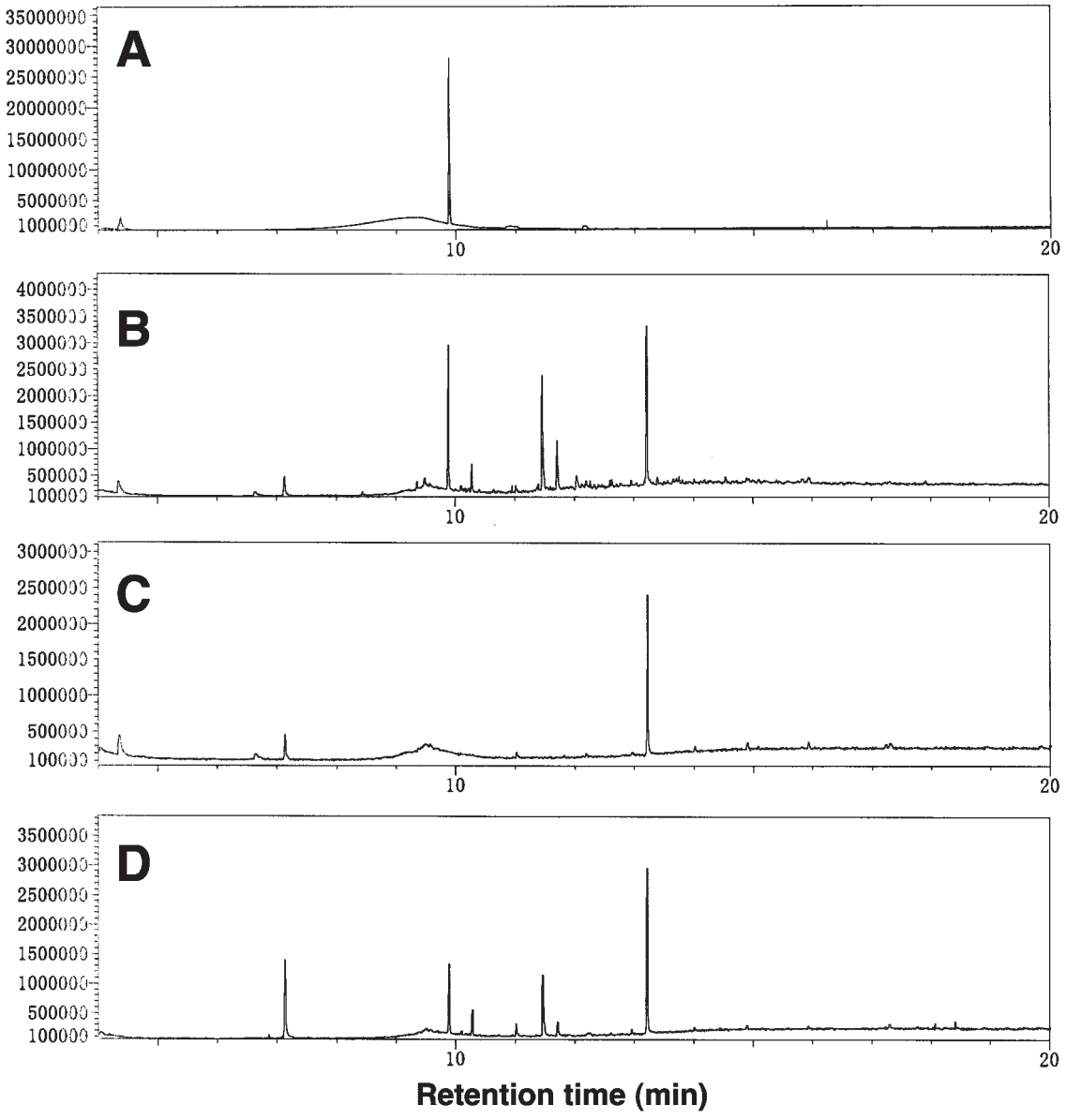


**Fig. 7.** GC-MS analysis of extracts from cultured broth of *S. avermitilis* and its mutants. (A) Authentic sample of geosmin (**1**, rt 9.89 min, $[M]^+$ *m/z* 182), (B) *n*-hexane extract from wild type strain of *S. avermitilis*. The peak at 11.42 min is germacradienol (**3**, [$M^+$+1] *m/z* 223), (C) *n*-hexane extract from *⊿geoA::aad3"* and (D) *n*-hexane extract from exoconjugant of *geoA*-deletion mutant carrying an extra-copy of *geoA*. (The peak at rt 13.30 min is diethyl phthalate ($[M]^+$ *m/z* 222).)

mid into wild-type *S. avermitilis* by selection of the vector marker, thiostreptone-resistance, homologous recombination between the chromosome and the recombinant plasmid gave the desired *geoA*-deletion mutants, which were obtained by selection for the thiostreptone-sensitive and streptomycin/spectinomycin resistance phenotype. The *geoA* deletion mutants failed to produce either geosmin or germacradienol (Fig. 7C). Introduction of an extra copy of wild-type *geoA* into these deletion mutants restored the production of both geosmin and germacradienol (Fig. 7D), indicating that GeoA is essential for the formation of both geosmin and germacradienol. We next used PCR to amplify the 2178-bp coding region of SAV2163, using DNA from *S. avermitilis* cosmid CL_228_H03 as template, while introducing *Eco*RI and *Xho*I restriction sites at the respective 5'- and 3'-termini of the ORF. After ligation of the amplified DNA into the *Eco*RI/*Xho*I cloning sites of the pET21d(+) expression vector, the derived plasmid, pXH17, was purified from *Escherichia coli* XL-1 Blue and used to transform the T7 RNA polymerase-based expression host *E. coli* BL21(DE3). The resultant recombinant protein was obtained as insoluble inclusion bodies that were readily solubilized using 20 mM NaOH and purified to homogeneity, using a protocol previously developed for the homologous *S. coelicolor* A3(2) germacradienol/geosmin synthase. Incubation of 2.5 nM GeoA with 270 nM FPP for 3.5 h at 30ºC followed by GC-MS analysis of the pentane-soluble extract revealed the formation of germacradienol, germacrene D, octalin, and geosmin (Fig. 8) in a ratio of 66:24:2:8. The individual components were unambiguously identified by direct comparison of GC-retention times and EI-mass spectra with those of authentic samples that were generated from FPP in a separate incubation with recombinant *S. coelicolor* A3(2) germacradienol/geosmin synthase (51). A small amount (3%) of an additional, unidentified sesquiterpene hydrocarbon, *m/z* 204, was also detected in the product mixture. As previously observed for the homologous *S. coelicolor* A3(2) enzyme, no geosmin was detected after 20 min incubation time, while both the absolute yield and the relative proportion of geosmin increased with longer incubation times. The activity of recombinant GeoA, which was tested over a pH range from 5.4-9.5, showed optimal activity between pH 7.6 and 9.0. The reaction showed an absolute requirement for a divalent cation, $Mg^{2+}$ (10 mM) being preferred, with $Fe^{2+}$ and $Zn^{2+}$ exhibiting 50% activity of $Mg^{2+}$, and $Co^{2+}$, $Cu^{2+}$, or $Mn^{2+}$ each showing 10-20% activity. Neither $Ca^{2+}$ nor $Ni^{2+}$ supported turnover of FPP.

*Minimization of a linear chromosome of S. avermitilis.*

The linear chromosome (9,025,608 bp) of *S. avermitilis* contains 7,577 protein-coding genes, of which we assigned a putative function to 5,027 (66.3%). Out of the remaining 2,550 genes, 2,277 genes (30.1%) showed the conservation to hypothetical proteins of unknown function annotated in other genomes, and 273 genes (3.6%) had no significant similarity to data in the public databases. Clustering of the 7,574 genes by BLASTCLUST showed that 35% (2,664) of the genes were clustered into 721 paralogous families, ranging from 2 to 91 genes per family. These included two large gene families, composed of genes related to membrane-spanning components of the ATP binding cassette (ABC) transport and the two-component system transcriptional regulator family. We identified a putative origin of replication (*oriC*) at position 5,287,935-5,289,024 of the chromosome. This region contained at least 19 *dnaA*-box-like sequences (52) and the order of genes flanking this region is almost the same as that observed in circular bacterial chromosomes. The replication origin was positioned at the middle of the linear chromosome of *B. burgdorferi* (4), *A. tumefaciens* (5, 6) and *S. coelicolor* A3(2) (14)

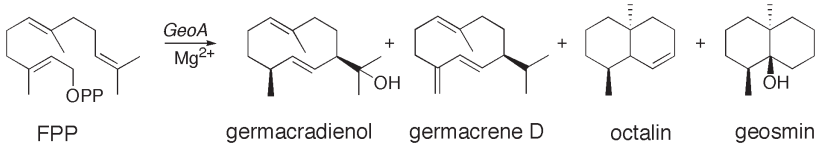


**Fig. 8.** Enzymatic reaction products identified by incubation of FPP with GeoA and $Mg^{2+}$.

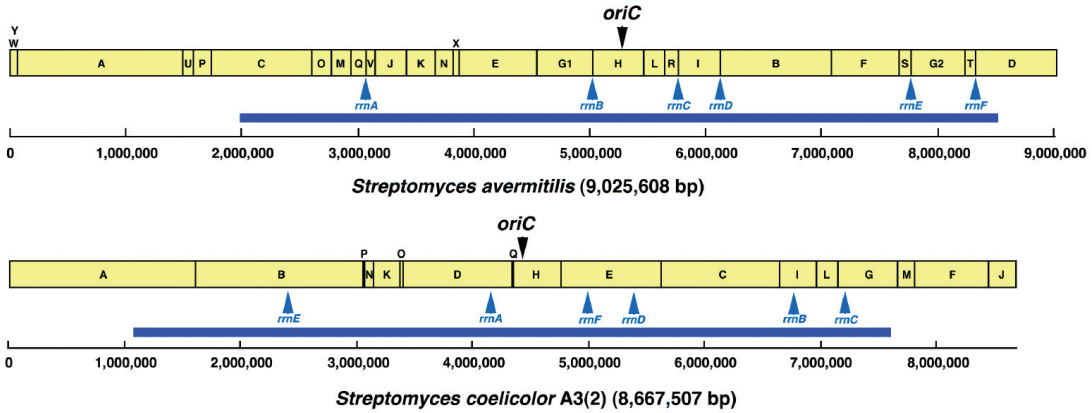


**Fig. 9.** *Ase*I-physical maps of *S. avermitilis* and *S. coelicolor* A3(2). Each blue bar corresponds to 6.5-Mb conserved region of both microorganisms. Up and down arrows indicate ribosomal operons (*rrn*) and origin of replication (*oriC*), respectively.

but the location of the *oriC* in the *S. avermitilis* chromosome shifted 776 kb away from the center toward the right end. *S. avermitilis* and *S. coelicolor* A3(2) showed the comprehensive conservation for the linearity and gene order along the chromosomes (Fig. 9). However, most of the highly conserved internal regions are structurally asymmetric between the *S. coelicolor* A3(2) and *S. avermitilis* chromosomes when placed each *oriC* with the same direction at the center of each chromosome. All of known essential genes are located in the 6.5-Mb highly conserved internal region (SAV1625-7142 in *S. avermitilis* and SCO1196-6804 in *S. coelicolor* A3(2), respectively). The gene content and location in the 6.5-Mb conserved region also showed syntenic feature with the circular chromosomes of Actinobacteria, *M. tuberculosis*, *C. diphtheriae* and *C. glutamicun*. The analysis also revealed that the regions near both telomeres are less conserved in both the sequence and ortholog distribution. These variable regions are located in the 2.0Mb region from left telomere and 0.5Mb region from right telomere in *S. avermitiliis* and designated the sub-telomeric region. Corresponding sub-telomeric regions in *S. coelicolor* A3(2) are 1.1Mb regions from both left and right telomeres. The sub-telomeric regions contained 1,020 of *S. avermitilis*-specific genes corresponding to 44.5% of the total 2,291 specific genes in *S. avermitilis*. Similarly, 972 (42.1%) of *S. coelicolor* A3(2)-specific 2,307 genes were located in the sub-telomeric regions.

Thus, the left 2-Mb sub-telomeric region contained non-essential genes and might not contain genes concerning supplement of precursors for secondary metabolite biosyntheses. As *S. avermitilis* has an ability to produce avermectins as the secondary metabolites in the industrial scale, the microorganism has extremely efficient regulatory systems; supplement of precursors and generation of cofactor and energy source for secondary metabolism. It suggests that *S. avermitilis* could be used as a versatile host for secondary metabolites by introducing foreign gene cluster(s) for secondary metabolite biosynthesis. Homologous recombination system was applied to minimize the linear chromosome of *S. avermitilis*. Two pieces of segments corresponding to nt 5,847 to 8,806, and nt 1,494,519 to 1,497,112 were purified from cosmid clones CL_090_H01 and CL_225_G12, respectively. A resistance gene (*aph*) was inserted between these two segments. After introducing the recombinant plasmid into oligomycin-deletion mutant, *S. avermitilis ΔolmA* (deletion at nt 3,557,725 to 3,594,005), by selection of the vector marker, thiostreptone-resistance, homologous recombination between the chromosome and the recombinant plasmid gave the desired large-deletion mutants, which were obtained by selection for the thiostreptone-sensitive and neomycin resistance phenotype. To remove resistance marker (*aph*) in the chromosome of large-deletion mutant, second homologous recombination event was done in a similar manner. Two segments (nt 5,847 to 7,734 and nt 1,494,893 to 1,497,112, respectively) from above two cosmid clones were li-

gated. After introducing the resultant recombinant plasmid into the above large-deletion mutants by selection of the vector marker, ultimately, objective clones were obtained by selection for the thiostreptone- and neomycin-sensitive phenotype. The growth and morphology of the large-deletion mutants were same as those of the wild type strain, and the large deletion mutants never required cofactors for growth on the defined minimal medium. To confirm the deletion region in the resultant large-deletion mutants, each chromosome was digested by rare-cutter and digests were analyzed by CHEF electrophoresis. Twenty-six fragments were generated from the wild-type chromosome by cutting with restriction enzyme *Ase*I (Fig. 10). The mutants deleted two regions on the chromosome at position nt 7,734 to 1,494,893 and nt 3,557,725 to 3,594,005, respectively. The former region contains a part of *Ase*I-W, *Ase*I-Y, *Ase*I-A, and a part of *Ase*I-U segments of the wild type chromosome. The deletion mutants lacked *Ase*I-A segment in the CHEF electrophoresis (Fig10). Smaller segments, *Ase*I-W and -U, also disappeared in FIGE (data not shown). These mutants constructed lacked 1,523,439-bp from the chromosome and the genome size is 7,502,169-bases long (Fig. 11) and contained at least 6,377 potential protein-coding genes. The deletion region in left side of the chromosome contains many gene clusters for secondary metabolite biosynthesis, in which carotenoid and melanin biosynthetic gene clusters are located. The deletion mutants failed to produce both pigments, carotenoid and melanin (Fig. 12). Since the deletion mutants lack three biosynthetic gene clusters for avermectin, filipin and oligomycin, which are major secondary metabolites of *S. avermitilis*, the mutants did not produce these metabolites. Although the deletion mutants lack some gene clusters for secondary metabolite biosynthesis, they retain genes for primary metabolism, some of which are involved in the supplement of precursors, cofactors and energy for secondary metabolism. *S. avermitilis* has the ability to produce many polyketide compounds, and the productivity for the precursors, malonyl-CoA and methylmalonyl-CoA,

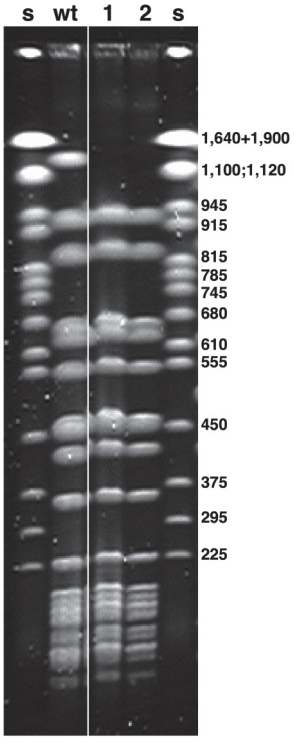


**Fig. 10.** CHEF electrophoresis of *Ase*I-digested wild type (wt) and deletion mutants (1 and 2) of *S. avermitilis* chromosome. The condition of electrophoresis is as follows; 1% agarose gel in 0.5 × TBE (50 mM Tris-borate, 1 mM EDTA, pH8.3), ramp time 70 sec for 24 hrs, 140 sec 24 hrs and 180 sec 24 hrs, 5 volts/cm at 12°C. Yeast chromosome (s) was used as a size marker (Each size is indicated in right side).

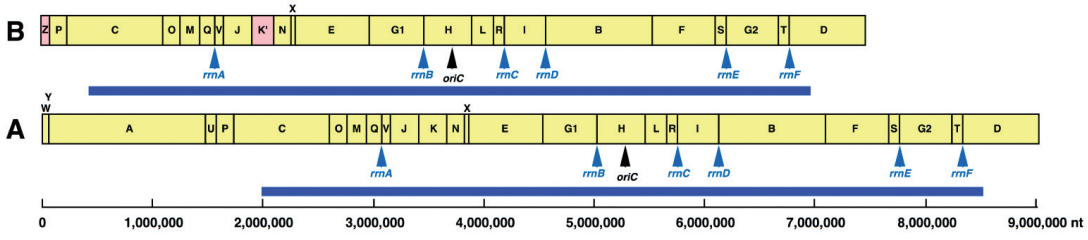


**Fig. 11.** *Ase*I-physical maps of (A) wild type and (B) deletion mutant of *S. avermitilis*. As to blue bars and arrows, see Fig. 9 legend.

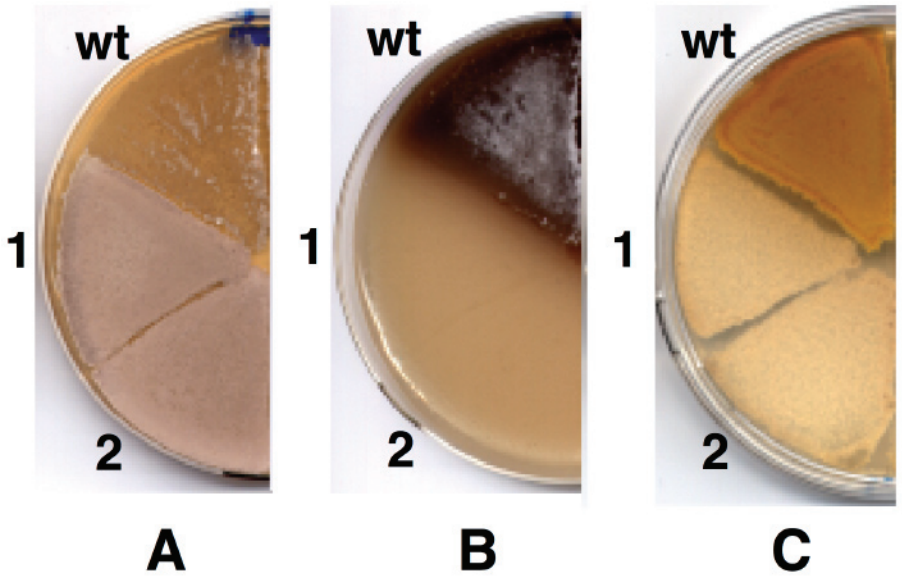


**Fig. 12.** Morphology and pigment production of wild type (wt) and deletion mutants (1 and 2) of *S. avermitilis* cultured on the following three differt kinds of agar media at 30°C for 1 week. (A) Yeast-malt extract agar, (B) soyflour-mannitol agar containing 1 mM $CuSO_4$ and 0.1% of L-tyrosine, and (C) Bennet agar containing 15% sucrose (under the light), were used for examination of morphology, melanin production and carotenoid production, respectively.

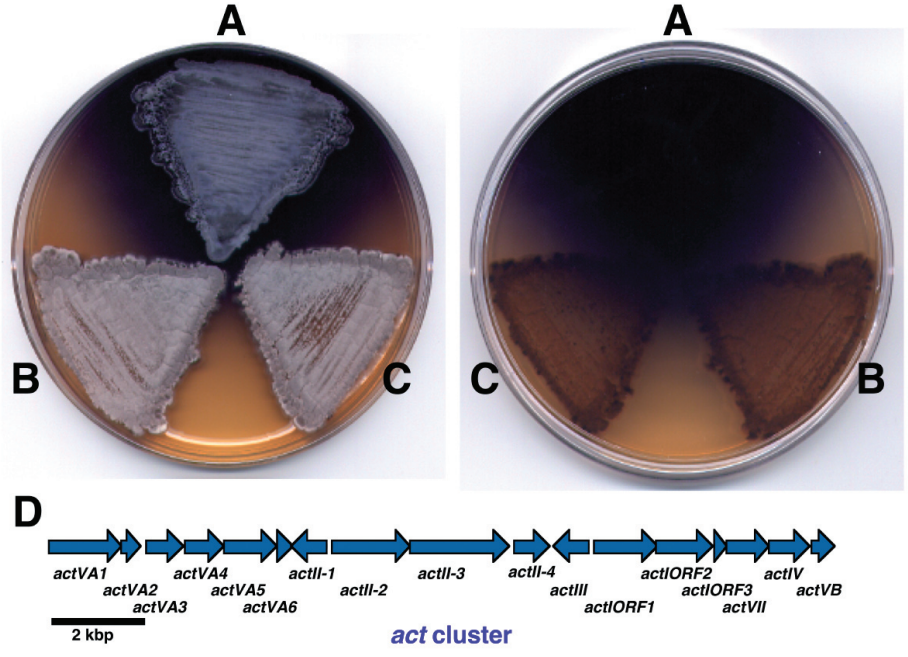


**Fig. 13.** Production of blue pigment antibiotic, actinorhodin, by (A) *S. avermitilis* deletion mutant carrying a gene cluster for actinorhodin biosynthesis, (B) *S. coelicolor* A3(2) and (C) *S. avermitilis* deletion mutant. Microorganisms were grown at 30°C for 5 days on yeast-malt extract agar. *S. coeliclolor* A3(2) produced a small amount of actinorhodin after 7 days incubation. The plate was photographed from surface (left) and back (right). The actinorhodin biosynthetic gene cluster of *S. coelicolor* A3(2) was presented in (D).

of the polyketide compounds would be more efficient rather than other streptomycetes. *S. avermitilis* does not produce aromatic polyketide compounds except for spore pigment, which might be synthesized by type II polyketide synthase using malonyl-CoA as a precursor. Introducing whole set of biosynthetic gene cluster for actinorhodin of *S. coelicolor* A3(2) into the deletion mutant of *S. avermitilis*, a large amount of aromatic polyketide, actinorhodin, was produced by the mutant as blue pigment (Fig. 13). Gene clusters for aminoglycoside antibiotic biosynthesis were not found in the genome of *S. avermitilis*. It is interesting that *S. avermitilis* acquired the ability to produce these compounds after introducing the biosynthetic gene clusters. Recently, it was found that the deletion mutants produced small amounts of ribostamycin after introducing gene cluster for ribostamycin biosynthesis of *S. ribosidificus*.

## Discussion

The increasing availability of complete microbial genome sequences has recently opened up the possibility of the top-down characterization of the molecular genetics and biochemistry of entire biosynthetic pathways whose genes are frequently organized in discrete clusters. As an essential first step in the elucidation of the enzymology and genetics of pentalenolactone biosynthesis in *S. avermitilis*, we have established that *ptlA* (SAV2998), one of 13 ORFs within a 13.4-kb cluster, encodes a 336-aa protein that catalyzes the cyclization of FPP to pentalenene, the well-established sesquiterpene hydrocarbon precursor of the pentalenolactone family of metabolites. The pentalenolactone biosynthetic pathway is functional in *S. avermitilis*, as confirmed by the isolation of both pentalenolactone F and the shunt metabolite pentalenic acid. Deletion of the entire *ptl*-cluster from *S. avermitilis* abolished the production of pentalenolactone metabolites, while transfer of this cluster to the naïve host, *S. lividans* 1326, the transformants were endowed with the ability to generate pentalenic acid, accompanied by trace amounts of pentalenolactones.

The results firmly establish the biochemical function of the *ptlI* gene product, which is shown to catalyze the three-step oxidation of pentalenene to 1-deoxypentalenic acid. The work reported here fills the biosynthetic gap between pentalenene, generated by PtlA-catalyzed cyclization of FPP, and 1-deoxypentalenic acid. Although *S. avermitilis* contains six putative ferredoxin reductases and nine ferredoxins, the natural electron transport pair for PtlI is unknown. The experimental results also establish the biochemical function of the *ptlH* gene product, which is shown to catalyze the Fe(II)- and $\alpha$-ketoglutarate-dependent hydroxylation of 1-deoxypentalenic acid to 11$\beta$-hydroxy-1-deoxypentalenic acid. Further conversion of 1-deoxypentalenic acid to pentalenolactone D may involve oxidation of 1-deoxypentalenic acid to the 11-oxo-1-deoxypentalenic acid by PtlF, an apparent $NAD^+$-dependent dehydrogenase, followed by Baeyer-Villiger-like oxidaton of 11-oxo-1-deoxypentalenic acid mediated by PtlE, which has 49% identity and 62% similarity over 591 aa to the cyclodecanone-lauryl lactone dioxygenase of *Rhodococcus ruber* (Genbank AY052630.1).

Germacradienol was first identified in 1995 as a cometabolite of geosmin in *S. citreus* (44, 53). Since that time, germacradienol has frequently been observed as a cometabolite of geosmin in streptomycetes, myxobacteria, and liverworts, often accompanied by germacrene D (45, 46, 54). Consistent with the demonstration that *S. coelicolor* A3(2) harbors a germacradienol synthase encoded by the SCO6073 gene, and that this gene is essential for geosmin production, both germacradienol and geosmin were found in the culture broth of *S. avermitilis*. The observed ~5:6 ratio of germacradienol/geosmin was essentially the same in the several media examined. A *geoA* (SAV2163) deletion mutant constructed by homologous recombination produced neither geosmin nor germacradienol, while production of both compounds could be restored by complementation of the mutation by introducing an extra copy of the *geoA* gene, confirming that GeoA is essential for geosmin biosynthesis.

We have established that the GeoA protein of *S. avermitilis*, encoded by *geoA*, which exhibits a high degree of sequence similarity to the *S. coelicolor* A3(2) enzyme SCO6073p, catalyzes the predicted conversion of FPP to a mixture of germacradienol, ger-

macrene D, and geosmin, as well as the presumed intermediate, octalin. Recombinant *S. avermitilis* GeoA has a product profile, divalent metal ion dependence, pH optimum, and steady-state kinetic parameters that are essentially the same as those previously determined for the *S. coelicolor* A3(2) germacradienol/geosmin synthase. Significantly, for both enzymes, the relative proportion of geosmin to germacradienol was enhanced by increasing the concentration of synthase or by employing longer incubation times. One would not expect such a result if both geosmin and germacradienol were to be generated by partitioning of a single series of enzyme-bound intermediates. Instead, it appears likely that a substantial fraction of the initially generated germacradienol is released into solution before being subsequently rebound and further converted to geosmin.

From the comparative analysis of *S. avermitilis* with *S. coelicolor* A3(2), it was found that the 6.5-Mb highly conserved internal region where most of known essential genes are located with the similar order and direction exists, and this also has the structural similarity to the circular chromosome of other bacteria. This finding implies that the 6.5-Mb internal region is the underlying backbone of the *Streptomyces* chromosomes and may have evolved from an ancestor common to bacteria having circular chromosomes existing to date. On the other hand, it was also found the variable and less conserved regions near both telomeres designated sub-telomeric regions. Interestingly, more than half of the genes related to the secondary metabolites were found to be located in the sub-telomeric regions where no known essential gene was found at all. Also, the sub-telomeric regions contained most of mobile elements as well as about half of genes specific to *S. avermitilis* but not relevant to the secondary metabolites. Similar organization at the sub-telomeric regions was also found in *S. coelicolor* A3(2). These findings suggest that frequent gene duplication may have preferentially occurred in the sub-telomeric regions in the *Streptomtces* chromosomes. About 1.4Mb-deletion at the left sub-telomeric region did not affect the growth and morphological changes. The results were reconfirmed that no known essential genes are located in this region. Moreover, the deletion mutants carrying foreign gene cluster for biosynthesis of an aromatic polyketide antibiotic, actinorhodin, produced a larger amount of actinorhodin than that the original strain *S. coelicolor* A3(2) did, suggesting that the constructed deletion mutants possess genes related to primary metabolism for supplement of precursors, cofactors and energy. The information and materials in this study will be of great value to make the *Streptomyces* more useful for the production of secondary metabolites including antibiotics and bioactive substances.

**References**


(1) Burg, R.W., Miller, B.M., Baker, E.E., Birnbaum, J., Currie, S.A., Hartman, R., Kong, Y.-L., Monaghan, R.L., Olson, G., Putter, I., Tunac, J.B., Wallick, H., Stapley, E.O., Oiwa, R., Omura, S. *Antimicrob. Agents Chemother*. **15**, 361−367 (1979)

(2) Witt, D., Stackenbrandt, E. *Syst. Appl. Microbiol*. **13**, 361−371 (1990)

(3) Lin, Y.-S., Kieser, H.M., Hopwood, D.A., Chen, C.W. *Mol. Microbiol*. **10**, 923−933 (1993)

(4) Fraser, C.M., Casjens, S., Huang, W.M., Sutton, G.G., Clayton, R., Lathigra, R., White, O., Ketchum, K.A., Dodson, R., Hickey, E.K., Gwinn, M., Dougherty, B., Tomb, J.F., Fleischmann, R.D., Richardson, D., Peterson, J., Kerlavage, A.R., Quackenbush, J., Salzberg, S., Hanson, M., van Vugt, R., Palmer, N., Adams, M.D., Gocayne, J., Venter, J.C. *Nature* **390**, 580−586 (1997)

(5) Wood, D.W., Setubal, J.C., Kaul, R., Monks, D.E., Kitajima, J.P., Okura, V.K., Zhou, Y., Chen, L., Wood, G.E., Almeida, N.F. Jr, Woo, L., Chen, Y., Paulsen, I.T., Eisen, J.A., Karp, P.D., Bovee, D. Sr., Chapman, P., Clendenning, J., Deatherage, G., Gillet, W., Grant, C., Kutyavin, T., Levy, R., Li, M.J., McClelland, E., Palmieri, A., Raymond, C., Rouse, G., Saenphimmachak, C., Wu, Z., Romero, P., Gordon, D., Zhang, S., Yoo, H., Tao, Y., Biddle, P., Jung, M., Krespan, W., Perry, M., Gordon-Kamm, B., Liao, L., Kim, S., Hendrick, C., Zhao, Z.Y., Dolan, M., Chumley, F., Tingey, S.V., Tomb, J.F., Gordon, M.P., Olson, M.V., Nester, E.W. *Science* **294**, 2317−2323 (2001)

(6) Goodner, B., Hinkle. G., Gattung, S., Miller, N., Blanchard, M., Qurollo, B., Goldman, B.S., Cao, Y., Askenazi, M., Halling, C., Mullin, L., Houmiel, K., Gordon, J., Vaudin, M., Iartchouk, O., Epp, A., Liu, F., Wollam, C., Allinger, M., Doughty, D., Scott, C., Lappas, C., Markelz, B., Flanagan, C., Crowell, C., Gurson, J., Lomo, C., Sear, C., Strub, G., Cielo, C., Slater, S. *Science* **294**, 2323−2328 (2201)

(7) Demain, A.L. *Appl. Microbiol. Biotechnol*. **52**, 455−463 (1999)

(8) Cole, S.T., Brosch, R., Parkhill, J., Garnier, T., Churcher, C., Harris, D., Gordon, S.V., Eiglmeier, K., Gas, S., Barry, C.E.3rd., Tekaia, F., Badcock, K., Basham, D., Brown, D., Chillingworth, T., Connor, R., Davies, R., Devlin, K., Feltwell, T., Gentles, S., Hamlin, N., Holroyd, S., Hornsby, T., Jagels, K., Barrell, B.G. *Nature* **393**, 537−544 (1998)

(9) Fleischmann, R.D., Alland, D., Eisen, J.A., Carpenter, L., White, O., Peterson, J., DeBoy, R., Dodson, R., Gwinn, M., Haft, D., Hickey, E., Kolonay, J.F., Nelson, W.C., Umayam, L.A., Ermolaeva, M., Salzberg, S.L., Delcher, A., Utterback, T., Weidman, J., Khouri, H., Gill, J., Mikula, A., Bishai, W., Jacobs, Jr. W.R. Jr., Venter, J.C., Fraser, C.M. *J. Bacteriol*. **184**, 5479−5490 (2002)

(10) Cole, S.T., Eiglmeier, K., Parkhill, J., James, K.D., Thomson, N.R., Wheeler, P.R., Honore, N., Garnier, T., Churcher, C., Harris, D., Mungall, K., Basham, D., Brown, D., Chillingworth, T., Connor, R., Davies, R.M., Devlin, K., Duthoy, S., Feltwell, T., Fraser, A., Hamlin, N., Holroyd, S., Hornsby, T., Jagels, K., Lacroix, C., Maclean, J., Moule, S., Murphy, L., Oliver, K., Quail, M.A., Rajandream, M.A., Rutherford, K.M., Rutter, S., Seeger, K., Simon, S., Simmonds, M., Skelton, J., Squares, R., Squares, S., Stevens, K., Taylor, K., Whitehead, S., Woodward, J.R., Barrell, B.G. *Nature* **409**, 529, 1007−1011 (2001)

(11) Cerdeno-Tarrage, A.M., Efstratiou, A., Dover, L.G., Holden, T.G., Pallen, M., Bentley, S.D., Besra, G.S., Churcher, C., James, K.D., De Zoysa1, A., Chillingworth, T., Cronin, A., Dowd, L., Feltwell, T., Hamlin, N., Holroyd, S., Jagels, K., Moule, S., Quail, M.A., Rabbinowitsch, E., Rutherford, K.M., Thomson, N.R., Unwin, L., Whitehead, S., Barrell, B. G., Parkhill, J. *Nucleic Acids Res*., 6516−6523 (2003)

(12) Ikeda,M. and Nakagawa, S. *Appl. Microbiol. Biotechnol*. **62**, 99−109 (2003)

(13) Ishikawa, J., Yamashita, A., Mikami, Y., Hoshino, Y., Kurita, H., Hotta, K., Shiba, T., Hattori, M. *Proc. Natl. Acad. Sci. USA*. **101**, 14925−14930.

(14) Bentley, S.D., Chater, K.F., Cerdeno-Tarraga, A.M., Challis, G.L., Thomson, N.R., James, K.D., Harris, D.E., Quail, M.A., Kieser, H., Harper, D., Bateman, A., Brown, S., Chandra, G., Chen, C.W., Collins, M., Cronin, A., Fraser, A., Goble, A., Hidalgo, J., Hornsby, T., Howarth, S., Huang, C.H., Kieser, T., Larke, L., Murphy, L., Oliver, K., O' Neil, S., Rabbinowitsch, E., Rajandream, M.A., Rutherford, K., Rutter, S., Seeger, K., Saunders, D., Sharp, S., Squares, R., Squares, S., Taylor, K., Warren, T., Wietzorrek, A., Woodward, J., Barrell, B.G., Parkhill, J., Hopwood, D.A. *Nature* **417**, 141 −147 (2002)

(15) Omura, S., Ikeda, H., Ishikawa, J., Hanamoto, A., Takahashi, C., Shinose, M., Takahashi, Y., Horikawa, H., Nakazawa, H., Osonoe, T., Kikuchi, H., Shiba, T., Sakaki, Y., Hattori, M. *Proc. Natl. Acad. Sci. USA* **98**, 12215−12220 (2001)

(16) Ikeda, H., Ishikawa, J., Hanamoto, A., Shinose, M., Kikuchi, H., Shiba, T., Sakaki, Y., Hattori, M., Omura, *Nature Biotechnol*. **21**, 526−531 (2003)

(17) Koe, B.K., Sobin, B.A., Celmer, W.D. *Antibiot. Annu*. 672−675 (1957)

(18) Martin, D.G., Slomp, G., Mizsak, S., Duchamp, D.J., Chidester, C.G. *Tetrahedron Lett*. 4901−4904 (1970)

(19) Keller-Schierlein, W., Lemke, J., Nyfeler, R., Zähner, H. Stoffwechselprodukte von Mikroorganismen, **105**. Arenaemycin E, D, und C. *Arch. Mikrobiol*. **84**, 301−316 (1972)

(20) Takahashi, S., Takeuchi, M., Arai, M., Seto, H., Otake, N. *J. Antibiot*. **36**, 226−228 (1983)

(21) Okazaki, T., Enokita, R., Torikata, A., Inukai, M., Takeuchi, M., Takahashi, S., Arai, M. *Ann. Rep. Sankyo Res. Lab*. **31**, 94−103 (1979)

(22) English, A.R., McBride, T.J., Lynch, J.E. *Antibiot.*

*Annu*., 682−687 (1957)
(23) Nakagawa, A., Tomoda, H., Hao, M. V., Okano, K., Iwai, Y., Omura, S. *J. Antibiot*. **38**, 1114−1115 (1985)
(24) Ikeda, M., Fukuda, A., Takagi, M., Morita, M., Shimada, Y. *Eur. J. Pharm*. **411**, 45−53 (2001)
(25) Duszenko, M., Balla, H., Mecke, D. *Biochim. Biophys. Acta* **714**, 344-350 (1982)
(26) Hartmann, S., Neeff, J., Heer, U., Mecke, D. *FEBS Lett*. **93**, 339−342 (1978)
(27) Cane, D.E., Sohng, J.-K. *Arch. Biochem. Biophys*. **270**, 50−61 (1989)
(28) Cane, D.E., Sohng, J.-K. *Biochemistry* **33**, 6524−6530 (1994)
(29) Maurer, K.-H., Mecke, D. *J. Antibiot*. **39**, 266−271 (1986)
(30) Maurer, K.H., Pfeiffer, F., Zehender, H., Mecke, D. *J. Bacteriol*. **153**, 930−936 (1983)
(31) Frohlich, K.U., Kannwischer, R., Rudiger, M., Mecke, D. *Arch. Microbiol*. **165**, 179−186 (1996)
(32) Tillman, A. M., Cane, D. E. Pentalenolactone F, *J. Antibiot*. **36**, 170−172 (1983)
(33) Helliwell, C.A., Chandler, P.M., Poole, A., Dennis, E.S., Peacock, W.J. *Proc. Natl. Acad. Sci. USA*. **98**, 2065−2070 (2001)
(34) Pikuleva, I.A., Babiker, A., Waterman, M.R., Bjorkhem, I. *J. Biol. Chem*. **273**, 18153−18160 (1998)
(35) Ro, D.K., Paradise, E.M., Ouellet, M., Fisher, K.J., Newman, K.L., Ndungu, J.M., Ho, K.A., Eachus, R.A., Ham, T.S., Kirby, J., Chang, M.C.Y., Withers, S.T., Shiba, Y., Sarpong, R., Keasling, J.D. *Nature* **440**, 940−943 (2006)
(36) Sono, M., Roach, M.P., Coulter, E.D., Dawson, J.H. *Chem. Rev*. **96**, 2841−2887 (1996)
(37) Peterson, J.A., Lorence, M. C., Amarneh, B. *J. Biol. Chem*. **265**, 6066−6073 (1990)
(38) Jenkins, C.M., Waterman, M.R. *J. Biol. Chem*. **269**, 27401−27408 (1994)
(39) Jenkins, C.M., Waterman, M. R. *Biochemistry* **37**, 6106−6113 (1998)
(40) Mihalik, S.J., Rainville, A.M., Watkins, P.A. *Eur. J. Biochem*. **232**, 545−551 (1995)
(41) Gerber, N.N. *Phytochemistry* **10**, 185−189 (1971)
(42) Gerber, N.N., Lechevalier, H.A. *Appl Microbiol* **13**, 935−938 (1965)
(43) Gerber, N.N. *Tetrahedron Lett*., 2971−2974 (1968)
(44) Pollak, F.C., Berger, R.G. *Appl Environ Microbiol* **62**, 1295−1299 (1996)
(45) Dickschat, J.S., Wenzel, S.C., Bode, H.B., Muller, R., Schulz, S. *Chembiochem*. **5**, 778−787 (2004)
(46) Dickschat, J.S., Bode, H.B., Wenzel, S.C., Muller, R., Schulz, S. *Chembiochem*. **6**, 2023−2033 (2005)
(47) Lu, G., Edwards, C.G., Fellman, J.K., Mattinson, D.S., Navazio, J. *J. Agric. Food Chem*. **51**, 1026−1029 (2003)
(48) Gerber, N.N. *CRC Crit. Rev. Microbiol*. **7**, 191−214 (1979)
(49) La Guerche, S., Chamont, S., Blancard, D., Dubourdieu, D., Darriet, P. *Antonie Van Leeuwenhoek* **88**, 131−139 (2005)
(50) Cane, D.E., Watt, R.M. *Proc. Natl. Acad. Sci. USA*. **100**, 1547−1551 (2003)
(51) Jiang, J., He, X., Cane, D.E. *J. Am. Chem. Soc. in press*
(52) Jakimowicz, D., Majka, J., Messer, W., Speck, C., Fernandez, M., Martin, M.C., Sanchez, J., Schauwecker, F., Keller, U., Schrempf, H., Zakrzewska-Czerwinska, J. *Microbiol*. **144**, 1281−1290 (1998)
(53) Gansser, D., Pollak, F.C., Berger, R.G. *J. Nat. Prod*. **58**, 1790−1793 (1995)
(54) Toyota, M., Yoshida, T., Matsunami, J., Asakawa, Y. *Phytochemistry* **44**, 293−298 (1997)

# Fluctuation of Drug Susceptibility of *Vibrio cholerae* O1 and Analysis of the Drug Resistance Genes

**Masaaki Iwanaga**

*Division of Bacterial Pathogenesis, Department of Molecular Biology, Graduate School of Medicine, University of the Ryukyus, 207 Uehara, Nishihara, Okinawa 903-0215, Japan*

## Introduction

Cholera is a life-threatening disease associated with severe watery diarrhea. *Vibrio cholerae* O1, a causative agent of cholera, has been susceptible to the therapeutic antibiotics. Although outbreaks of cholera due to drug-resistant *V. cholerae* O1 were occasionally reported in some areas, the resistant strains soon disappeared, especially after preventive medication was stopped (1, 2). Cholera can be treated with fluid infusion, and antibiotic therapy is not essential. However, antibiotic therapy has been routinely performed, as the duration of diarrhea can be shortened (3).

Usually, drug resistant bacterial pathogens appear sporadically depending on the use of antibiotics, and the prevalence of the resistant bacteria gradually increases. However, drug resistant *V. cholerae* in the past decade suddenly appeared in a wide district, and almost all epidemic strains became resistant at the same time regardless of antibiotic use. Besides, in some occasion, the resistance suddenly disappeared in the next epidemic. Cholera epidemic in a wide district started within a limited period suggested that the infection foci are multiple and the clone of the pathogens must be different.

Before 1995, e.g., in 1980 or thereabout, only a few cases of cholera epidemic due to drug resistant strains were reported. In those epidemics, the pathogens were highly resistant to many antibiotics, and the resistance was mediated by plasmid. In the late 1990s, *V. cholerae* O1 throughout the world simultaneously started to become resistant to a variety of antibiotics (4-7), however, the antibiogram was quite different from those previously reported. Most of these strains had specific genetic elements such as class I integron or SXT constin (a conjugative, self-transmissible, integrating element) that could contribute to the spread of the drug resistance. Integrons are gene capturing systems that usually contain a few antibiotic-resistance genes. SXT constin is a transmissible genetic element that contains some regions (hot spots) for insertion of additional DNA such as drug-resistance genes (8). Dalsgaard *et al*. characterized *V. cholerae* O1 isolated in Vietnam from 1979 to 1996 and found that the strains isolated after 1990 were resistant to streptomycin and harbored class I integrons which contain a gene cassette encoding resistance to streptomycin (9). Nguyen et al. reported that *V. cholerae* O1 isolates in Vietnam in 1995 were sensitive to and those in 2000 were resistant to tetracycline and chloramphenicol (10).

It thus seems that the characteristics of *V. cholerae* O1 in the recent epidemic are variable. The purpose of this study is to clarify genetic composition responsible for the drug resistance, and to elucidate the reason why in the past decade, epidemic *V. cholerae* strains changed the drug susceptibilities with one accord from an epidemic to another.

## Materials and Methods

*Bacterial strains.*

*V. cholerae* strains used in this study were isolated from cholera patients and from environmental water in the Lao PDR and Vietnam. Human isolates were col-

lected during the period between 1993 and 2004. The environmental isolates were collected in 2005. The isolates were stored in a butt of soft agar at room temperature until use.

*Isolation of V. cholerae.*

*V. cholerae* from cholera patients were isolated from diarrheal stools by the routine laboratory work. For isolation of the organisms from the environmental water, Moor swabs (11, 12) and immuno-magnetic beads were used. Moor swabs were placed in the surface water of a stream or river near the residential area. The swabs were left as they were until heavy biofilm was formed (usually 24 to 48 hours). The swabs coated with heavy biofilm were put into alkaline peptone water, and incubated at 37ºC for 8 to 20 hours to proliferate the organisms. A kit of immuno-magnetic beads, sensitized with anti-*V. cholerae* O1 antibody, (DYNABEADS M-280) was used to select *V. cholerae* O1 among the heavy growth of the other organisms in the culture. Twenty micro-liter of the immuno-beads suspension (in PBS Tween buffer) was added to 1 ml of the incubated alkaline peptone water culture in a small tube, and mixed under gentle agitation for 10 minutes at room temperature. Then the tubes were set in the Dynal MPC-S rack with magnetic plate at the lateral side of the tubes. After a few minutes, the fluid was removed using micropipette (the organisms attached to the beads were left on the tube wall faced to the magnetic plate ). Then the beads were washed 5 times with 1 ml of PBS Tween buffer, and finally suspended in 0.2 ml of the buffer. All apparatus in this method were the preparations by Dynal AS, Oslo, Norway.

*Drug susceptibility test.*

Eight therapeutic drugs: ampicillin (Meiji), tetracycline (Nakarai), chloramphenicol (Wako), erythromycin (Dainihon), ofloxacin (Daiichi), nalidixic acid (Wako), sulfamethoxazol-trimethoprim (sulfamethoxazol: Wako, trimethoprim: Sigma), and streptomycin (Wako) were used to determine the minimum inhibitory concentrations (MICs) against the organisms. The MICs were determined by the plate dilution method. A series of heart infusion agar plates containing two-fold dilutions of the drugs from 100 $\mu$g/ml to 0.0125 $\mu$g/ml were prepared.

MIC of the compound drug sulfamethoxazol-trimethoprim was determined as follows. The ratio of sulfamethoxazol to trimethoprim in the mixture was 19 to 1, and the concentration of the drug was expressed as the total amount of sulfamethoxazol and trimethoprim. A dilution series from 640 $\mu$g/ml to 0.078 $\mu$g/ml of the drug combination in heart infusion agar plates (608 $\mu$g/ml to 0.0742 $\mu$g/ml of sulfamethoxazol and 32 $\mu$g/ml to 0.0039 $\mu$g/ml of trimethoprim) was prepared.

A 10-fold diluted overnight broth culture of test organisms was inoculated onto each plate containing serially diluted concentration of the drug with a Microplanter (Sakuma Co. model MITP #00257), and incubated at 37ºC for 24 hours. The susceptibility of the organisms to the drug was expressed as the MIC ($\mu$g/ml) of each drug.

*PCR amplification.*

All primers used in this study are listed in Table 1. DNA was extracted as previously described (13). Class I integrase (*intI1*) was detected by PCR using primers inDS-F and inDS-B. DNAs from strains yielding PCR product with these primers were subsequently amplified with the integron primers in-F and in-B, which amplify the region between the 5' and 3' CSs. The primers in-F and aadA-B were used to assess whether the integron contained a gene cassette encoding resistance to streptomycin and spectinomycin (*aadA1*). To investigate the presence of an SXT constin, primers INT1 and INT2, specific for SXT integrase (*intSXT*), were used. Antibiotic-resistant genes included in the SXT constin were detected using primers reported by others (14, 15) or designed in this study. The location of the *tetA* gene within the SXT constin was assessed based upon a strategy of different PCR amplifications using combination of several primers based on the sequence of the antibiotic resistance gene element of *V. cholerae* strain V21 (DDBJ accession number AB114188).

**Table 1.** Primers used in this study

| Primer | Sequence (5' to 3') | Locus (direction)[a] | Reference |
|---|---|---|---|
| inDS-F | CGG AAT GGC CGA GCA GAT C | *intI1* (–) | 6 |
| inDS-B | CAA GGT TCT GGA CCA GTT GCG | *intI1* (+) | 6 |
| in-F | GGC ATC CAA GCA GCA AGC | 5'-CS | 6 |
| in-B | AAG CAG ACT TGA CCT GAT | 3'-CS | 6 |
| aadA-B | ATT GCC CAG TCG GCA GCG | *aadA* (–) | 6 |
| TetA-F | GTA ATT CTG AGC ACT GTC GC | *tetA* (+) | 15 |
| TetA-R | CTG CCT GGA CAA CAT TGC TT | *tetA* (–) | 15 |
| INT1 | GCT GGA TAG GTT AAG GGC GG | *int*SXT (–) | 18 |
| INT2 | CTC TAT GGG CAC TGT CCA CAT TG | *nt*SXT (+) | 18 |
| LEND4 | CCT TTG GTT ACA CAT TCG C | *tnp* (+) | 18 |
| RUMA | CGA GCA ATC CCC ACA TCA AG | Intergenic | 18 |
| FLOR-F | TTA TCT CCC TGT CGT TCC AGC | G *floR* (+) | 18 |
| FLOR-2 | CCT ATG AGC ACA CGG GGA GC | *floR* (–) | This study |
| strB-F | GGC ACC CAT AAG CGT ACG CC | *strB* (–) | This study |
| strB-R | TGC CGA GCA CGG CGA CTA CC | *strB* (+) | This study |
| STRA-F | TTG ATG TGG TGT CCC GCA ATG C | *strA* (+) | 18 |
| STRA-B | CCA ATC GCA GAT AGA AGG CAA | *strA* (–) | 18 |
| SUL2-F | AGG GGG CAG ATG TGA TCG AC | *sulII* (+) | 18 |
| SUL2-B | TGT GCG GAT GAA GTC AGC TCC | *sulII* (–) | 18 |
| TMP-F | TGG GTA AGA CAC TCG TCA TGG G | *dfr18* (+) | 18 |
| TMP-B | ACT GCC GTT TTC GAT AAT GTG G | *dfr18* (–) | 18 |
| DFR1-F | CGA AGA ATG GAG TTA TCG GG | *dfrA1* (+) | This study |
| DFR1-B | TGC TGG GGA TTT CAG GAA AG | *dfrA1* (–) | This study |
| TMP3 | CAT GCT GTT TCT CGA CGG TG | *npB* (+) | 18 |
| TMP4 | GAT CCG ATC TGT TTG TTC AG | *sO13* (–) | 18 |
| YL6 | TGT GGA ACG GCT TTC TGA CG | *sO73* (+) | 18 |
| YL3 | CGT TGG TTT GGG GTA ACA CC | *orfC5A* (+) | 18 |
| traF-R | GGG GTT CTC ATT GTC AGC TC | *traF* (–) | This study |
| EXO-F | AGC GGA TCG TTC TCG AAT CC | *orf1* (+) | This study |
| EXO-R | CAC ATG TGG TTT ACA TGG CG | *orf1* (–) | This study |

[a] +, oligonucleotides corresponding to the coding strand (forward primer);
–, oligonucleotides corresponding to the noncoding strand (backward primer).

*DNA sequencing.*

Amplified DNA was purified with a GFX column (Amersham Pharmacia, Little Chalfont, United Kingdom) before sequencing, and the nucleotide sequence was determined by cycle sequencing with a Big Dye Terminator Cycle Sequencing FS Ready Reaction kit and analyzed with an ABI PRISM 310 Genetic Analyzer or 3730 DNA Analyzer (Applied Biosystems, Foster City, Calif.). The identities of the determined sequences were analyzed by comparison with the gene sequences in databases using BLAST software (16).

*Conjugation.*

The ampicillin-resistant *V. cholerae* O34 strain 88UDT119/pGV3 (17) was used as the recipient in

conjugation experiments with SXT constin positive strains, and the chloramphenicol-resistant *V. cholerae* O34 strain AM15 was used as the recipient in conjugation experiments with class I integron-positive strains. After mating on nonselective Luria-Bertani agar incubated at 37°C for 16 h, exconjugants were harvested, and appropriate dilutions of the harvest were spread on Luria-Bertani agar containing 100 $\mu$g of ampicillin/ml and 32 $\mu$g of trimethoprim/ml to investigate SXT conjugation, and on Luria-Bertani agar containing 5 $\mu$g of chloramphenicol/ml and 20 $\mu$g of streptomycin/ml to investigate the presence of a conjugative plasmid carrying the integron. Exconjugants were analyzed by PCR to exclude possible spontaneous antibiotic-resistant mutants.

*Cloning of $SXT^{LAOS}$-specific fragment.*

The region between *sO73* and *traF* of *V. cholerae* Lao strains was amplified by PCR using the primers YL6 and traF-R and DNA from *V. cholerae* O1 strain 00LA1 as the template. The 5-kbp PCR product was cloned into the pCR 2.1 vector, and the nucleotide sequence of the inserted PCR product was determined by primer walking.

## Results

*Drug susceptibility of V. cholerae O1 in Lao PDR and in Vietnam.*

In Laos, we have continuously monitored cholera epidemic and drug resistant *V. cholerae* since 1993. Before 1997, almost all epidemic strains were susceptible to all drugs examined except streptomycin. But we did not pay attention to this resistance, because streptomycin is not used for the treatment of cholera. There was no cholera case in 1997 in Laos, and when cholera epidemic came again in 1998, almost all isolates were resistant to tetracycline, chloramphenicol, sulfamethoxazol-trimethoprim, and streptomycin. Epidemic due to these resistant strains repeated in 1999 and 2000 (Table 2). However in Laos, there has been no cholera since 2001 to date. In Vietnam, all human isolates in 1995 had a good sensitivity to all drugs examined except streptomycin. The epidemic due to drug resistant *V. cholerae* were seen in 2000 and 2001. The organisms were moderately resistant to TC and CP, and highly resistant to co-trimoxazol as seen in Laos. However, in 2002 and 2003, all epidemic isolates suddenly became well sensitive to all drugs including streptomycin (Table 3). The antibiogram of the organisms in Laos and Vietnam were essentially the same.

Environmental *V. cholerae* non-O1 were examined in 2005 in Laos and Vietnam. Drug susceptibility of these organisms was so variable. Majority of the environmental isolates (34/43) were highly resistant to sulfamethoxazol-trimethoprim. By contrast, only 2 of 43 were moderately resdistant to tetracycline.

*Distribution of class I integron and SXT constin.*

The strains isolated in the Lao PDR can be divided into four groups according to the antibiograms and

**Table 2.** Drug susceptibility of epidemic *V. cholerae* O1 in Lao PDR

| Drugs | MICs of each drug ($\mu$g/ml) | |
|---|---|---|
| | 1993 ~ 1996 | 1998 ~ 2000 |
| Tetracycline | 0.4 ~ 0.8 | 3.13 ~ 6.25 |
| Chloramphenicol | 0.8 ~ 1.6 | 6.25 ~ 12.5 |
| Ampicillin | 3.13 ~ 6.25 | 3.13 ~ 12.5 |
| Erythromycin | 3.13 ~ 6.25 | 3.13 ~ 6.25 |
| Nalidixic acid | 0.2 ~ 0.4 | 0.2 ~ 0.4 |
| Ofloxacin | 0.025 > | 0.025 > |
| Co-trimoxazol | 2.5 ~ 20 | 640 < |
| Streptomycin | 25 ~ 100 | 25 ~ 100 |

**Table 3.** Drug susceptibility of epidemic *V. cholerae* O1 in Vietnam

| Drugs | MICs of each drug ($\mu$g/ml) | | |
|---|---|---|---|
| | 1995 | 2000&2001 | 2002 |
| Tetracycline | 0.4 ~ 0.8 | 3.13 ~ 6.25 | 0.2 ~ 0.4 |
| Chloramphenicol | 0.8 ~ 1.6 | 6.25 ~ 12.5 | 0.8 ~ 1.6 |
| Ampicillin | 3.13 ~ 6.25 | 3.13 ~ 12.5 | 3.13 ~ 6.25 |
| Erythromycin | 3.13 ~ 6.25 | 6.25 ~ 12.5 | 3.13 ~ 6.25 |
| Nalidixic acid | 0.1 ~ 0.2 | 0.2 ~ 0.8 | 0.2 ~ 0.4 |
| Ofloxacin | 0.025 > | 0.025 > | 0.025 > |
| Co-trimoxazol | 2.5 ~ 20 | 640 < | 2.5 ~ 10 |
| Streptomycin | 25 ~ 100 | 25 ~ 100 | 6.25 ~ 12.5 |

**Table 4.** Characteristics of *V. cholerae* (Lao strains)

| Group | No. of isolates | Yr of isolation | Antibiogram[a] | 5'-CS | *aadA1* | *intSXT* |
|---|---|---|---|---|---|---|
| A | 24 | 1993-1996 | SM | + | + | − |
| B | 2 | 1993-1996 | | − | − | − |
| C | 20 | 1998-2000 | SM, CP, TC, S-T | − | − | + |
| D | 4 | 1998-2000 | | − | − | + |

[a] SM, streptomycin; CP, chloramphenicol; TC, tetracycline; S-T, trimethoprim-sulfamethoxazole.

Note: No cholera in 1997, 2001 and thereafter.

year of isolation (Table 4). Group A comprises 24 strains isolated between 1993 and 1996 that were streptomycin resistant. Group B comprises two strains isolated in 1995 that were susceptible to all the antibiotics tested. Group C comprises 20 strains isolated between 1998 and 2000 that were resistant to streptomycin, chloramphenicol, tetracycline, and trimethoprim-sulfamethoxazole. Group D comprises four strains isolated between 1998 and 2000 that were susceptible to all of the antibiotics tested.

PCR with the primers inDS-F and inDS-B yielded a PCR product of ~800 bp from each of the 24 streptomycin-resistant strains belonging to group A. Strains belonging to groups B, C, and D did not yield an amplicon with these primers, indicating that class I integrons were not present. A PCR product of ~1,000 bp was obtained from each of the 24 class I integron-positive strains using the in-F and in-B primers. DNA sequencing of the 1,000-bp amplicons from three isolates confirmed the presence of the gene cassette *aadA1*, which conferred resistance to streptomycin on the host bacteria. PCR with the in-F and aadA-B primers yielded an ~750-bp amplicon from all isolates that yielded a product with the in-F and in-B primers. Streptomycin resistance encoded by the class I integron could not be transferred by conjugation, indicating that the class I integron was not carried in a conjugative plasmid. PCR for detection of *intSXT* showed that all strains belonging to groups C and D yielded a 592-bp amplicon of a size identical to those of the positive controls *V. cholerae* O139 strain MO45 and *V. cholerae* O1 strain CRC182.

*Analysis of SXT constin in group C V. cholerae.*

Conjugation experiments showed that *intsxt* was transferable by conjugation. Antimicrobial susceptibility testing of the *V. cholerae* transconjugants showed that the resistance genes contained in the SXT element were transferred and expressed in each of the transconjugants (Table 5). PCR assays designed to detect the genes that encode resistance to chloramphenicol (*floR*), streptomycin (*strA* and *strB*), sulfamethoxazole (*sulII*), and tetracycline (*tetA*) yielded the expected PCR products of 526 (*floR*), 383 (*strA*), 459 (*strB*), 625 (*sulII*), and 950 (*tetA*) bp for each of the 20 strains of group C

**Table 5.** MICs of various antibiotics and PCR results for *V. cholerae* strains used in conjugation experiments and obtained transconjugants

| Description | Strain | MIC ($\mu$g/ml) | | | | | PCR | |
|---|---|---|---|---|---|---|---|---|
| | | ABPC | CP | SM | S-T | TC | *int*SXT | *tetA* |
| Donor | 99LA79 | 3.13 | 12.5 | 100 | 640 | 3.13 | + | + |
| Donor | 00LA1 | 3.13 | 12.5 | 100 | 640 | 6.25 | + | + |
| Recipient | 119/pGV3 | 100 | 0.8 | 6.25 | 5 | 0.4 | − | − |
| Transconjugant | TC79-8 | 100 | 6.25 | 100 | 640 | 3.13 | + | + |
| Transconjugant | TC002 | 100 | 6.25 | 100 | 640 | 3.13 | + | + |

ABPC, ampicillin ; CP, chloramphenicol ; SM, streptomycin; S-T, trimethoprim-sulfamethoxazole; TC, tetracycline.
+, present; −, absent.
Transconjugant TC79-8; obtained by mating strains 99LA79 and 88UDT119/pGV3.
Transconjugant TC002; obtained by mating strains 00LA1 and 88UDT119/pGV3.

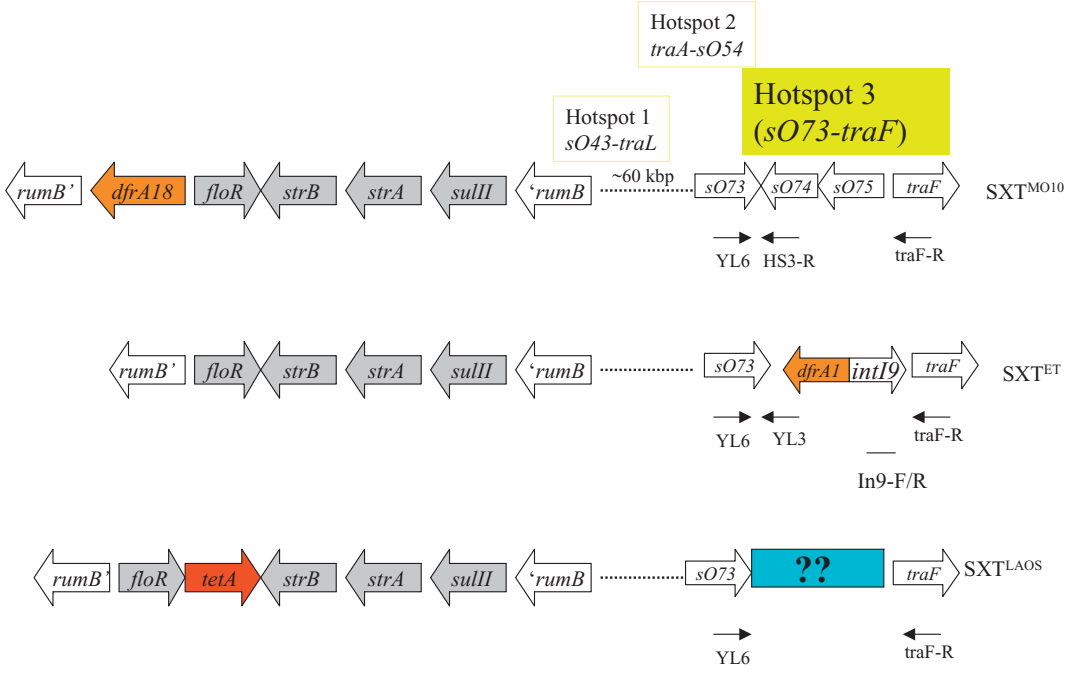


**Fig. 1.** Schema of SXT constins. Only antibiotic resistant genes and some adjacent *orfs* are presented. Primers used in PCR analysis to investigate the insertion sequence between *sO73-traF* are indicated.

in Table 4, while strains in group D failed to react. As *tetA* was also transferable by conjugation, we investigated the location of *tetA* within the SXT constin. In PCR analysis, an amplicon of ~2.3 kbp was obtained with TetA-F and strB-R, and an amplicon of ~3.0 kbp was obtained with TetA-F and STRA-F (Figure 1, $SXT^{LAOS}$). The presence of *tetA* upstream of *strB* was also confirmed by nucleotide sequence analysis of the 2.3-kbp amplicon obtained with primers TetA-F and strB-R.

*Analysis of SXT constin in group D V. cholerae.*

PCR assays utilizing the primers LEND4 and RUMA, which flank the antibiotic resistance genes in SXTMO10, yielded a product of ~3.3 kbp for each of

the four strains in group D in Table 4. Partial sequencing of these products revealed that there was a deletion of the antibiotic resistance genes as previously reported for *V. cholerae* O139 strain 2055 by Hochhut et al. (18).

*$SXT^{LAOS}$ is different from previously reported SXTs.*

All strains in group C in Table 4 failed to give an amplicon with primers designed to detect *dfr18* and *dfrA1*, which are the trimethoprim resistance determinants reported for $SXT^{MO10}$ and $SXT^{ET}$, respectively (18). PCR with primers TMP3 and TMP4, which anneal to sequences that flank *dfr18* in $SXT^{MO10}$, gave a PCR product of 1.3 kbp. These primers give a PCR product of 5.35 kbp with *V. cholerae* O139 DNA as a template (18). The results revealed that a 3.34-kbp fragment which included *dfr18* is missing in $SXT^{LAOS}$ as in $SXT^{ET}$. However, $SXT^{LAOS}$ is distinct from $SXT^{ET}$ in that no PCR product was obtained with primers YL6 and YL3. To further characterize $SXT^{LAOS}$, PCR with primers YL6 and traF-R was performed. An amplicon of ~5 kbp was obtained for $SXT^{LAOS}$, as well as $SXT^{MO10}$ and $SXT^{ET}$. Nucleotide sequencing of this fragment from $SXT^{LAOS}$ revealed the presence of two novel open reading frames (ORFs) (*orf1*, 1,875 bp, and *orf2*, 1,605 bp) (Table 6). The deduced amino acid sequence of ORF1 had 36% identity and 54% similarity to that of an exonuclease (encoded by *sO24*) found in the genomic island associated with the multidrug resistance region of *Salmonella enterica* serovar Typhimurium DT104 (19), while the deduced amino acid sequence of ORF2 had 26% identity and 45% similarity to that of a helicase (encoded by *sO23*) found downstream of the exonuclease in the same genomic island (18). PCR analysis with primers EXO-F and EXO-R showed that only $SXT^{LAOS}$ gave the expected amplicon of 890 bp.

*Class I integron and SXT constin in the environmental isolates.*

Among 43 strains examined, Class I integron was found in one and SXT constin in 5. A strain with Class I integron revealed resistance to many antibiotics but not to streptomycin. SXT constin carrying 5 strains showed different patterns of drug susceptibility. The three isolates showed resistance only to sulfamethoxazol-trimethoprim, one was resisrtant to chloramphenicol, sulfamethoxazol-trimethoprim and streptomycine, and another was resistant to tetracycline, chloramphenicol, nalidixic acid, sulfamethoxazol-trimethoprim and streptomycin. Class I integron positive strain was resistant to many antibiotics but not to streptomycin, so different from human isolates. Thus, a variety of antibiograms were observed in the environmental isolates.

## Discussion

We have studied the drug susceptibility and the genetic determinants of drug resistance in *V. cholerae* strains isolated in the Lao PDR and in Vietnam. In the Lao PDR, *V. cholerae* in cholera epidemic has been collected every year between 1993 and 2000. While in Vietnam, the strains were collected in 1995 and every year between 2000 and 2004 .

Strains isolated before 1997 (a year without cholera) in the Lao PDR were clearly different from those isolated after 1997. A class I integron with an *aadA1* gene cassette was present in pre-1997 strains, while an SXT constin was present in the reemerged (post-1997) El Tor O1 strains. Recently, Amita et al. (19) have reported that a class I integron with an *aadA1* gene cassette was widely distributed among the pre-1992 O139 O1 strains isolated in India. In contrast, most of the

**Table 6.** Analysis of novel ORFs in hotspot-3 of $SXT^{LAOS}$

| Gene | Length (bp) | Closest similarity to | Similarity % |
|---|---|---|---|
| orf1 | 1875 | *sO24* exonuclease * | 54% |
| orf2 | 1605 | *sO23* helicase* | 45% |

**sO24* and *sO23* genes located in the genomic island associated with multidrug resistance region of *Salmonella enterica* Typhimurium DT104.

post-1992 O139 O1 strains contained the SXT constin and were devoid of the class I integron. Although *V. cholerae* O139 has not been isolated in the Lao PDR, it seems that strains isolated in the Lao PDR after 1997 are similar to Indian post-1992 O139 O1 strains, as they showed resistance to trimethoprim-sulfamethoxazole, chloramphenicol, and streptomycin, the resistance genes of which are encoded in an SXT constin. However, strains from Laos are tetracycline resistant, in constrast to Indian strains which were susceptible to this antibiotic (19). *V. cholerae* O1 strains isolated in Mozambique and South Africa in 1998 were also reported to be tetracycline-resistant (20). Tetracycline resistance in African strains, as well as Laotian strains, is encoded by *tetA*. In Laotian strains, as well as *V. cholerae* strain V21 isolated in Vietnam, *tetA* is located within the SXT element. PCR analysis of the SXT constin showed that $SXT^{LAOS}$ is different from the $SXT^{MO10}$ and $SXT^{ET}$ reported previously. Comparison of two conjugative integrating elements, SXT of *V. cholerae* and R391 of *Providencia rettgeri* (21), revealed that the conserved backbone apparently contains three hot spots for insertion of additional DNA sequences, the first between *sO43* and *traL*, the second between *traA* and *sO54*, and the third between *sO73* and *traF*. $SXT^{ET}$ contains a class 9 integron in hot spot *sO73-traF* that harbors *dfrA1* as a gene cassette (14). We first hypothesized that this integron structure has a different gene cassette in $SXT^{LAOS}$; however, PCR of integrase IntI9 (14) failed to produce a reaction (data not shown). The nucleotide sequence of this hot-spot region of $SXT^{LAOS}$ revealed the presence of two ORFs possibly involved in conjugal transfer (19). A trimethoprim resistance determinant was not found in this region, and we therefore could not identify the gene responsible for trimethoprim resistance. Trimethoprim resistance was also transferred by conjugation, and we hypothesized that the responsible gene is located within $SXT^{LAOS}$, as in previously reported SXTs. However, the possibility that the trimethoprim resistance determinant is located on the chromosome outside the SXT constin and cotransfers with the SXT constin in an Hfr-like manner cannot be ruled out (22).

Gene compositions of Vietnam strains were essentially the same with Laotian strains. Pre-1997 strains of Lao-isolates corresponded to Vietnam isolates in 1995. Post-1997 Laotian isolates corresponded to Vietnam isolates in 2000 and 2001.

A rapidly changing antibiotic resistance pattern was also observed among *V. cholerae* O139 strains (23, 24; R. Mitra, A. Basu, D. Dutta, G. B. Nair, and Y. Takeda, Letter, Lancet **348**:1181, 1996). *V. cholerae* O139 strains are becoming increasingly resistant to nalidixic acid but are susceptible to trimethoprim- sulfamethoxazole and streptomycin. Our results suggested that variation within sequences inserted in the hot spots and the antibiotic resistance gene cluster might occur in *V. cholerae* strains, allowing rapid adaptation to changing environment. SXT constins are present in virtually all recent clinical *V. cholerae* isolates from Asia, and SXT variants are arising in a manner similar to the *Salmonella* genomic island 1 multidrug resistance regions from serovars Typhimurium DT104 and Agona (25). The presence of IntSXT-positive, antimicrobial-susceptible strains should also be carefully monitored, since "empty SXT constins" (group D) are capable of inserting not only antibiotic resistance genes but also other virulence factors which could be easily transferred to other strains by conjugation.

Distribution of environmental *V. cholerae* O1 must be a key to predict cholera epidemic in the near future. Although in this study period, we tried to isolate *V. cholerae* O1 for a few days in August and failed to isolate the organism in spite of an intensive work. However, many strains of the same species *V. cholerae* non-O1 were isolated from the environment, so, they were analyzed. It was revealed that some strains of *V. cholerae* in the environment carry Class I integron or SXT element with drug resistance genes. A variety of antibiograms in the environmental vibrios suggested a frequent exchange of the drug resistance genes. Environmental *V. cholerae* O1 should cause cholera epidemic, so which category of the organisms plays an important role in the epidemic is to be clarified. Therefore the study on the environmental *V. cholerae* just before the epidemic is important, and continuous study through the whole year is required.

## References


(1) Mhalu FS, Mmari PW and Ijumba J. Rapid emergence of El Tor *Vibrio cholerae* resistant to antimicrobial agents during the first six months of fourth cholera epidemic in Tanzania. Lancet 1979; **i**: 345−347.

(2) Glass RI, Huq I, Alim ARMA and Yunus M. Emergence of multiply antibiotic-resistant *Vibrio cholerae* in Bangladesh. J Infect Dis 1980; **142**: 939−942.

(3) Lindenbaum, JW, Greenough B and Islam MR. Antibiotic therapy of cholera. Bull WHO 1967; **36**: 871−878

(4) Dalsgaard A, Forslund A, Serichantalergs O and Sandvang D. Distribution and content of class 1 integrons in different *Vibrio cholerae* O-serotype strains isolated in Thailand. Antimicrob Agents Chemother 2000; **34**: 642−650.

(5) Dalsgaard A, Forslund A, Petersen A, *et al*. Class 1 integron-borne, multiple-antibiotic resistance encoded by a 150-kilobase conjugative plasmid in epidemic *Vibrio cholerae* O1 strains isolated in Guinea-Bissau. J Clin Microbiol 2000; **38**: 3774 −3779.

(6) Dalsgaard A, Forslund A, Sandvang D, Arntzen L and Keddy K. *Vibrio cholerae* O1 outbreak in Mozambique and South Africa in 1998 are multiple-drug resistant, contain the SXT element and the *aadA2* gene located on class 1 integrons. J Antimicrob Chemother 2001; **48**: 827−838.

(7) Phantouamath B, Sithivong N, Sisavath L, *et al*. Transition of drug susceptibilities of *Vibrio cholerae* O1 in Lao People's Democratic Republic. Southeast Asian J Trop Med Public Health 2001; **32**: 95−99.

(8) Hochhut B, Lotfi Y, Mazel D, Faruque SM, Woodgate R and Waldor MK. Molecular analysis of antibiotic resistance gene clusters in *Vibrio cholerae* O139 and O1 SXT constins. Antimicrob Agents Chemother 2001; **45**: 2991−3000.

(9) Dalsgaard A, Forslund A, Tam NV, Vinh DX and Cam PD. Cholera in Vietnam: changes in genotypes and emergence of class I integrons containing aminoglycoside resistance gene cassettes in *Vibrio cholerae* O1 strains isolated from 1979 to 1996. J Clin Microbiol 1999; **37**: 734−741.

(10) Nguyen BM, Higa N, Kakinohana S and Iwanaga M. Characterization of *Vibrio cholerae* O1 isolated in Vietnam. Jpn J Trop Med Hyg 2002; **30**: 103−107.

(11) Spira WM and Ahmed QS. Gauze filtration and enrichment procedures for recovery of *Vibrio cholerae* from contaminated waters. Appl Environ Microbiol 1981; **42**: 730−733.

(12) Barrett J, Timothy B, Paul A, Morris KG, Puhr DN, Bradford BH and Wells GJ. Use of Moore swabs for isolating *Vibrio cholerae* from sewage. J Clin Miclobiol 1980; **11**: 385−388.

(13) Toma C, Lu Y, Higa N, Nakasone N, Chinen I, Baschkier A, Rivas M and Iwanaga M. Multiplex PCR for identification of human diarrheagenic *Escherichia coli*. J Clin Microbiol 2003; **41**: 2669−2671.

(14) Hochhut B, Lotfi Y, Mazel D, Faruque SM, Woodgate R and Waldor MK. Molecular analysis of antibiotic resistance gene clusters in *Vibrio cholerae* O139 and O1 SXT constins. Antimicrob Agents Chemother 2001; **45**: 2991−3000.

(15) Schmidt AS, Bruun MS, Dalsgaard I and Larsen JL. Incidence, distribution, and spread of tetracycline resistance determinants and integron-associated antibiotic resistance genes among motile aeromonads from a fish farming environment. Appl Environ Microbiol 2001; **67**: 5675−5682.

(16) Altschul SF, Madden TL, Schaffer AA, Zhang J, Zhang Z, Miller W and Lipman DJ. Gapped BLAST and PSI-BLAST: a new generation of protein database search programs. Nucleic Acids Res 1997; **25**: 3389−3402.

(17) Toma C, Kuroki H, Nakasone N, Ehara M and Iwanaga M. Minor pilin subunits are conserved in *Vibrio cholerae* type IV pili. FEMS Immunol Med Microbiol 2002; **33**: 35−40.

(18) Boyd D, Peters GA, Cloeckaert A, Boumedine KS, Chaslus-Dancla E, Imberechts H and Mulvey MR. Complete nucleotide sequence of a 43-kilobase genomic island associated with the multidrug resistance region of *Salmonella enterica* se-

rovar Typhimurium DT104 and its identification in phage type DT120 and serovar Agona. J Bacteriol 2001; **183**: 5725−5732.
(19) Amita S, Chowdhury R, Thungapathra M, Ramamurthy T, Nair GB and Ghosh A. Class I integrons and SXT elements in El Tor strains isolated before and after 1992 *Vibrio cholerae* O139 outbreak, Calcutta, India. Emerg Infect Dis 2003; **9**: 500−502.
(20) Dalsgaard A, Forslund A, Sandvang D, Arntzen L and Keddy K. *Vibrio cholerae* O1 outbreak isolates in Mozambique and South Africa in 1998 are multiple-drug resistant, contain the SXT element and the *aadA2* gene located on class 1 integrons. J Antimicrob Chemother 2001; **48**: 827−838.
(21) Beaber JW, Burrus V, Hochhut B and Waldor MK. Comparison of SXT and R391, two conjugative integrating elements: definition of a genetic backbone for the mobilization of resistance determinants. Cell Mol Life Sci 2002; **59**: 2065−2070.
(22) Hochhut B, Marrero J and Waldor MK. Mobilization of plasmids and chromosomal DNA mediated by the SXT element, a constin found in *Vibrio cholerae* O139. J Bacteriol 2000; **182**: 2043−2047.
(23) Faruque SM, Siddique AK, Saha MN, Asadulghani M, Rahman M, Zaman K, Albert MJ, Sack DA and Sack RB. Molecular characterization of a new ribotype of *Vibrio cholerae* O139 Bengal associated with an outbreak of cholera in Bangladesh. J Clin Microbiol 1999; **37**: 1313−1318.
(24) Mukhopadhyay AK, Basu A, Garg P, Bag PK, Gosh A, Bhattacharya SK, Takeda Y and Nair GB. Molecular epidemiology of reemergent *Vibrio cholerae* O139 Bengal in India. J Clin Microbiol 1998; **36**: 2149−2152.
(25) Boyd D, Cloeckaert A, Chaslus-Dancla E and Mulvey MR. Characterization of variant *Salmonella* genomic island 1 multidrug resistance regions from serovars Typhimurium DT104 and Agona. Antimicrob Agents Chemother 2002; **46**: 1714−1722.

# Development of Novel Approach for Treatment of Infectious Diseases Targeting Bacterial Cell-to-Cell Signaling: Focusing on an Opportunistic Pathogen *Pseudomonas aeruginosa*

**Keizo Yamaguchi**

*Department of Microbiology and Infectious Diseases, Toho University School of Medicine, Ohmorinishi, Ohta-ku, Tokyo 143-8540, Japan*

## Introduction

*Pseudomonas aeruginosa* is an opportunistic pathogen that causes a wide range of acute and chronic infections, including sepsis, wound and pulmonary infections [1]. In particular, this organism is a major cause of pulmonary damage and mortality in patients with cystic fibrosis (CF), diffuse panbronchiolitis (DPB) and other forms of bronchiectasis [2, 3]. Colonization of the respiratory tract with *P. aeruginosa* leads to an exuberant inflammatory response in the airways, characterized with large numbers of neutrophils [4]. Although the mechanisms by which the organism evades neutrophils-defenses are unclear, *P. aeruginosa* persists in the tissues, resulting in chronic colonization and infection of the lungs of these patients. Despite treatment with potent antibiotics, infection of these patients' lungs by *P. aeruginosa* typically leads to death by respiratory failure or other complications.

This organism is known to produce a variety of virulence factors, such as pigment, proteases and exotoxins. The synthesis of these factors is regulated by a cell-to-cell signaling mechanism referred to quorum sensing [5], which was originally described in *Vibrio fischeri* as a LuxR/LuxI-type system [6]. *Las* and *Rhl* are known to be two major quorum-sensing components in *P. aeruginosa*, and this mechanism enables bacteria to coordinately turn on and off genes in a density-dependent manner by the production of small diffusible molecules called autoinducers. *P. aeruginosa* predominantly produces two autoinducers, *N*-3-oxododecanoyl homoserine lactone (3-oxo-$C_{12}$-HSL) and *N*-butyryl-L-homoserine lactone ($C_4$-HSL) [7, 8]. The expression of these autoinducer-regulated virulence factors directly contributes to the colonization and dissemination of the bacteria, which may determines the course and outcome of the disease of the individuals infected with *P. aeruginosa*.

A break-through of antibiotic chemotherapy for patients with chronic *P. aeruginosa* pulmonary infection was brought by a case with DPB. This patient happened to be treated with erythromycin over years, and Dr. Shoji Kudoh noticed dramatic improvement of the patient, including clinical symptoms, respiratory function and chest X-ray findings. After that, Kudoh and associates conducted an open trial study and reported for the first time clinical efficacy of long-term erythromycin therapy in DPB patients [9, 10]. The recent progress in the clinical trial data demonstrated successful extension of application of the long-term macrolide therapy, not only to DPB patients, but also to other types of chronic respiratory infection, such as chronic sinusitis, bronchiectasis and CF. In contrast to accumulating clinical evidence of macrolide efficacy, mechanisms of its action are still unknown, although many investigators are working on two major research directions, effects of macrolide on host inflammatory and immune systems or on bacterial virulence factors. Recently we have reported that azithromycin, a

15-membered macrolide, suppresses quorum-sensing systems of *P. aeruginosa* at sub-MIC, without affecting growth of the bacteria [11].

In this project, we examined potential of several strategies to inhibit bacterial quorum-sensing systems as a novel therapeutic approach for treatment of infectious diseases. Especially, effects of sub-MIC macrolides on quorum-sensing of *P. aeruginosa* were of our great interest, and some promising data were obtained. Additionally, search for autoinducer analogues as a quorum-sensing inhibitor, vaccine strategy against 3-oxo-$C_{12}$-HSL, in addition to interspecies communication and interference by *P. aeruginosa* autoinducer, were explored.

## 1. Quorum-sensing systems and *P. aeruginosa* infection

Quorum sensing is an important mechanism for the regulation of genes in many Gram-negative and Gram-positive bacteria. *P. aeruginosa* quorum-sensing systems consist of two separate but interrelated systems, *las* and *rhl* [12, 13]. As the bacterial population increases, the autoinducer signal molecules produced by *P. aeruginosa*, 3-oxo-$C_{12}$-HSL and $C_4$-HSL, accumulate, and as soon as they reach intracellular threshold concentrations, these molecules bind to and activate their cognate transcriptional regulators (Figure 1). Both systems have been found to regulate the production and expression of multiple virulence factors, such as extracellular toxins (e.g. elastase, alkaline protease, exotoxin A), rhamnolipid and pyocyanin. In addition, Glessner and associates have reported that the *las* and *rhl* quorum-sensing systems are required for pilus-dependent twitching motility and the ability of *P. aeruginosa* to adhere to human bronchial epithelial cells is also found to be dependent on the *rhl* system [14]. To investigate the effects of quorum-sensing systems during infections, strains of *P. aeruginosa* that contain deletions in one or more of the quorum-sensing genes were tested in various infection models. These include a burnt-mouse model, a murine model of acute pneumonia and a rat model of chronic lung infection [15-18]. General observation obtained from these models is that strains containing a mutation in quorum-sensing genes were found to be less virulent compared with wild-type *P. aeruginosa*. Another interesting aspect in quorum-sensing research is contribution and association of this system in biofilm formation. Accumulating data demonstrate that quorum-sensing systems are essential for differentiation and maturation of biofilm in *P. aeruginosa* infection [19-23].

There is increasing evidence that quorum-sensing is functionally active during *P. aeruginosa* infections in humans. Sputum samples from CF patients chronically colonized with *P. aeruginosa* contain mRNA transcripts of the quorum-sensing genes [24]. The production of autoinducer molecules *in vivo* was corrobo-

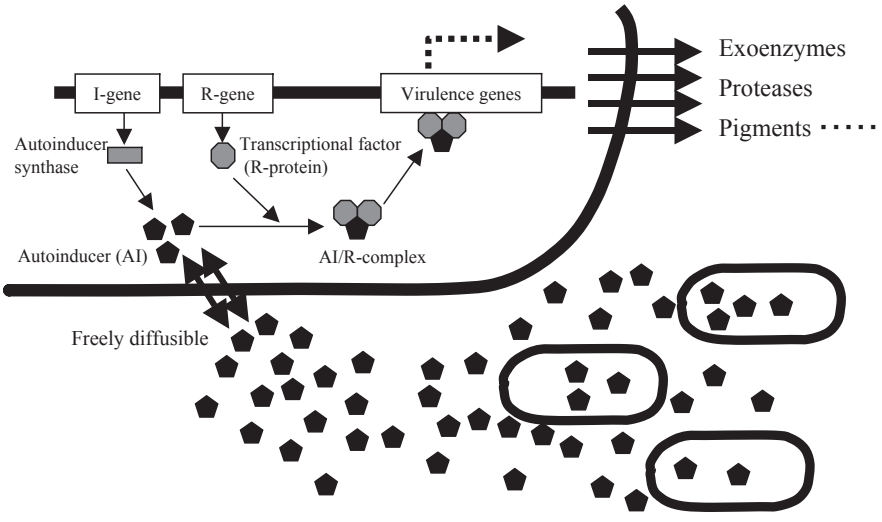


**Fig. 1.** Schema of quorum-sensing systems in *P. aeruginosa*.

rated in a human disease setting by studies that sputum from *P. aeruginosa*-colonized CF patients was able to produce both 3-oxo-$C_{12}$-HSL and $C_4$-HSL [19]. Subsequently, the autoinducer molecules were directly extracted from the sputum of CF patients colonized with *P. aeruginosa* [25]. These samples contained approximately 20 nM 3-oxo-$C_{12}$-HSL and 5 nM $C_4$-HSL. In contrast, in experiments where bacteria were grown in a biofilm, concentrations of 300-600 $\mu$M 3-oxo-$C_{12}$-HSL were measured in association with the bacteria [26]. Although it is difficult to define exact concentrations of autoinducer molecules at the site of infection, particularly in biofilm, these results demonstrate that quorum-sensing systems are active during *P. aeruginosa* infection and it potentially regulates the expression of various genes *in vivo*.

Advances in researches in the past several years have demonstrated that the quorum sensing signal molecule 3-oxo-$C_{12}$-HSL is also a potent stimulator of multiple eukaryotic cells and thus may alter the host responses to *P. aeruginosa* infection. In vitro experiments have shown that 3-oxo-$C_{12}$-HSL stimulates the production of the inflammatory cytokine IL-8 from human lung bronchial epithelial cells [27, 28]. It was subsequently demonstrated that 3-oxo-$C_{12}$-HSL could stimulate a broad-spectrum of responses *in vivo* by inducing several inflammatory cytokines and chemokines [17]. It has also been shown that 3-oxo-$C_{12}$-HSL can inhibit the production of IL-12 and TNF-$\alpha$ from LPS-activated mouse peritoneal exudate cells or human peripheral blood mononuclear cells [29, 30]. These data demonstrate that, under certain conditions, 3-oxo-$C_{12}$-HSL also acts as an immunosuppressor. More recently, we have reported that 3-oxo-$C_{12}$-HSL at a concentration of 12 $\mu$M induces apoptosis in certain types of cells, such as macrophages and neutrophils, but not in epithelial cells [31]. Taken together, these data suggest that the quorum-sensing molecules have a critical role in the pathogenesis of *P. aeruginosa* infection, not only in the induction of bacterial virulence factors but also in the modulation of host responses. Precise mechanisms in bacterial quorum-sensing systems and their regulation have been reviewed elsewhere [32-35].

## 2. Potential of macrolides as a quorum-sensing inhibitor

There are two broad strategies for the control of bacterial infection: either to kill the organisms, or to attenuate their virulence by making the organisms fail to adapt to the host environment thus resulting in clearance of the organisms by the innate defenses of the host. The discovery that gram-negative bacteria employ HSL autoinducer molecules to regulate globally the production of virulence determinants offers a novel target. The ability to interfere with bacterial virulence by jamming signal generation or signal transduction in the quorum-sensing is intellectually attractive and pharmaceutically appealing, and may be clinically timely. These strategies may include chemical antagonists and specific antibody to inhibit the autoinducers, HSL-destroying enzyme lactonase, and suppression of quorum-sensing by interfering with the associated genes and their products. Several investigators have reported potential of HSL-analogues [36, 37] and synthetic derivatives of natural furanone in inhibition of bacterial quorum-sensing systems [38].

To find a quorum-sensing inhibitor, clinical and experimental data described above provided a hint that certain macrolides and their analogues may be a candidate as *Pseudomonas* quorum-sensing inhibitors. Particularly, it became more realistic after we knew that long-term azithromycin therapy is effective to chronic *P. aeruginosa* pulmonary infection, irrespective of underlying disease, DPB or CF. These facts prompted us to examine whether clinically achievable concentrations of macrolides affect the quorum-sensing systems in *P. aeruginosa*. Previously we have reported that 2 $\mu$g/ml of azithromycin suppressed transcription of *lasI* by 80% and *rhlI* by 50% in *P. aeruginosa* PAO1 [11]. Well correlated to these data, the production of 3-oxo-$C_{12}$-HSL and $C_4$-HSL was inhibited to approximately 6% and 28% of the control, respectively. In contrast, azithromycin treatment did not affect expression of the *xcpR* gene, which codes for a structural protein belonging to the type II secretion pathway. These data suggested that the effects of azithromycin on *P. aeruginosa* may be selective, but not nonspecific. In complementary study, the addition of exogenous autoinducers

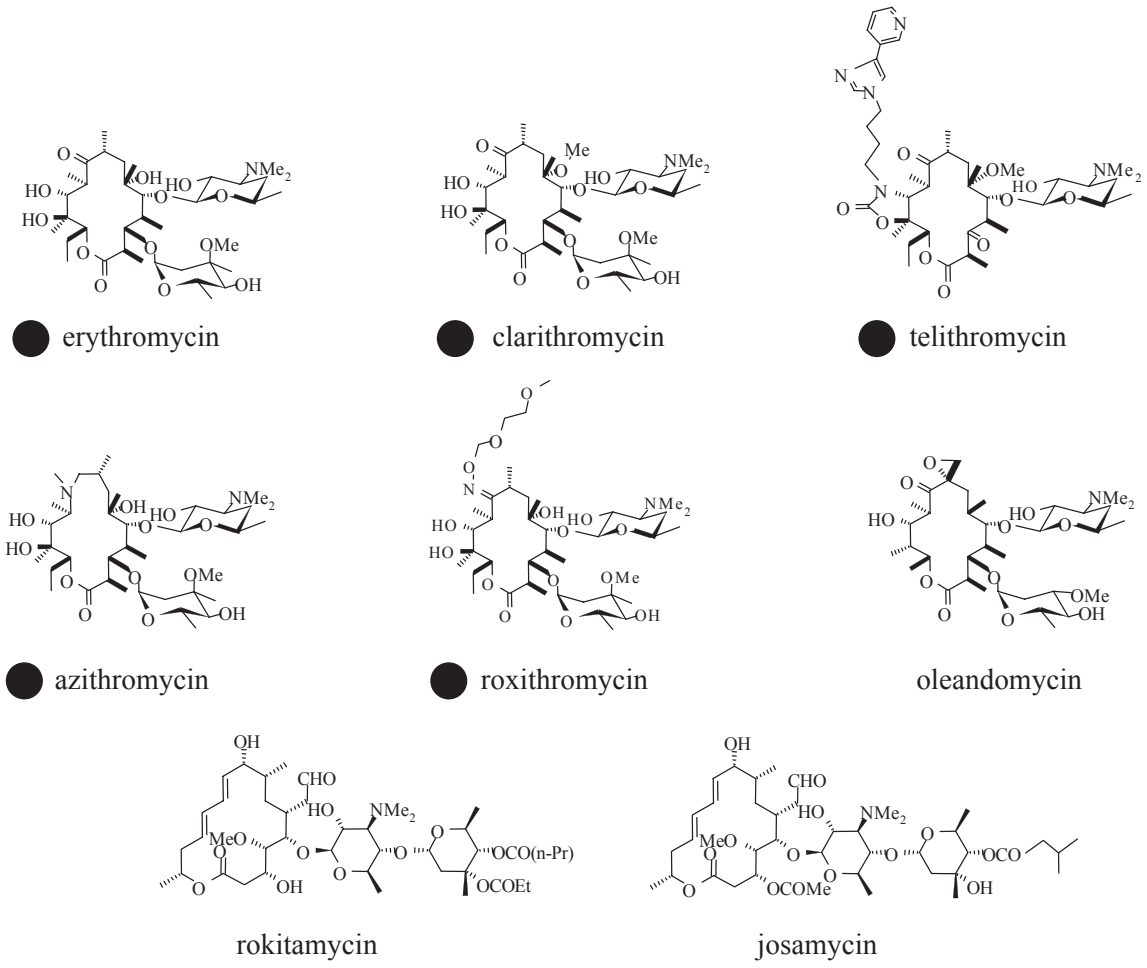


**Fig. 2.** Structures of macrolide antibiotics and their effects on quorum-sensing systems of *P. aeruginosa*.
● positive for quorum-sensing suppressive activity.

restored the expression of transcriptional regulator *lasR* and *rhlR*, which were associated with restoration of virulence factor expression. In contrast, no effect of supplementation of autoinducers was observed in transcription of autoinducer synthase gene *lasI*. Importantly, we have observed suppression of *lasI* gene expression by erythromycin, clarithromycin and roxithromycin, in addition to azithromycin, but not by oleandomycin and josamycin (Figure 2). These results suggested that clinically effective macrolides are also active for suppression of quorum-sensing system, and macrolides might reduce the production of *Pseudomonas* virulence factors by inhibiting the synthesis of the autoinducer molecules.

How macrolides interfere with the transcription of genes belonging to the quorum-sensing circuitry remains fully unknown. The absence of a reduction of *xcpR* transcription suggests that macrolides do not act in a nonspecific manner. Macrolides inhibit protein synthesis at the ribosomal level, and therefore a direct effect of macrolides on gene transcription seems unlikely. As the expression of *lasI* could not be complemented by exogenous autoinducers, we hypothesize that macrolides might interfere with the translation of a so-far-unidentified protein important for the transcription of the autoinducer.

## 3. Agonistic and antagonistic activities of HSL-analogues

Quorum-sensing is a bacterial intercellular communication device for controlling gene expression

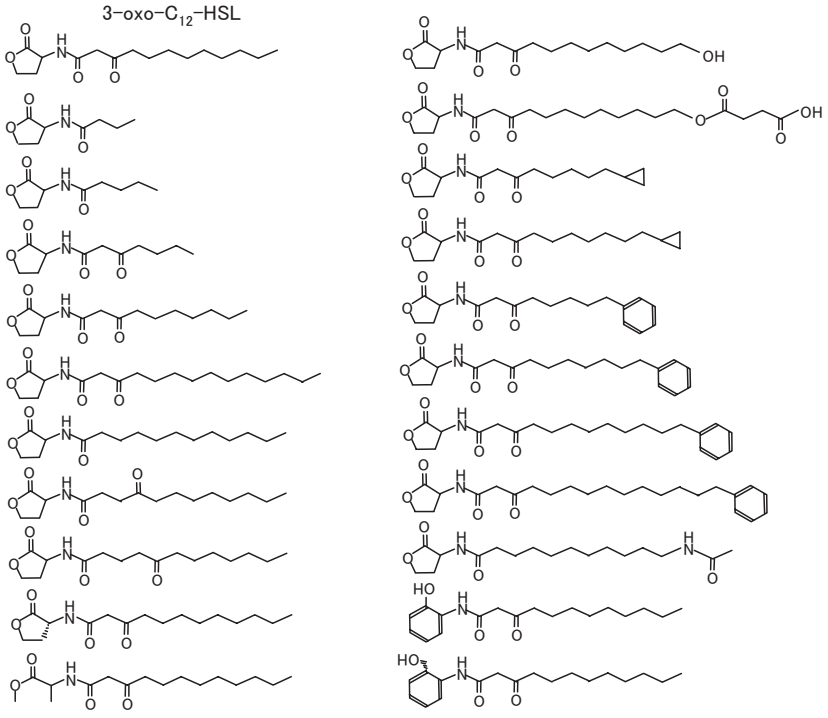


**Fig. 3.** *P. aeruginosa* 3-oxo-$C_{12}$-HSL and its derivatives examined.

through production of a small signal molecule, autoinducer. Recently, we have reported that 3-oxo-$C_{12}$-HSL, but not $C_4$-HSL, induces apoptosis and chemokine MIP-2 production in eukaryotic cells [31], although mechanisms of the action of 3-oxo-$C_{12}$-HSL are largely unknown. We explored molecular basis and cellular signaling in biological activities of the autoinducer, in addition to screening of quorum-sensing antagonist from a panel of derivatives of the autoinducer. We synthesized a panel of 3-oxo-$C_{12}$-HSL analogs to characterize critical structures of autoinducer (Figure 3). These compounds were evaluated in their antagonistic activities in several ways: induction of apoptosis, apoptosis markers, such as caspase 3 and histone-associated DNA fragmentation activity, and IL-8 production in eukaryotic cells. To explore cellular signaling mechanisms, responses of macrophages from receptor-deficient mice (Fas, FasL, toll-like receptor 2 and 4) were examined. Effects of 3-oxo-$C_{12}$-HSL on cellular signaling factors, such as caspases and MAP kinases, were investigated. The structure-activity correlation demonstrated that fine structures of 3-oxo-$C_{12}$-HSL, such as presence of 3-oxo, length of acyl-side chain and hydrophobicity, are crucial for apoptosis-inducing activity in macrophages. A few compounds inhibited virulence factor expression to some extents. Caspase and MAP kinase inhibitors prevented apoptosis and IL-8 production caused by 3-oxo-$C_{12}$-HSL, respectively. These data demonstrated that fine structures of autoinducer may be crucial in maximum activity of this molecule [39]. Our data suggest potential of certain autoinducer analogs as antagonist to *P. aeruginosa* quorum-sensing.

## 4. Vaccine strategy against autoinducer molecule 3-oxo-$C_{12}$-HSL

Quorum-sensing systems have been reported to play a critical role in pathogenesis of several bacterial infections. Recent data demonstrated that *Pseudomonas* 3-oxo-$C_{12}$-HSL, but not $C_4$-HSL, induces apoptosis in macrophages and neutrophils. In this study, effects of active immunization with 3-oxo-$C_{12}$-HSL/carrier protein conjugate were investigated on acute *P. aeruginosa* lung infection in mice. Immunization of mice with 3-oxo-$C_{12}$-HSL/bovine serum albu-

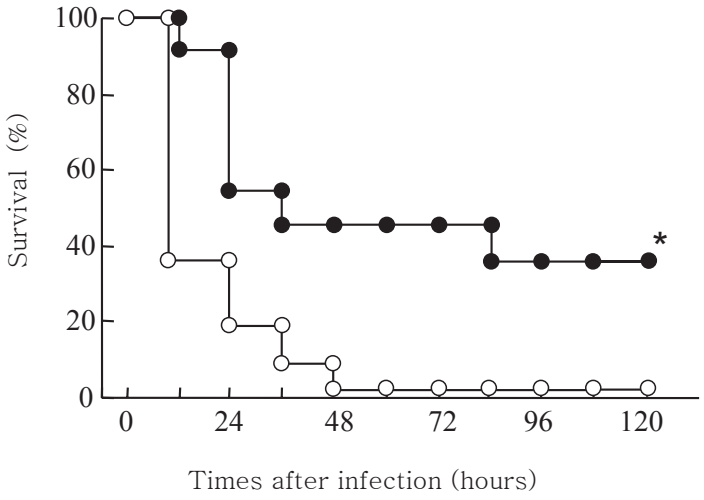


**Fig. 4.** Effects of vaccination against 3-oxo-$C_{12}$-HSL on survival of mice with acute pulmonary *P. aeruginosa* infection.
Balb/c mice were immunized with carrier-protein conjugated 3-oxo-$C_{12}$-HSL (closed circle) or not (control. open circle), and then were intranasally infected with *P. aeruginosa* PAO1 (3.0 x $10^6$ CFU/mouse). Survival of mice was monitored for 7 days after infection (n=11).
*$P$<0.05, compared to control.

min conjugate (subcutaneous, 4 times, at 2-week intervals) elaborated significant amounts of specific antibody in the serum. Control and immunized mice were intranasally challenged with approximately $3\times10^6$ CFU of *P. aeruginosa* PAO1, and then survival was compared. All control mice died by day 2 post bacterial challenge, while 36% of the immunized mice survived to day 4 ($P$<0.05) (Figure 4) [40]. Interestingly, bacterial number in the lungs was not different between the control and immunized groups, whereas the levels of pulmonary TNF-$\alpha$ in the immunized mice were significantly lower than those of the control mice ($P$<0.05). Furthermore, the extractable 3-oxo-$C_{12}$-HSL levels in the serum and lung homogenate were also significantly low in the immunized mice. *In vitro*, immune serum completely rescued macrophages from reduction of cell viability by 3-oxo-$C_{12}$-HSL-mediated apoptosis. These results demonstrated that specific antibody to 3-oxo-$C_{12}$-HSL plays a protective role in acute *P. aeruginosa* infection, probably through blocking of host inflammatory responses, without altering lung bacterial burden. The present data identify a promising potential of vaccine strategy targeting bacterial quorum-sensing molecules, including autoinducers.

## 5. Effects of *P. aeruginosa* 3-oxo-$C_{12}$-HSL on other bacteria: Potential of interspecies communication and interference

Bacteria commonly communicate each other by a cell-to-cell signaling mechanism referred to as quorum-sensing. Recent studies have shown that *Las*-quorum-sensing autoinducer 3-oxo-$C_{12}$-HSL of *Pseudomonas aeruginosa* possesses a variety of functions, not only intra-species signaling, but also inter-species and inter-kingdom communications. We examined effects of *Pseudomonas* 3-oxo-$C_{12}$-HSL on growth and virulence factor expression of other species of bacteria, which frequently co-localize the lesion with *P. aeruginosa* in nature. Type strains and clinical isolates of *Legionella pneumophila*, *Serratia marcescens*, *Proteus mirabilis*, *Ecsherichia coli*, *Alcaligenes faecalis* and *Stenotrophomonas maltophilia* were used in this study. The bacteria were incubated in liquid medium with or without synthetic 3-oxo-$C_{12}$-HSL or its analogues (5–50 $\mu$M), and 24 h later their growths were examined by plating. Effect of filter-sterilized culture supernatants of *P. aeruginosa* PAO1 and its *Las*-quorum-sensing deficient mutant was examined. Expressions of

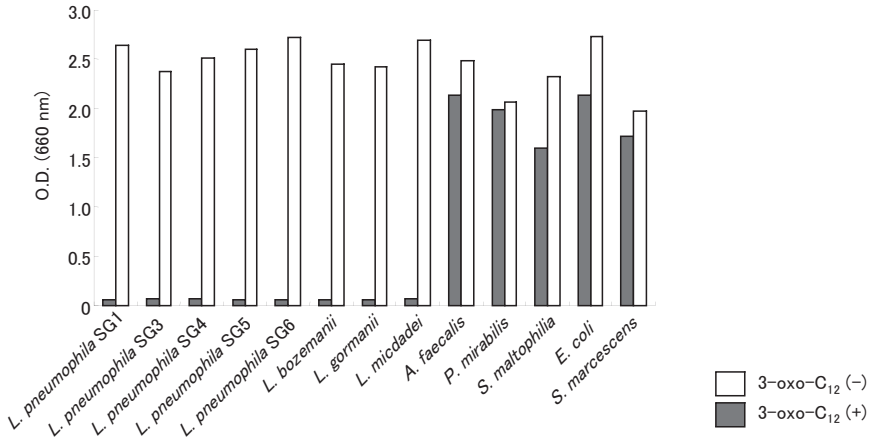


**Fig. 5.** Effects of 3-oxo-$C_{12}$-HSL on growth of *L. pneumophila* and other bacteria.

virulence factor genes (*dotA*, *rtxA* or *lvh*) were explored in *L. pneumophila* by RT-PCR in the presence of 3-oxo-$C_{12}$-HSL. 3-oxo-$C_{12}$-HSL, but not its analogues, suppressed growth of *L. pneumophila* in a dose-dependent manner (Figure 5) [41]. We also observed growth suppression of *L. pneumophila* by culture supernatant of PAO1, but not that of *Las*-quorum-sensing mutant. The growth of *L. pneumophila* was completely inhibited by 50 $\mu$M of 3-oxo-$C_{12}$-HSL, and interestingly, significant suppressions of virulence factor genes were demonstrated in *L. pneumophila* exposed to *Pseudomonas* 3-oxo-$C_{12}$-HSL. Our results suggest that *Pseudomonas* quorum-sensing autoinducer 3-oxo-$C_{12}$-HSL possesses bacteriostatic and virulence factor-suppressing activity against *L. pneumophila*. These data identify a novel activity of quorum-sensing autoinducer in bacterial inter-species communication.

## 6. Conclusions

The potential of macrolides as a prototypic inhibitor of bacterial quorum-sensing systems was explored. Given that clinical efficacy of macrolides is associated with suppression of bacterial virulence, including quorum-sensing activity, further investigation aimed at characterizing molecular mechanisms involved may prove fruitful in identifying novel strategies of antimicrobial chemotherapy against disease caused by antibiotic resistant organisms and biofilm disease. Also, the present data demonstrated potential of multiple approaches to inhibit bacterial cell-to-cell signaling systems, through autoinducer antagonists, vaccine strategy and interspecies interference.

This study was done in collaboration with Kazuhiro Tateda of this Department.

## References

(1) Richards MJ, Edwards JR, Culver DH and Gaynes RP. Nosocomial infections in medical intensive care units in the United States. National Nosocomial Infections Surveillance System. Crit Care Med 1999; **27**: 887−92.
(2) Hoiby N. Diffuse panbronchiolitis and cystic fibrosis: East meets West. Thorax 1994; **49**: 531−2.
(3) Wilson R, Dowling RB. Lung infections. 3. *Pseudomonas aeruginosa* and other related species. Thorax 1998; **53**: 213−9.
(4) Baltimore RS, Christie CD and Smith GJ. Immunohistopathologic localization of *Pseudomonas aeruginosa* in lungs from patients with cystic fibrosis. Implications for the pathogenesis of progressive lung deterioration. Am Rev Respir Dis 1989; **140**: 1650−61.
(5) Passador L, Cook JM, Gambello MJ, Rust L and Iglewski BH. Expression of *Pseudomonas aeruginosa* virulence genes requires cell-to-cell communication. Science 1993; **260**: 1127−30.

(6) Kaplan HB, Greenberg EP. Diffusion of autoinducer is involved in regulation of the *Vibrio fischeri* luminescence system. J Bacteriol 1985; **163**: 1210−4.
(7) Pearson JP, Gray KM, Passador L, et al. Structure of the autoinducer required for expression of *Pseudomonas aeruginosa* virulence genes. Proc Natl Acad Sci U S A 1994; **91**: 197−201.
(8) Pearson JP, Passador L, Iglewski BH and Greenberg EP. A second N-acylhomoserine lactone signal produced by *Pseudomonas aeruginosa*. Proc Natl Acad Sci U S A 1995; **92**: 1490−4.
(9) Kudoh S, Uetake T, Hagiwara K, et al. [Clinical effects of low-dose long-term erythromycin chemotherapy on diffuse panbronchiolitis]. Nihon Kyobu Shikkan Gakkai Zasshi 1987; **25**: 632−42.
(10) Kudoh S, Azuma A, Yamamoto M, Izumi T and Ando M. Improvement of survival in patients with diffuse panbronchiolitis treated with low-dose erythromycin. Am J Respir Crit Care Med 1998; **157**: 1829−32.
(11) Tateda K, Comte R, Pechere JC, Kohler T, Yamaguchi K and Van Delden C. Azithromycin inhibits quorum sensing in *Pseudomonas aeruginosa*. Antimicrob Agents Chemother 2001; **45**: 1930−3.
(12) Gambello MJ, Iglewski BH. Cloning and characterization of the *Pseudomonas aeruginosa* lasR gene, a transcriptional activator of elastase expression. J Bacteriol 1991; **173**: 3000−9.
(13) Ochsner UA, Koch AK, Fiechter A and Reiser J. Isolation and characterization of a regulatory gene affecting rhamnolipid biosurfactant synthesis in *Pseudomonas aeruginosa*. J Bacteriol 1994; **176**: 2044−54.
(14) Glessner A, Smith RS, Iglewski BH and Robinson JB. Roles of *Pseudomonas aeruginosa* las and rhl quorum-sensing systems in control of twitching motility. J Bacteriol 1999; **181**: 1623−9.
(15) Rumbaugh KP, Griswold JA, Iglewski BH and Hamood AN. Contribution of quorum sensing to the virulence of *Pseudomonas aeruginosa* in burn wound infections. Infect Immun 1999; **67**: 5854−62.
(16) Pearson JP, Feldman M, Iglewski BH and Prince A. *Pseudomonas aeruginosa* cell-to-cell signaling is required for virulence in a model of acute pulmonary infection. Infect Immun 2000; **68**: 4331−4.
(17) Smith RS, Harris SG, Phipps R and Iglewski B. The *Pseudomonas aeruginosa* quorum-sensing molecule N-(3-oxododecanoyl)homoserine lactone contributes to virulence and induces inflammation in vivo. J Bacteriol 2002; **184**: 1132−9.
(18) Wu H, Song Z, Givskov M, et al. *Pseudomonas aeruginosa* mutations in lasI and rhlI quorum sensing systems result in milder chronic lung infection. Microbiology 2001; **147**: 1105−13.
(19) Singh PK, Schaefer AL, Parsek MR, Moninger TO, Welsh MJ and Greenberg EP. Quorum-sensing signals indicate that cystic fibrosis lungs are infected with bacterial biofilms. Nature 2000; **407**: 762−4.
(20) Parsek MR, Greenberg EP. Quorum sensing signals in development of *Pseudomonas aeruginosa* biofilms. Methods Enzymol 1999; **310**: 43−55.
(21) Parsek MR, Greenberg EP. Acyl-homoserine lactone quorum sensing in gram-negative bacteria: a signaling mechanism involved in associations with higher organisms. Proc Natl Acad Sci USA 2000; **97**: 8789−93.
(22) De Kievit TR, Iglewski BH. Quorum sensing, gene expression, and *Pseudomonas* biofilms. Methods Enzymol 1999; **310**: 117−28.
(23) Sauer K, Camper AK, Ehrlich GD, Costerton JW and Davies DG. *Pseudomonas aeruginosa* displays multiple phenotypes during development as a biofilm. J Bacteriol 2002; **184**: 1140−54.
(24) Storey DG, Ujack EE, Rabin HR and Mitchell I. *Pseudomonas aeruginosa* lasR transcription correlates with the transcription of lasA, lasB, and toxA in chronic lung infections associated with cystic fibrosis. Infect Immun 1998; **66**: 2521−8.
(25) Erickson DL, Endersby R, Kirkham A, et al. *Pseudomonas aeruginosa* quorum-sensing systems may control virulence factor expression in the lungs of patients with cystic fibrosis. Infect Immun 2002; **70**: 1783−90.
(26) Charlton TS, de Nys R, Netting A, et al. A novel and sensitive method for the quantification of N-3-oxoacyl homoserine lactones using gas chro-

matography-mass spectrometry: application to a model bacterial biofilm. Environ Microbiol 2000; **2**: 530−41.
(27) DiMango E, Zar HJ, Bryan R and Prince A. Diverse *Pseudomonas aeruginosa* gene products stimulate respiratory epithelial cells to produce interleukin-8. J Clin Invest 1995; **96**: 2204−10.
(28) Smith RS, Fedyk ER, Springer TA, Mukaida N, Iglewski BH and Phipps RP. IL-8 production in human lung fibroblasts and epithelial cells activated by the *Pseudomonas* autoinducer N-3-oxododecanoyl homoserine lactone is transcriptionally regulated by NF-kappa B and activator protein-2. J Immunol 2001; **167**: 366−74.
(29) Telford G, Wheeler D, Williams P, et al. The *Pseudomonas aeruginosa* quorum-sensing signal molecule N-(3-oxododecanoyl)-L-homoserine lactone has immunomodulatory activity. Infect Immun 1998; **66**: 36−42.
(30) Chhabra SR, Harty C, Hooi DS, et al. Synthetic analogues of the bacterial signal (quorum sensing) molecule N-(3-oxododecanoyl)-L-homoserine lactone as immune modulators. J Med Chem 2003; **46**: 97−104.
(31) Tateda K, Ishii Y, Horikawa M, et al. The *Pseudomonas aeruginosa* autoinducer N-3-oxododecanoyl homoserine lactone accelerates apoptosis in macrophages and neutrophils. Infect Immun 2003; **71**: 5785−93.
(32) de Kievit TR, Iglewski BH. Bacterial quorum sensing in pathogenic relationships. Infect Immun 2000; **68**: 4839−49.
(33) Miller MB, Bassler BL. Quorum sensing in bacteria. Annu Rev Microbiol 2001; **55**: 165−99.
(34) Whitehead NA, Barnard AM, Slater H, Simpson NJ and Salmond GP. Quorum-sensing in Gram-negative bacteria. FEMS Microbiol Rev 2001; **25**: 365−404.
(35) Schauder S, Bassler BL. The languages of bacteria. Genes Dev 2001; **15**: 1468−80.
(36) Reverchon S, Chantegrel B, Deshayes C, Doutheau A and Cotte-Pattat N. New synthetic analogues of N-acyl homoserine lactones as agonists or antagonists of transcriptional regulators involved in bacterial quorum sensing. Bioorg Med Chem Lett 2002; **12**: 1153−7.
(37) Smith KM, Bu Y and Suga H. Induction and inhibition of *Pseudomonas aeruginosa* quorum sensing by synthetic autoinducer analogs. Chem Biol 2003; **10**: 81−9.
(38) Hentzer M, Wu H, Andersen JB, et al. Attenuation of *Pseudomonas aeruginosa* virulence by quorum sensing inhibitors. Embo J 2003; **22**: 3803−15.
(39) Fuse T. Etsu et al. Novel insight in biological activities of quorum-sensing autoinducer in *Pseudomonas aeruginosa*: molecular basis, cellular signaling and search for antagonist. Submitted.
(40) Miyairi S. et al. Immunization with 3-oxododecanoyl-L-homoserine lactone/protein conjugate protects mice from lethal *Pseudomonas aeruginosa* lung infection. J Med Microbiol In press.
(41) Kimura S. et al. *Pseudomonas aeruginosa Las*-quorum-sensing autoinducer suppresses growth of and virulence factors in *Legionella pneumophila*. Submitted.

# Effects of Synthetic *N*-Acyl Homoserine Lactones and Eel Lectin on Oral Pathogens

**Tetsuo Kato**

*Department of Microbiology, Tokyo Dental College, 1-2-2 Masago, Mihama-ku, Chiba 261-8502, Japan*

## Introduction

Dental plaque is a biofilm formed by numerous organisms bound tightly to the tooth surface and is closely associated with the etiology of oral infectious diseases. The biofilm formation is associated with intercellular communication, quorum sensing (QS) (1). For QS, bacteria synthesize and secrete extracellular signaling molecules, autoinducer (2). When a critical threshold concentration of the autoinducer is attained, a signal transduction cascade is triggered, resulting in the density dependent regulation of gene expression and a change in behavior of the organism for facilitating environmental adaptation (3). The predominant signaling molecules of gram-positive bacteria are peptides, while in gram-negative bacteria, some different systems of QS, which use different types of signaling molecules, have so far been described (4). The autoinducer of gram-negative bacteria has been identified as an *N*-acyl homoserine lactone (*N*-acyl HSL) (5). Frias *et al*. (6) suggested that the gram negative periodontal organisms do not possess *N*-acyl HSL-dependent signaling systems. However, several of these organisms such as *Porphyromonas gingivalis* and *Actinobacillus actinomycetemcomitans* secrete signals functionally related to AI-2 (7-10).

*P. gingivalis* has frequently been isolated from periodontal lesions and shown to be related to the onset and progression of periodontal disease (11, 12). Although previous researchers were unable to obtain any evidence to suggest that the gram negative anaerobe *P. gingivalis* employs *N*-acyl HSL-mediated QS, they have demonstrated that this periodontopathic bacteria produces a diffusible signal molecule capable of activating the *V. harveyi* AI-2 biosensor (6-8). To determine whether *N*-acyl HSLs play a role in *P. gingivalis*, we investigated the influence of synthetic *N*-acyl HSLs on the growth and production of proteins in this organism.

Cariogenic bacteria and periodontopathic bacteria live in dental plaques as oral biofilms and induce respective infections. Recent studies have suggested that these bacteria are associated with systemic disease (13, 14); therefore the need for oral care in a systemic health regimen has also been emphasized. In this study, the inhibitory effect of the lectin purified from the skin mucus of Japanese eels on biofilm formation by oral bacteria was also evaluated.

## Materials and Methods

*Bacterial strains and culture conditions.*

*P. gingivalis* ATCC 33277, ATCC 53977, Su63 and W50; *Prevotella intermedia* ATCC 15032, ATCC 25611 and ATCC 49046; *A. actinomycetemcomitans* Y4, ATCC 29523 and ATCC 29524; *Streptococcus sobrinus* 6715 and B13; *Streptococcus mutans* MT8148R and JC2 were used in this study. These strains were maintained anaerobically on blood agar plates containing trypticase soy agar (Becton Dickinson Microbiology System, Cockeysville, MD, USA) supplemented with 10% defibrinated horse blood, hemin (5 $\mu$g/ml; Sigma Chemical Co., St. Louis, MO, USA) and menadione (0.5 $\mu$g/ml; Wako Pure Chemical Industries, Osaka, Japan). The bacterial strains were cultured anaerobically in trypticase soy broth (TSB; Becton Dick-

inson Microbiology System) supplemented with hemin and menadione at 37ºC.

*Effect of synthetic N-acyl HSLs or acyl coenzyme A on the growth of bacteria.*

*N*-butyryl-DL-homoserine lactone (HSL), *N*-hexanoyl HSL, *N*-heptanoyl HSL, *N*-octanoyl HSL, and *N*-tetradecanoyl (myristoyl) HSL were used as synthetic *N*-acyl HSLs (Sigma-Aldrich Co., Steinheim, Germany). Each *N*-acyl HSL was added to the culture broth at various concentrations (100 $\mu$M, 10 $\mu$M and 100 nM), and its influence on the growth of test bacteria was evaluated. Growth was monitored by optical density (OD) at 660 nm for 48 h. In order to confirm survival for 48 h, 100 $\mu$l aliquots were taken from cultures with *N*-acyl HSL showing no increase in OD, inoculated onto blood agar plates, and cultured for one week under anaerobic conditions.

In order to study the effect of acyl coenzyme A (acyl CoA) on *P. gingivalis* autoinducer synthesis, *P. gingivalis* ATCC 33277 cells were cultured in the broth containing myristoyl CoA or lauroyl CoA (100 $\mu$M and 10 $\mu$M; Doosan Serdary Research Laboratories, Toronto, Canada). Growth was monitored by OD at 660 nm.

*SDS-polyacrylamide gel electrophoresis (SDS-PAGE) analysis.*

*P. gingivalis* ATCC 33277 and ATCC 53977 were cultured with/without *N*-tetradecanoyl HSL for 24 h. Cells were harvested by centrifugation. Harvested cells were suspended in distilled water, and disrupted by sonication. The protein content of the sonicated sample was adjusted to 1 mg protein per ml. The adjusted samples were suspended in SDS-PAGE loading buffer (15) and boiled for 10 min. The samples were loaded on the gel. SDS-PAGE was done in 10 to 20% gradient micro slab gels (Daiichi Pure Chemical Co., Tokyo, Japan) and stained with Coomassie brilliant blue (CBB; Amersham Biosciences AB, Uppsala, Sweden).

*Purification of eel lectin AJL-1.*

The lectin, AJL-1 (16), was purified from the skin mucus of the Japanese eel, *Anguilla japonica*. Skin was gathered from ice-chilled eels and immediately bufferized with 0.02 M Tris-HCl buffer (pH 7.5). The extract was fractionated with gel filtration chromatography and affinity chromatography (17).

*Effect of AJL-1 on biofilm formation of oral bacteria.*

Aliquots of 10 $\mu$l of precultured cells were inoculated into wells of 96-well (flat-bottom) cell culture plates (Sumitomo Bakelite Co, Ltd, Tokyo, Japan) containing 25, 50, or 100 $\mu$g/ml of AJL-1 in 100 $\mu$l of broth. The plates were anaerobically incubated for 24 h or 48 h. After incubation, the biofilm formations on the bottom of wells were quantified.

*Quantification of biofilm.*

Quantification of biofilm was achieved by using the protocol of Yamanaka *et al*. (18). Briefly the culture medium containing floating bacteria was removed. The wells were washed with 200 $\mu$l of distilled water. The adherent bacteria were stained with 50 $\mu$l of 0.1% crystal violet for 15 min at room temperature. After rinsing with 200 $\mu$l of distilled water twice, the dye bound to biofilm was extracted with 200 $\mu$l of ethanol for 20 min. Biofilm formation was then quantified by measuring the OD of the extract at 595 nm with a microplate reader (Model 3550, Bio-Rad Laboratories, Hercules, CA).

## Results

*Effects of synthetic N-acyl HSLs or acyl CoA on the growth of P. gingivalis.*

*N*-tetradecanoyl HSL completely inhibited the growth of all *P. gingivalis* strains tested in this study at 100 $\mu$M (Table 1). Growth inhibition of this *N*-acyl HSL was dose-dependent. Myristoyl CoA also inhibited *P. gingivalis* growth in a dose- dependent manner (Table 2). However lauroyl CoA showed no inhibitory effect on the growth of *P. gingivalis* (Table 2). *P. gingivalis* cells from cultures showing no increase in OD formed many colonies on blood agar plates (data not

**Table 1.** Effects of *N*-acyl HSLs on the growth of *P. gingivalis* strains

| *N*-acyl HSLs | *P. gingivalis* strains | | | |
|---|---|---|---|---|
| | ATCC 33277 | ATCC 53977 | W50 | Su63 |
| Control | ++ | + | ++ | ++ |
| *N*-tetradecanoyl HSL | | | | |
| 100 $\mu$M | − | − | − | − |
| 10 $\mu$M | + | − | + | ± |
| 100 nM | ++ | + | ++ | ++ |
| *N*-butyryl HSL | | | | |
| 100 $\mu$M | ++ | + | ++ | ++ |
| *N*-hexanoyl HSL | | | | |
| 100 $\mu$M | ++ | + | ++ | ++ |
| *N*-heptanoyl HSL | | | | |
| 100 $\mu$M | ++ | + | ++ | ++ |
| *N*-octanoyl HSL | | | | |
| 100 $\mu$M | + | ± | ++ | + |

Growth was monitored by optical density (OD) at 660 nm.
++: $0.25 \leq OD_{660}$ +: $0.1 \leq OD_{660} < 0.25$ ±: $0.05 \leq OD_{660} < 0.1$ −: $OD_{660} < 0.05$

**Table 2.** Inhibitory effect of acyl CoA on the growth of *P. gingivalis* ATCC 33277 strain

| Acyl CoA | Concentration | Culture time | |
|---|---|---|---|
| | | 24 h | 48 h |
| Control | − | ++ | ++ |
| Myristoyl CoA | 100 $\mu$M | − | − |
| | 10 $\mu$M | − | + |
| Lauroyl CoA | 100 $\mu$M | + | + |
| | 10 $\mu$M | ++ | ++ |

Growth was monitored by optical density (OD) at 660 nm.
++: $0.25 \leq OD_{660}$ +: $0.1 \leq OD_{660} < 0.25$ +: $0.05 \leq OD_{660} < 0.1$ −: $OD_{660} < 0.05$

shown), indicating that this microorganism survived at least 48 h in the broth containing *N*-tetradecanoyl HSL or myristoyl CoA.

*Effect of N-tetradecanoyl HSL on the protein expression of P. gingivalis.*

We compared the SDS-PAGE profiles of sonicated samples of *P. gingivalis* cells cultured with or without *N*-tetradecanoyl HSL. The effects of *N*-tetradecanoyl HSL on the protein expression of *P. gingivalis* ATCC 33277 and ATCC 53977 are shown in Fig. 1. We found that protein production of *P. gingivalis* was changing by addition of *N*-tetradecanoyl HSL. We confirmed that the alteration of the protein profile was not due to contamination by black-pigment produced by bacteria themselves.

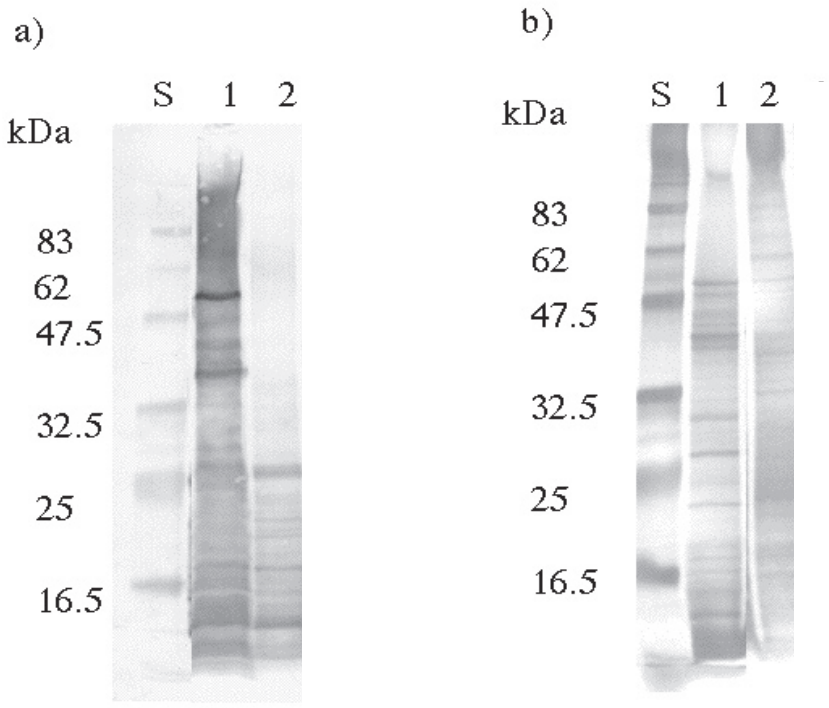


**Fig. 1.** SDS-PAGE profile (CBB staining) of *P. gingivalis* sonicated samples. Lanes, S; molecular weight standards, 1; sonicated sample of *P. gingivalis* cells in control culture, 2; sonicated sample of *P. gingivalis* cells cultured with 100 $\mu$M *N*-tetradecanoly HSL. a) ATCC 33277, b) ATCC 53977.

**Table 3.** Effects of AJL-1 on the biofilm formation of oral bacteria

| | Amounts of biofilm (Optical density at 595 nm) | | | |
|---|---|---|---|---|
| | AJL-1 ($\mu$g/ml) | | | |
| Bacterial strains | 0 (control) | 25 | 50 | 100 |
| *S. sobrinus* 6715 | 0.59 ± 0.14 | 0.35 ± 0.09* | 0.39 ± 0.14* | 0.96 ± 0.18* |
| *S. sobrinus* B13 | 1.41 ± 0.32 | 0.51 ± 0.25* | 0.52 ± 0.18* | 0.52 ± 0.25* |
| *S. mutans* JC2 | 0.87 ± 0.54 | 0.39 ± 0.36* | 0.76 ± 0.64 | 0.80 ± 0.66 |
| *S. sobrinus* MT8148R | 1.60 ± 0.46 | 1.44 ± 0.32 | 1.44 ± 0.42 | 1.61 ± 0.22 |
| *A. actinomycetemcomitans* Y4 | 0.90 ± 0.11 | 0.31 ± 0.06* | 0.17 ± 0.07* | 0.11 ± 0.02* |
| *A. actinomycetemcomitans* ATCC 29523 | 0.20 ± 0.07 | 0.06 ± 0.02* | 0.02 ± 0.01* | 0.02 ± 0.03* |
| *A. actinomycetemcomitans* ATCC 29524 | 0.51 ± 0.25 | 0.06 ± 0.04* | 0.04 ± 0.05* | 0.03 ± 0.03* |
| *P. gingivalis* ATCC 33277 | 0.37 ± 0.07 | 0.43 ± 0.18 | 0.44± 0.15 | 0.37 ± 0.16 |
| *P. gingivalis* 381 | 1.15 ± 0.24 | 1.12 ± 0.47 | 1.31 ± 0.57 | 1.01 ± 0.35 |
| *P. intermedia* ATCC 15032 | 1.16 ± 0.29 | 1.13 ± 0.22 | 1.00 ± 0.33 | 1.26 ± 0.34 |
| *P. intermedia* ATCC 25611 | 0.73 ± 0.08 | 0.69 ± 0.12 | 0.76 ± 0.09 | 0.71 ± 0.12 |
| *P. intermedia* ATCC 49046 | 1.18 ± 0.28 | 1.08 ± 0.25 | 1.02 ± 0.18 | 0.93 ± 0.42 |

*$p<0.05$ vs. control

*Effect of AJL-1 on oral bacterial biofilm formation.*

The effects of AJL-1 on oral bacterial biofilm formation on the 96-well plates are shown in Table 3. AJL-1 significantly reduced biofilm formation of all *A. actinomycetemcomitans* strains tested and *S. sobrinus* B13 in a dose dependent manner (Mann Whitney *U* test, $p<0.05$). However, no inhibitory activity was shown against all *P. gingivalis* and *P. intermedia* strains tested in this study at any concentrations.

## Discussion

Since bacteria within the biofilms reach a high density, it has been suggested that QS might play a key role in bacterium-bacterium communication and, therefore, in the formation of biofilm (1). QS mechanisms control the production of virulence factors in some species of bacteria (19-21). *P. gingivalis* has long been considered one of the main periodontopathic bacteria, playing an important role in bone and tissue destruction (22). To facilitate adaptation for life within the oral cavity, *P. gingivalis* must be capable of sensing and responding to prevailing environmental conditions, including variations in temperature, oxygen tension, pH, nutrient availability and the presence of other cells (23, 24).

Several investigators (6-8) suggested that periodontal bacteria including *P. gingivalis* do not possess *N*-acyl HSL dependent signaling circuits. In their reports, those bacteria were tested for production of extracellular autoinducer-like activities that stimulates the expression of the genes for biosensors of *V. harveyi* or *Chromobacterium violaceum*. It suggests that *P. gingivalis* does not employ *N*-acyl HSLs which are able to stimulates the biosensors. The objective of the present study is to investigate whether *P. gingivalis* possesses *N*-acyl HSL system as one of the QS signal by the assay using synthetic *N*-acyl HSLs. *N*-tetradecanoyl HSL inhibited the growth and affected protein production in *P. gingivalis*. The growth of *P. gingivalis* was inhibited by myristoyl CoA but not by lauroyl CoA, suggesting that *P. gingivalis* responds to auto-produced *N*-tetradecanoyl (myristoyl) HSL-like molecule(s), and slows their growth.

CinI, LuxI homologue, produces the *N*-(3-hydroxy-7-*cis* tetradecanoyl) HSL, and CinR is a LuxR-type regulator (25). CerI, which is also LuxI homologue, in *Rhodobacter sphaeroides* synthesizes *N*-(7-*cis*-tetradecanoyl) HSL (26). Laue *et al*. (27) demonstrated that *Pseudomonas fluorescens* F113 makes at least three different *N*-acyl HSLs including *N*-(3-hydroxy-7-*cis* tetradecanoyl) HSL and identified a gene *hdtS* which does not belong to the LuxI or LuxM family of *N*-acyl HSL synthases. Interrogation to the *P. gingivalis* W83 genome sequence database (www.tigr.org) for homologues of *N*-acyl HSL synthases belonging to either the LuxI or LuxM family failed to identify any candidates. However, one open reading frame (ORF) with significant homology with HdtS amino acid sequence was identified (TIGR locus: PG1249, 1-acyl-sn-glycerol-3-phosphate acetyltransferase, putative). The ORF showed 25% identity and 48% amino acid similarity with the HdtS at over 201 amino acids. The ORF possesses two motifs which are conserved in the lysophosphatidic acid acyltransferases (28, 29). It is possible that the ORF is an acyltransferase which transfers acyl-chains onto a substrate to generate some *N*-acyl HSLs. Further study is required to define its function for *N*-acyl HSL formation.

Animal lectins are classified as C-type (30), galectin family (31, 32), P-type (33), I-type (34) or others (35). The eel lectin AJL-1 was composed of 142 amino acid residues, and showed homology to member of the galectin family (16). This lectin showed agglutinating activity against pathogenic bacteria, *Streptococcus difficile*. This suggests that AJL-1 plays an important role as a defensive factor at the body surface in eel. AJL-1 showed agglutinating activity against *S. sobrinus* B13, but not against any other bacteria tested (data not shown). The present study shows that the eel lectin effectively inhibits biofilm formation by some oral bacteria such as *S. sobrinus* and *A. actinomycetemcomitans*. We intend to confirm these effects *in vivo* and apply them clinically.

## Conclusions

The present study suggests that *P. gingivalis* responds to *N*-tetradecanoyl HSL-like signaling molecule and changes protein production to become more fit for habitation in the worse environment.

The eel lectin AJL-1 effectively inhibited biofilm formation by some oral pathogens.

This study was done in collaboration with Eiichi Saitoh, Department of Applied Chemistry and Biotechnology, Niigata Institute of Technology, and Akiyo Ito, Department of Periodontology, Tokyo Dental College.

## References

(1) McNab, R., Ford, S. K., El-Sabaeny, A., Barbieri, B., Cook, G. S. and Lamont, R. J. (2003) LuxS-based signaling in *Streptococcus gordonii*: autoinducer 2 controls carbohydrate metabolism and biofilm formation with *Porphyromonas gingivalis*. J. Bacteriol. **185**, 274−284.

(2) Miller, M. B. and Bassler, B. B. (2001) Quorum sensing in bacteria. Annu. Rev. Microbiol. **55**, 165−199.

(3) Engebrecht, J., Nealson, K. and Silverman, M. (1983) Bacterial bioluminescence: isolation and genetic analysis of functions from *Vibrio fischeri*. Cell **32**, 773−781.

(4) Bassler, B. L. (1999) How bacteria talk to each other: regulation of gene expression by quorum sensing. Curr. Opin. Microbiol. **2**, 582−587.

(5) Shaw, P. D., Gao, F., Daly, S. L., Cha, C., Cronan Jr, J. E. M., Rinehart, K. L. and Farrand, S. K. (1997) Detecting and characterizing N-acylhomoserine lactone signal molecules by thin-layer chromatography. Proc. Natl. Acad. Sci. USA. **94**, 6036−6041.

(6) Frias, J., Olle, E. and Alsina, M. (2001) Periodontal pathogens produce quorum sensing signal molecules. Infect. Immun. **69**, 3431−3434.

(7) Burgess, N. A., Kirke, D. F., Williams, P., Winzer, K., Hardie, K. R., Meyers, N. L., Aduse-Opoku, J., Curtis, M. A. and Cámara, M. (2002) LuxS-dependent quorum sensing in *Porphyromonas gingivalis* modulates protease and haemagglutinin activities but is not essential for virulence. Microbiology **148**, 763−772.

(8) Chung, W. O., Park, Y., Lamont, R. J., McNab, R., Barbieri, B. and Demuth, D. R. (2001) Signaling system in *Porphyromonas gingivalis* based on a LuxS protein. J. Bacteriol. **183**, 3903−3909.

(9) Fong, K. P., Chung, W. O., Lamont, R. J. and Demuth, D. R. (2001) Intra- and interspecies regulation of gene expression by *Actinobacillus actinomycetemcomitans* LuxS. Infect. Immun. **69**, 7625−7634.

(10) Fong, K. P., Gao, L. and Demuth, D. R. (2003) *luxS* and *arcB* control aerobic of *Actinobacillus actinomycetemcomitans* under iron limitation. Infect. Immun. **71**, 298−308.

(11) Mayrand, D. and Holt, S. C. (1988) Biology of asaccharolytic black-pigmented Bacteroides species. Microbiol. Rev. **52**, 134−152.

(12) Slots, J. and Listgarten, M. A. (1988) *Bacteroides gingivalis*, *Bacteroides intermedius* and *Actinobacilus actinomycetemcomitans* in human periodontal diseases. J. Clin. Periodontol. **15**, 85−93.

(13) Okuda, K., Kato, T. and Ishihara, K. (2004) Involvement of periodontopathic biofilm in vascular diseases. Oral Dis. **10**, 5-12.

(14) Okuda, K., Kimizuka, R., Abe, S., Kato, T. and Ishihara, K. (2005) Involvement of periodontopathic anaerobes in aspiration pneumonia. J Periodontol. **76**, 2154−2160.

(15) Laemmli, U. K. (1970) Cleavage of structural proteins during the assembly of the head of bacteriophage T4. Nature (London) **227**, 680−685.

(16) Tasumi, S., Yang, W.-J., Usami, T., Tsutsui, S., Ohira, T., Kawazoe, I., Wilder, M. N., Aida, K. and Suzuki, Y. (2004) Characterization and primary structure of a galectin in the skin mucus of the Japanese eel, *Anguilla japonica*. Dev. Comp. Immunol. **28**, 325−335.

(17) Saitoh, E., Isemura, S., Chiba, A., Oka, S. and Odani, S. (2005) A novel cysteine protease inhibitor with lectin activity from the epidermis of the Japanese eel *Anguilla japonica*. Comp. Biochem.

Physiol. B Biochem. Mol. Biol. **141**, 103−109.
(18) Yamanaka, A., Kimizuka, R., Kato, T. and Okuda, K. (2004) Inhibitory effects of cranberry juice on attachment of oral streptococci and biofilm formation. Oral Microbiol. Immunol. **19**, 150−154.
(19) De Kievit, T. R. and Iglewski, B. H. (2000) Bacterial quorum sensing in pathogenic relationships. Infect. Immun. **68**, 4839−4849.
(20) Passador, L., Cook, J. M., Gambello, M. J., Rust, L. and Iglewski, B. H. (1993) Expression of *Pseudomonas aeruginosa* virulence genes requires cell-to-cell communication. Science **260**, 1127−1130.
(21) Winzer, K. and Williams, P. (2001) Quorum sensing and the regulation of virulence gene expression in pathogenic bacteria. Int. J. Med. Microbiol. **291**, 131−143.
(22) Holt, S. C., Kesavalu. L., Walker, S. and Genco, C. A. (1999) Virulence factors of *Porphyromonas gingivalis*. Periodontol. 2000 **20**, 168−238.
(23) Lamont, R. J. and Jenkinson, H. F. (1998) Life below the gum line: pathogenic mechanisms of *Porphyromonas gingivalis*. Micrbiol. Mol. Biol. Rev. **62**, 1244−1263.
(24) Xie, H., Cai, S. and Lamont, R. J. (1997) Environmental regulation of fimbrial gene expression in *Porphyromonas gingivalis*. Infect. Immun. **65**, 2265−2271.
(25) Lithgow, J. K., Wilkinson, A., Hardman, A., Rodelas, B., Wisniewski-Dye, F., Williams, P. and Downie, J. A. (2000) The regulatory locus *cinRI* in *Rhizobium leguminosarum* controls a network of quorum sensing loci. Mol. Microbiol. **37**, 81−97.
(26) Puskas, A., Greenberg, E. P., Kaplan, S. and Schaefer, A. L. (1997) A quorum-sensing system in the free-living photosynthetic bacterium *Rhodobacter sphaeroides*. J. Bacteriol. **179**, 7530−7537.
(27) Laue, B. E., Jiang, Y., Chhabra, S. R., Jacob, S., Stewart, G. S. A. B., Hardman, A., Downie, J. A., O'Gara, F. and Williams, P. (2000) The biocontrol strain *Pseudomonas fluorescens* F113 produces the *Rhizobium small* bacteriocin, *N*-(3-hydroxy-7-cis-tetradecanoyl) homoserine lactone, via HdtS, a putative novel *N*-acylhomoserine lactone synthase. Microbiology **146**, 2469−2480.
(28) Shih, G. C., Kahler, C. M., Swartley, J. S., Rahman, M. M., Coleman, J., Carlson, R. W. and Stevens, D. S. (1999) Multiple lysophosphatidic acid acyltransferases in *Neisseria meningitides*. Mol. Microbiol. **32**, 942−952.
(29) West, J., Tompkins, C. K., Balantac, N., Nudelman, E., Meengs, B. and White, T. (1997) Cloning and expression of two human lysophosphatidic acid acyltransferase cDNAs that encode cytokine-induced signalling response in cells. DNA Cell Biol. **16**, 691−701.
(30) Dey, A. J. (1994) The C-type carbohydrate recognition domain (CRD) superfamily. Biochem. Soc. Trans. **22**, 83−88.
(31) Barondes, S. H., Cooper, D. N. W., Gitt, M. A. and Leffler, H. (1994) Galectins. Structure and function of a large family of animal lectins. J. Biol. Chem. **269**, 20807−20810.
(32) Kasai, K. and Hirabayashi, J. (1996) Galectins: a family of animal lectins that decipher glycocodes. J. Biolchem. **119**, 1−8.
(33) Kornfeld, S. (1992) Structure and function of the mannose 6-phosphate/insulinlike growth factor II receptors. Annu. Rev. Biochem. **61**, 307−330.
(34) Powell, L. D. and Varki, A. (1995) I-type lectins. J. Biol. Chem. **270**, 14243−14246.
(35) Kilpatrick, D. C. (2000) Handbook of animal lectins. Chichesters, Wiley.

# Role of Prostaglandin $D_2$ in Remodeling of Pulmonary Artery Affected by Pulmonary Hypertension

**Hidero Kitasato**

*Laboratory of Microbiology, Department of Medical Laboratory Sciences, School of Allied Health Sciences Kitasato University, 1-15-1 Kitasato, Sagamihara, Kanagawa 228-8555, Japan*

## Introduction

In 1972, a group of patients with overlapping features of systemic lupus erythematosus (SLE), systemic sclerosis (SSc) and polymyositis, associated with the serum autoantibodies to nuclear RNP, was described, and this condition was designated as mixed connective tissue disease (MCTD) (1). In addition, pulmonary hypertension (PH) with particularly severe intimal and medial thickening of the blood vessel has been reported in the patients of MCTD (2, 3).

Prostaglandin D synthase (PGDS) produces $PGD_2$ from $PGH_2$, which is the common precursor of prostaglandins (PGs) synthesized from arachidonic acid (AA) by cyclooxygenase I and II (Fig. 1). Two kinds of PGDS have been isolated and designated as lipocaline-type PGDS and hematopoietic PGDS, respectively. Lipocaline PGDS is a brain enzyme and its product, $PGD_2$, is the most potent somnogenic substance so far known and is involved in various physiological events, such as regulation of sleep and pain responses (4). He-

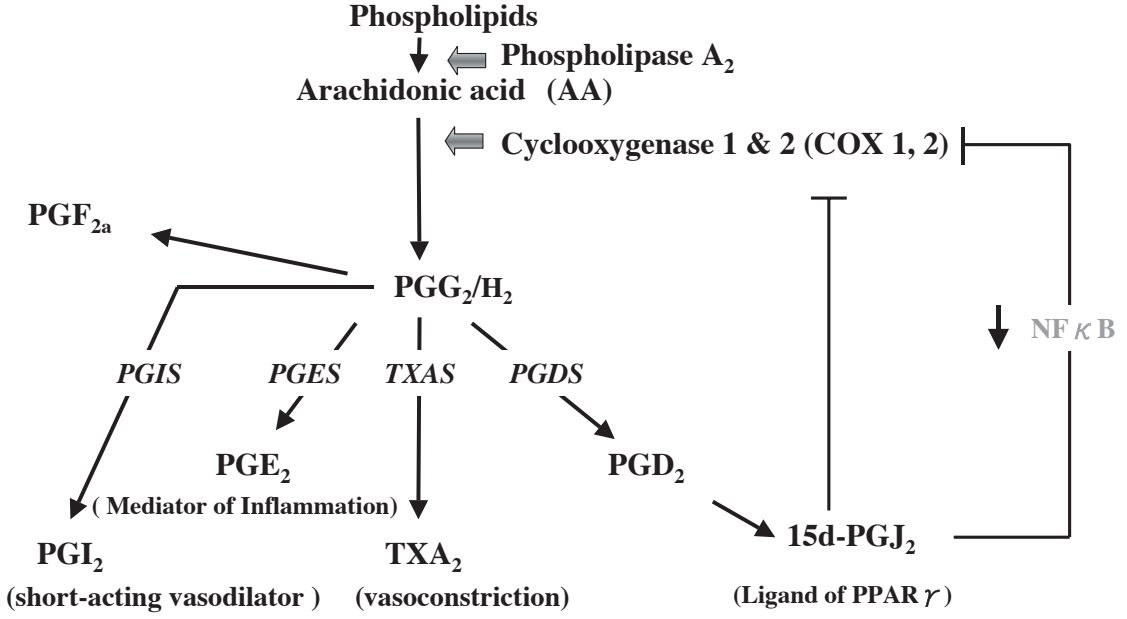


**Fig. 1.** Arachidonic acid cascade and metabolites. Prostaglandin D synthase (PGDS) produces $PGD_2$ from $PGG_2/H_2$ and one of its non-enzymatically converted metabolite, 15d-$PGJ_2$, directly or via NF$\kappa$-B suppresses Cox-II. Prostaglandin I synthase (PGIS) produces $PGI_2$, short-acting vasodilator, from $PGG_2/PGH_2$.

matopoietic PGDS is a splenic enzyme and is expressed in antigen-presenting dendritic cells as well as in mast cells of various organs. Its product $PGD_2$ and one of its metabolites, cyclopentenone 15-deoxy-$\Delta^{12,14}$-$PGJ_2$ (15d-$PGJ_2$), have the capability to down-regulate inflammatory cytokine production via peroxisome proliferator-activated receptor $\gamma$ (5). In addition, prostacyclin ($PGI_2$) produced from $PGH_2$ by PGIS is a potent short-acting vasodilator and inhibitor of platelet aggregation produced by vascular endothelium (Fig. 1). Indeed, epoprostanol (prostacyclin) was used as oral vasodilator therapy (6) and continuous intravenous infusion (7), for the treatment of pulmonary hypertension. In addition, an animal model of prostacyclin gene therapy for human pulmonary hypertension has been done using $PGI_2$ synthase gene incorporated HVJ liposomes to monocrotaline (MCT)-induced pulmonary hypertensive rats (8).

Endothelin-1 (ET-1) is known to have potent effects on contraction and proliferation of vascular smooth muscle cells and is also known to induce myocardial cell hypertrophy. In addition, endogenous ET-1 contributes to the progression of cardiopulmonary alteration in rats with MCT-induced pulmonary hypertension (9). Two ET-1 receptors, $ET_A$ and $ET_B$ are considered to contribute to vasoconstriction and proliferation of vascular smooth muscle cells, and clearance of ET-1 in endotherial cells, respectively (10).

Based on those findings, we tried to cure the MCT-induced pulmonary hypertension of rats by cell therapy using $PGI_2$- or $PGD_2$- producing cells, in order to clarify the role of those prostaglandins, and ET-1 and its receptors in remodeling of pulmonary artery affected by pulmonary hypertension.

## Materials and Methods

*Rats, cells and cell lines.*

Male SD rats (age 6 weeks, b.w. 200 g) were purchased from CLEA and fed standard chow pellets and water *ad libitum*. Human pulmonary artery endotherial cells (HUVEC) were purchased from Cambrex Bio Science Walkersville, Inc and cultured with endotherial cell medium- 2 (EGM- 2) bullet kits (Cambrex Bio Science Walkersville, Inc) supplemented with 2% heat inactivated fetal calf serum (Hyclone) in a 5% $CO_2$ atmosphere at 37ºC. Human smooth muscle cells (HPAEC) derived from artery were purchased from Asahitechno Glass then cultured with normal human muscle cell system (Asahi-techno) supplemented with 2% heat inactivated fetal calf serum (Hyclone) in the same culture condition as that for HUVEC. C57BL/6J (C57) cells were purchased from Riken, and normal rat kidney (NRK) cells were gift from Dr. Hayashi (Kitasato University). C57 cells expressing human prostaglandin D synthase by retrovirus vector pLXSN (BD Biosciences Clontech), and C57 cells expressing pLXSN alone were designated as C57-PGDS and C57-EV, respectively (11). Similarly, NRK cells expressing rat prostaglandin I synthase by pLSXN and NRK cells expressing pLXSN alone were designated as NRK-PGIS and NRK-EV, respectively. Those cells were cultured in Dulbecoo's modified Eagle's medium (Sigma) supplemented with 10% heat-inactivated fetal calf serum (Hyclone) in a 5% $CO_2$ atmosphere at 37°C.

*The cell-therapy for monocrotaline-induced pulmonary hypertension (MCTPH) of rats using $PGD_2$- or $PGI_2$-producing cells.*

MCTPH rats were prepared according to the previous report (10); 60 mg monocrotaline (Wako) /kg b.w. was injected to the neck of the rats.

The cell-therapy was carried out as follows: 0.5 ml PBS (Takara) containing 2.5 x $10^5$ cells of C57-PGDS or C57-EV or C57-PGIS or the same volume of PBS not containing cells (control) were intravenously injected into the tail vein of the rats.

*Measurement of systemic and right ventricular blood pressure.*

Three weeks after the injection of the $PGD_2$- or $PGI_2$-producing cells, the MCTPH rats were anesthesized with Nembtal (50 mg/kg b.w., i.p., Abbot), and systemic arterial and right ventricular blood pressure were measured under tracheal intubation for respiration with volume-regulated respirator (tidal volume 1 ml/kg, rate 60 breaths/min).

**Table 1.** Oligonucleotide primers used for reverse transcriptase-polymerase chain reaction

| Target gene | Product length, bp | Primer (5'-3') | Description |
|---|---|---|---|
| Rat ET-1 | 148 | CCATGCTGGCTGGGATCTTA | 20-mer |
| | | TGCTACCAGCGGATGCAAA | 19-mer |
| Rat $ET_A$ | 99 | CGCCATTGAAATTGTCTCCAT | 20-mer |
| | | TGCTCGCCCTTGTATTCGA | 19-mer |
| Rat $ET_B$ | 180 | TGGCCATTTGGAGCTGAGAT | 20-mer |
| | | TCCAAGAAGCAACAGCTCGAT | 21-mer |
| GAPDH | 380 | TTGGATCCGTCAGTGCCGGCCTCGTCTCATAG | 32-mer |
| | | TTCTCGAGGACCCTTTGGCACCACCCTTCAG | 32-mer |
| Human ET-1 | 147 | CTTCTGCCACCTGGACATCAT | 20-mer |
| | | TTGGCTAGCACATTGGCATCT | 20-mer |
| Human $ET_A$ | 93 | CACAGAGCTCAGCTTCCTGGTTA | 23-mer |
| | | AGTCTGCTGTGGGCAATAGTTGT | 23-mer |
| Human $ET_B$ | 147 | CCAATATCTTGATCGCCAGCTT | 22-mer |
| | | ACGGAGGCTTTCTGTATGAAAGG | 23-mer |

Wet weight of the lung, heart and right ventricle was also measured after sacrifice of the rats.

*Real time polymerase chain reaction (PCR) and reverse transcriptase (RT)-PCR.*

Total RNA was extracted from the lungs and right ventricle using a Trizol reagent (Invitrogen Life Technologies), and from the cultured cells using an RNeasy Mini Kit (Qiagen). The first stranded cDNA was synthesized from 1 $\mu$g of the total RNA using AMV reverse transcriptase and $p(dN)_6$ random primer (Roche Diagnostic). Oligonucleotide primers used for RT-PCR were listed in Table 1. Primers used for PGDS RT-PCR and COX 2 real time PCR were previously reported (11).

Prosta-5,13-dien-l-oicacid, 6, 9-epoxy-11,15-dihydroxy-, monosodium salt ($PGI_2$) and cyclopentenone 15-deoxy-$\Delta^{12,14}$-$PGJ_2$ (15d-$PGJ_2$) were purchased from Cayman Chemical.

## Results

*Characterization of C57-PGDS and NRK-PGIS.*

The first stranded cDNA was synthesized from the RNA extracted from C57-PGDS and NRK-PGIS, and expression of retrovirally transfected DNA and their transcripts were confirmed by specific DNA PCR and RT-PCR, respectively (data not shown). $PGD_2$ production and its biological activity concerning suppression of COX-2 expression were evaluated on C57-PGDS and C57-EV by $PGD_2$ ELISA (Cayman Chemical) and COX-2 real time PCR analysis, respectively.

The results of $PGD_2$ ELISA (Fig. 2A) show clearly that C57-PGDS produce significantly large amounts of $PGD_2$ in the presence of arachidonic acid (AA).

The COX-2 real time PCR analysis showed that expression of COX-2 induced by TNF$\alpha$ is significantly inhibited in C57-PGDS (Fig. 2B). This suggests that 15-d-$PGJ_2$ produced from $PGD_2$ suppresses COX-2 expression (see Fig. 1).

As an experiment in a similar lines, 6 keto PGF1$\alpha$, stable metabolite of $PGI_2$, was measured on

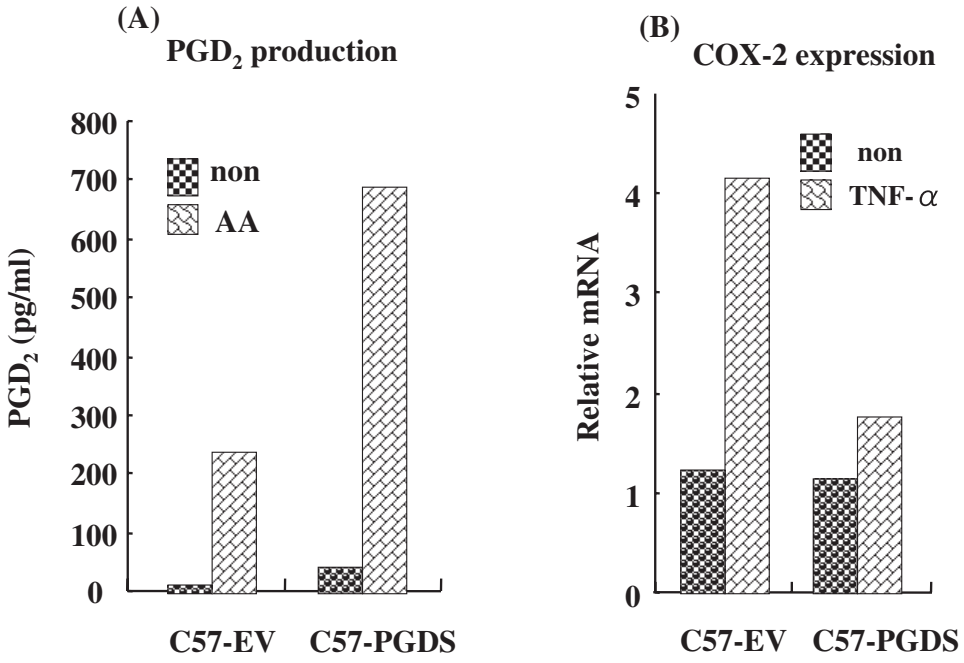


**Fig. 2.** Influence of introduced-PGDS gene on C57 cells. C57-PGDS and C57-EV were incubate with or without 10$\mu$M of arachidonic acid (AA) and measured $PGD_2$ by ELISA (A). C57-PGDS and C57-EV were incubated with or without 20 ng of TNF-$\alpha$ and cyclooxygenase (COX) 2 transcripts were evaluated by real time PCR. GAPDH transcript was used as internal control (B).

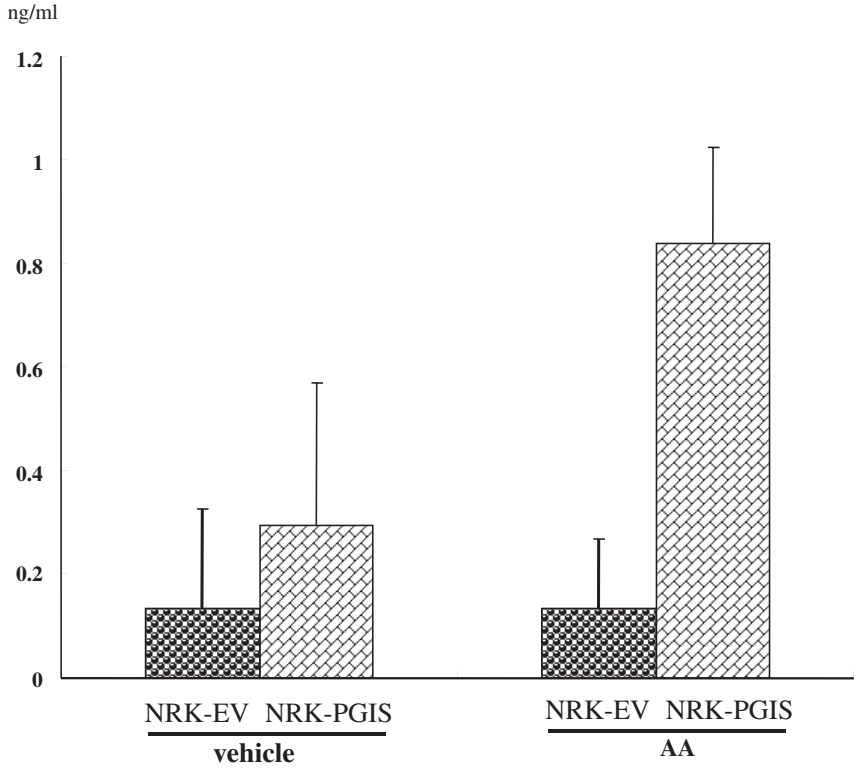


**Fig. 3.** $PGI_2$ production by NRK-PGIS. NRK-PGIS, NRK-EV were incubated with or without arachidonic acid (AA) and then 6-keto PGF1$\alpha$, stable metabolite of $PGI_2$, was measured by specific ELISA.

NRK-PGIS by ELISA. The results shown in Fig. 3 indicate that NRK-PGIS produce significant amounts of 6ketoPGF1$\alpha$ in the presence of arachidonic acid (AA).

Thus, all these results showed that retrovirally transfected PGDS and PGIS genes were successfully introduced into C57 cells and NRK cells, then transcribed and produced $PGD_2$ and $PGI_2$, respectively.

*Suppression of right ventricle blood pressure in MCTPH rats by C57-PGDS or NRK-PGIS cell therapy.*

Right ventricle blood pressure was measured on 4 groups of MCTPH rats inoculated with C57-EV, C57-PGDS, NRK-EV or NRK-PGIS, 21 days after the cell inoculation. As shown in Fig. 4, the results clearly indicated that C57-PGDS and NRK-PGIS cell therapy successfully improved the right ventricle blood pressure in comparison with controls inoculated with C57-EV or NRK-EV.

*Suppression of increase in wet weight of right ventricle by C57-PGDS and NRK-PGIS cell therapy.*

The rats in the preceding section were sacrificed after measurement of the right ventricle blood pressure, and then wet weight of their lungs (data not shown), heart (data not shown) and right ventricle was measured. No significant change in the wet weight of the lungs and heart was observed in the rats treated with MCT, but these rats showed significant increase in the wet weight of the right ventricle. This increase in the weight of the right ventricle caused by MCT was obviously suppressed by NRK-PGIS cell therapy and C57-PGDS cell therapy (Fig. 5).

*Expression of retrovirally transfected genes in the lungs of MCT-treated and C57-PGDS inoculated rats.*

RNA was extracted from the lungs of the rats in

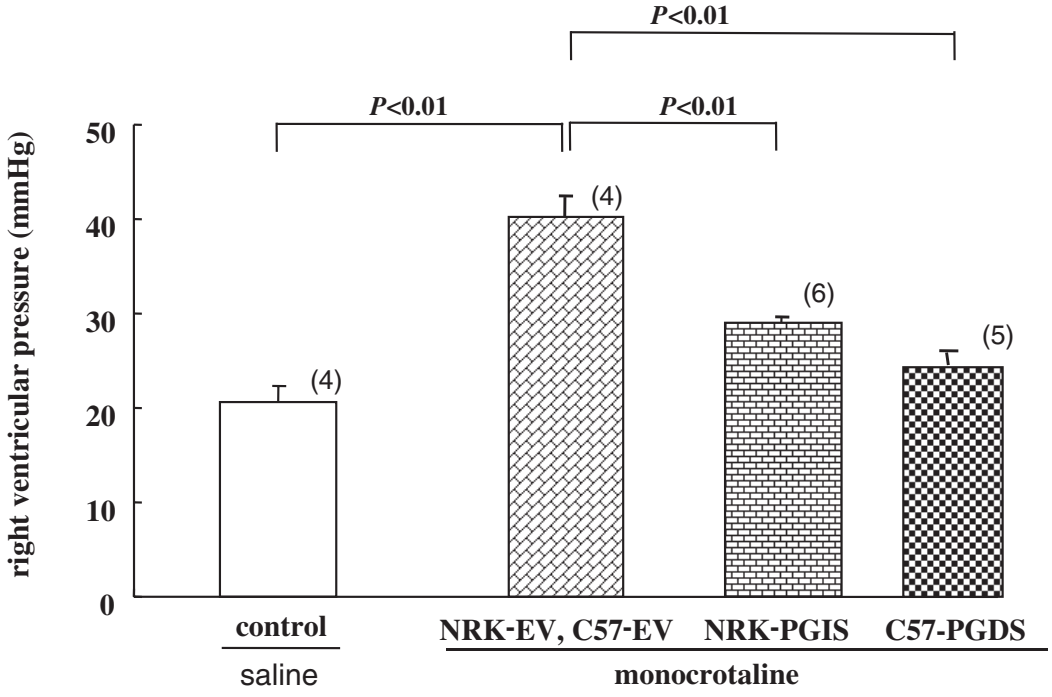


**Fig. 4.** Suppression of right ventricle blood pressure by C57-PGDS and NRK-PGIS cell therapy for MCTPH in rats. Monocrotaline (60 mg pro kg b.w.) was injected to the neck of rats. Then, 2.5 x $10^5$ cells of C57-EV or C57-PGDS or NRK-EV or NRK-PGIS were intravenously inoculated to the rats. 21 days after the cell inoculation, right ventricle blood pressure was measured under tracheal intubation for respiration with volume-regulated respirator.

the preceding section after measurement of the wet weight of the organs and used for PGDS-specific RT-PCR. The results (Fig. 6) showed clearly that retrovirally transfected PGDS genes were transcribed until day 19 of the cell inoculation. Similarly presence of PGIS gene transcripts in the lungs of the rats were also observed until day 19 of C57-PGIS inoculation (data not shown).

*Expression of ET-1, $ET_A$ and $ET_B$ in the right ventricle and the lungs of MCT-treated and C57-PGDS or NRK-PGIS inoculated rats.*

RNA was extracted from the right ventricle and lungs of MCT-treated and C57-PGDS or NRK-PGIS inoculated rats and subjected to the RT-PCR for rat ET-1, $ET_A$ and $ET_B$ transcripts. The results showed that $ET_B$ transcript increased in the right ventricle but not in the lungs, after C57-PGDS (Fig. 7A) or NRK-PGIS (Fig. 7B) cell therapy.

*Effect of 15d-$PGJ_2$ and $PGI_2$ on expression of ET-1, $ET_A$ and $ET_B$ on human pulmonary artery endotherial cells (HUVEC) and smooth muscle cells (HPAEC).*

We tried to retrovirally transfect PGDS or PGIS genes into HUVEC cells and HPAEC cells, but selection of the transfected cells was not successful. Therefore, we used $PGI_2$ and 15d-$PGJ_2$ to evaluate the effect on transcripts of ET-1, $ET_A$ and $ET_B$ by real time PCR assay. Approximately 1 x $10^5$ cells of HUVEC and HEPAEC were incubated with 1 x $10^{-6}$ M $PGI_2$, 1 x $10^{-7}$ M

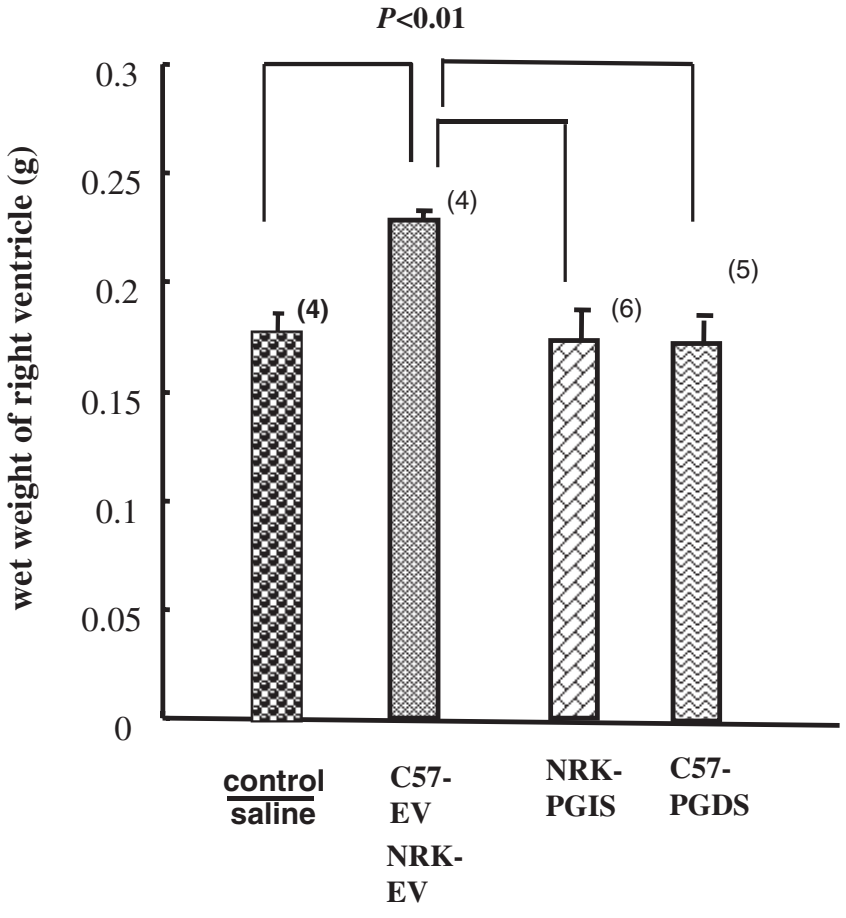


**Fig. 5.** Suppression of wet weight of right ventricle by C57-PGDS and NRK-PGIS cell therapy in MCTPH rats. Wet weight of right ventricle of MCTPH rats inoculated with C57-EV, C57-PGDS, NRK-EV or NRK-PGIS were measured after 21 days of cell inoculation.

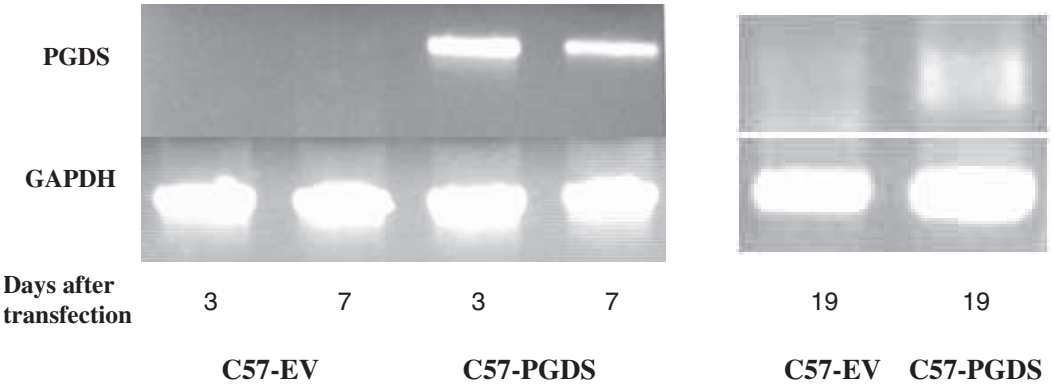


**Fig. 6.** Expression of PGDS mRNA in the lungs of MCT-treated rats after C57-PGDS cell therapy. RNA was extracted from the lungs of MCT-treated and C57-EV or C57-PGDS inoculated rats at 3, 7 and 19 days after the cell inoculation, and subjected to PGDS specific RT-PCR.

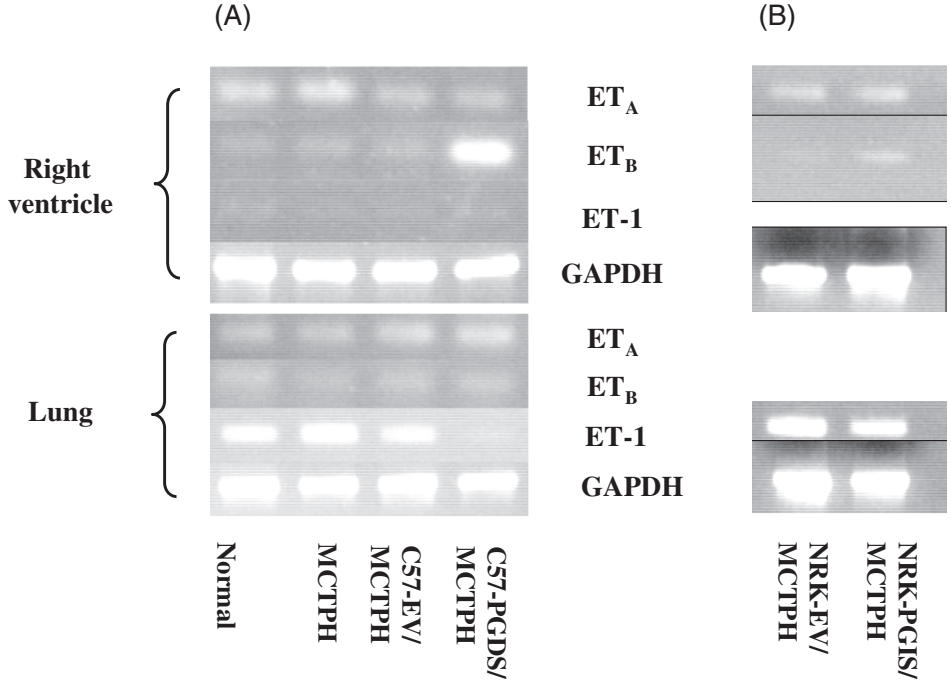


**Fig. 7.** Expression of ET-1, $ET_A$ and $ET_B$ in the right ventricle and lung of MCT-treated and C57-EV, C57-PGDS (A), NRK-EV, or NRK-PGIS (B) inoculated rats. RNA was extracted from the lungs and right ventricle of MCT-treated and C57-EV, C57-PGDS, NRK-EV or NRK-PGIS inoculated rats, and then was subjected to RT-PCR for ET-1, $ET_A$ and $ET_B$.

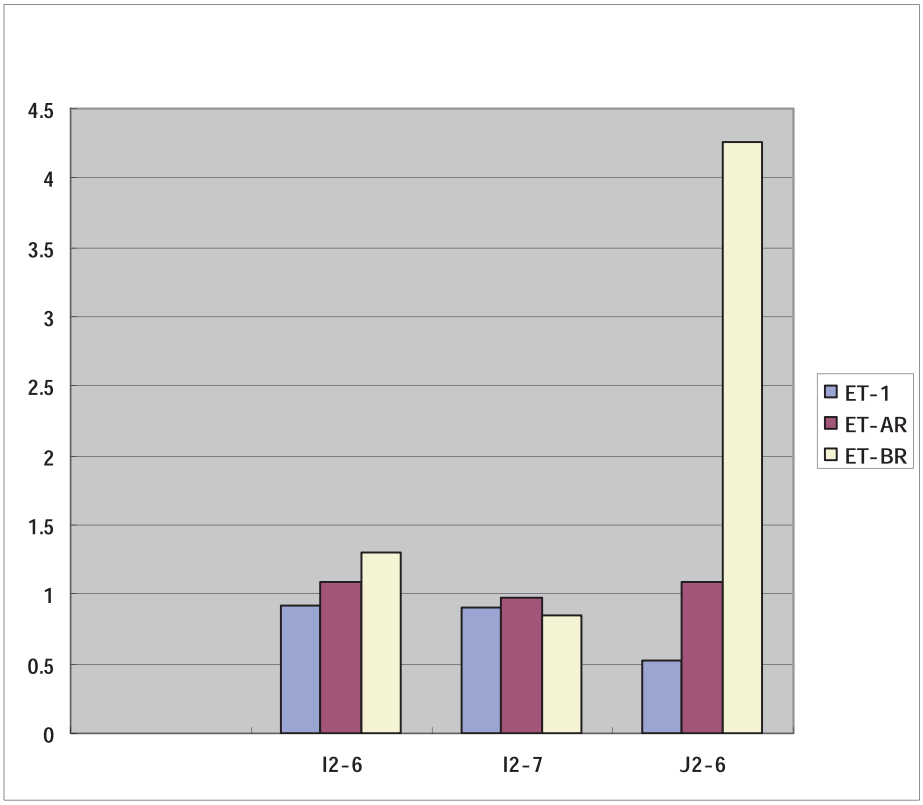


**Fig. 8.** Effect of 15d-$PGJ_2$ and $PGI_2$ on expression of ET-1, $ET_A$ and $ET_B$ on human smooth muscle cells (HEPAC). $PGI_2$ at concentration of $10^{-6}$M (I2−6), $10^{-7}$ M (I2−7), and 15d-$PGJ_2$ at concentration of $10^{-6}$M (J2−6) were added to approximately 1 x $10^5$ cells of HEPAC. RNA was extracted after 24 hours, and subjected to real time PCR for ET-1, $ET_A$ (ET-AR) and $ET_B$ (ET-BR). Control: 1.

$PGI_2$ or 1 x $10^{-6}$M 15d-$PGJ_2$ for 24 hours, and then were used for RNA extraction. The extracted RNA was subjected to the real time PCR analysis for transcripts of ET-1, $ET_A$, and $ET_B$. As shown in Fig. 8, 15d-$PGJ_2$ but not $PGI_2$ dramatically increased transcript of $ET_B$ on the smooth muscle cells, HPAEC. By contrast both $PGI_2$ and 15d-$PGJ_2$ did not affect the amounts of transcripts of ET-1, $ET_A$ and $ET_B$ on the endotherial cells, HUVEC (Fig. 9).

## Discussion

MCT-induced pulmonary hypertension was dramatically improved by C57-PGDS and NRK-PGIS cell therapy. Retrovirally transfected PGDS and PGIS genes were effectively transcribed and produced high concentration of their products (700-800 pg/ml). Inoculation of C57-PGDS or NRK-PGIS resulted in improvement of MCT-induced pulmonary hypertension of rats in terms of suppression of right ventricle blood pressure and weight of the ventricle, suggesting effectiveness of $PGD_2$ or $PGI_2$ produced by the inoculated cells.

*In vivo* experiments suggested that one of the mechanism of the cell therapy with those prostaglandin synthase genes, was up-regulation of $ET_B$ receptor which contributes to the clearance of ET-1 in the ventricle. This result seems to suggest that proliferation of smooth muscle cells by MCT is suppressed because of clearance of ET-1 via $ET_B$. Actually, proliferation of smooth muscle cells of pulmonary artery in MCT-treated rats was totally suppressed by C57-PGDS cell therapy when evaluated by histological findings (data not shown). *In vitro* experiments suggested that tran-

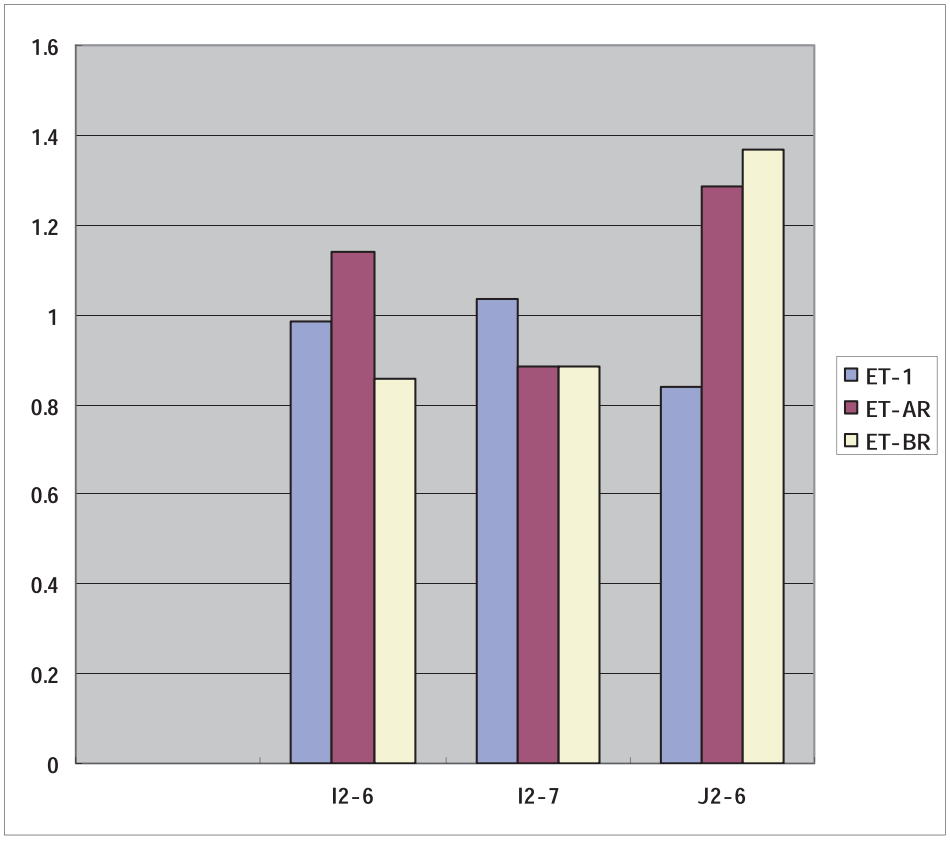


**Fig. 9.** Effect of 15d-$PGJ_2$ and $PGI_2$ on expression of ET-1, $ET_A$ and $ET_B$ on human pulmonary artery endotherial cells (HUVEC). $PGI_2$ at concentration of $10^{-6}$M (I2−6), $10^{-7}$ M (I2−7), and 15d-$PGJ_2$ at concentration of $10^{-6}$M (J2−6) were added to approximately 1 x $10^5$ cells of HUVEC. RNA was extracted after 24 hours, and subjected to real time PCR for ET-1, $ET_A$ (ET-AR) and $ET_B$ (ET-BR). Control: 1.

scripts of $ET_B$ in human smooth muscle cells (HPAEC) were up-regulated by 15d-$PGJ_2$ but not by $PGI_2$.

These results suggest the following important aspects; therapeutic effect of PGDS cell therapy and PGIS cell therapy on pulmonary hypertension should be achieved through different path-ways, and $ET_B$ on smooth muscle cells in the artery may be one of the important path-ways in the PGDS cell therapy. It is worth to note that $ET_A$ are mainly expressed on smooth muscle cells and $ET_B$ are on endotherial cells (10). Our present study revealed that $ET_B$ expressed on smooth muscle cells as minor ET-1 receptor played important role in the C57-PGDS cell therapy. Detail of the mechanism of the therapeutic effect of the PGDS through $ET_B$, together with the path-way in the therapeutic effect of PGIS cell therapy should be clarified in the future.

## Conclusion

Cell therapy using retrovirally transfected PGDS and PGIS genes successfully improved MCT-induced pulmonary hypertension in rats, and it was revealed that $ET_B$ on the smooth muscle cells should play important role in the C57-PGDS cell therapy.

## Acknowledgments

I would like to thank Mrs.Terumi Mizuno for excellent technical support. This study was supported by research grants from Waksman Foundation of Japan, The Ministry of Health, Labor, and Welfare of Japan

and Project Research from Kitasato University Graduate School of Medical Sciences. This study was done in collaboration with Izumi Hayashi (Prof., Nihon Pharmaceutical University), Hirahito Endo (Assoc. Prof., Kitasato University School of Medicine), Shinichi Kawai (Prof., Toho University School of Medicine), Hirobumi Kondo (Prof., Kitasato Institute Medical Center) and Masataka Majima (Prof., Kitasato University School of Medicine).

## References

(1) Sharp GC, Irvin WS, Tan EM, Gould RG, Holman RH. Mixed connective tissue disease; an apparently distinct rheumatic disease syndrome associated with a specific antibody to an extractable nuclear antigen. Am J Med 1972; **52**: 148−159.

(2) Graziano FM, Friedman LCV, Grossman J. Pulmonary hypertension in a patient with mixed connective tissue disease. Clin Exp Rheumatol 1983; **1**: 251−255.

(3) Sullivan WD, Hurst DJ, Harmaon CE, Esther JH, Agia GA, Maltby JD, Lillard SB, Held CN, Wolfe JF, Sunderrajan EV, Maricq HR, Sharp GC. A prospective evaluation emphasizing pulmonary involvement in patients with mixed connective tissue disease. Medicine 1984; **63**: 92−107.

(4) Urade Y, Hayashi O. Biochemical, structural, genetic, physiological, and pathophysiological features of lipocalin-type prostaglandin D synthase. Biochim Biophys Acta 2000; **1482**: 259−271.

(5) Kawahito Y, Knodo M, Tsubouchi Y, Hashiramoto A, Bishop-Bailey D, Inoue K, et al. 15-deoxy-$\Delta^{12,14}$-$PGJ_2$ induces synoviocyte apoptosis and suppresses adjuvant-induced arthritis in rats. J Clin Invest 2000; **106**: 189−197.

(6) Burst RJ, Rubin LJ, Long WA, McGoon MD, Rich S, Badesch DB, Groves BM, Tapson VF, Bourge RC, Brundage BH, Koerner SK, Langleben D, Keller CA, Murali S, Uretsky BF, Clayton LM, Jöbsis MM, Blackburn SD, Shortino D, Crow JW. A comparison of continuous intravenous epoprostenol (prostacyclin) with conventional therapy for primary pulmonary hypertension. N Engl J Med 1996; **334**: 296−301.

(7) Rubin LJ, Groves BM, Reeves JT, Frosolono M, Handel F, Cato AE. Prostacyclin-induced acute pulmonary vasodilatation in primary pulmonary hypertension. Circulation 1982; **66**: 334−338.

(8) Suhara H, Sawa Y, Fukushima N, Kagisaki K, Yokoyama C, Tanabe T, Ohtake S, Matsuda H. Gene transfer of human prostacyclin synthase into the liver is effective for the treatment of hypertension rats. J Thoracic Cardiovas Surg 2002; **123**: 855−861.

(9) Nishida M, Eshiro K, Okada Y, Takaoka M, Matsumura Y. Roles of endothelin ETA and ETB receptors in the pathogenesis of monocrotaline-induced pulmonary hypertension. J Cardiovasc Pharmacol 2004; **44**: 187−191.

(10) Miyauchi T, Yorikane R, Sakai S, Sakurai T, Okada M, Nishikibe M, Yano M, Yamaguchi I, Sugishita Y, Goto K. Contribution of endogenous endotherin-1 to the progression of cardiopulmonary alterations in rats with monocrotaline-induced pulmonary hypertension. Circulation Res 1993; **73**: 887−897.

(11) Murakami Y, Akahoshi T, Hayashi I, Endo H, Hashimoto A, Kono S, Kondo H, Kawai S, Inoue M, Kitasato, H. Inhibition of monosodium urate monohydrate crystal-induced acute inflammation by retrovirally transfected prostaglandin D synthase. Arthritis Rheum 2004; **48**: 2931−2941.

# Immunotherapy Targeting VEGFR-2 for Prevention from Pathological Retinal Angiogenesis

**Susumu Ishida**

*Laboratory of Retinal Cell Biology, Department of Ophthalmology, Keio University School of Medicine, Tokyo 160-8582, Japan*

## Introduction

Angiogenesis is a common progressed pathology in vision-threatening retinal diseases including diabetic retinopathy and age-related macular degeneration (AMD). These retinal diseases are the major causes of severe vision loss and blindness in the elderly in the developed countries. Therefore, a new therapy for suppressing ocular neovascularization needs to be urgently established in terms of both clinical ophthalmology and vascular biology.

Visual impairment in diabetic retinopathy results from ischemia-induced pathological retinal neovascularization, whereby new retinal vessels invade the vitreous cavity without physiological revascularization for the ischemic retina. Diabetic retinopathy characterized by pathological neovascularization is called 'proliferative diabetic retinopathy', which develops vitreous hemorrhage and traction retinal detachment.

In AMD, neovascularization develops beneath the macula (the central retina), or new vessels from the choroid invade the subretinal space. The process is termed 'choroidal neovascularization (CNV)', which complicates wet form of (exudative or neovascular) AMD with subretinal hemorrhage and exudative retinal detachment.

Previous analyses on human surgical samples and animal disease models have revealed that neovascularization seen in these retinal diseases depends on vascular endothelial growth factor (VEGF). VEGF has five isoforms generated from the single gene via alternative splicing. They are named VEGF121, VEGF145, VEGF165, VEGF189, and VEGF206, based on the number of amino acids comprised in each isoform (i.e., VEGF121 is a 121-amino-acid form of VEGF). Of these, two major isoforms constitutively expressed in the retina are VEGF121 and VEGF165. VEGF receptors expressed on vascular endothelial cells are known as VEGFR-1, VEGFR-2 and neuropilin-1. VEGFR-2, but not VEGFR-1, mediates intracellular signal transduction for endothelial cell mitogenicity and vascular permeability. Neuropilin-1 was shown to be a specific receptor for VEGF165, enhancing VEGF165 bioactivity through VEGFR-2. Indeed, our previous data revealed that coexpression of VEGFR-2 and neuropilin-1 increased the vascular density of fibrovascular proliferative tissues in diabetic retinopathy (1). Recently, pegaptanib, generated as a VEGF165-specific antagonist, proved to be useful for the treatment of neovascular AMD (2) and prolifertive diabetic retinopathy (3). The results of these clinical trials confirmed the important role of VEGF165-VEGFR-2/neuropilin-1 ligand-receptor system in these retinal diseases complicated by angiogenesis.

Our recent studies using the rodent models of diabetic retinopathy and proliferative retinopathy suggested that three major retinal pathologies (edema, ischemia and angiogenesis) are associated with inflammation and immunity, and that monocyte-lineage inflammatory cells and cytotoxic T lymphocytes (CTLs) function as positive and negative regulators for angiogenesis, respectively (4-7). Activated endothelial cells in the angiogenic state upregulate the expression of VEGFR-2. Based on the hypothesis that VEGFR-2-targeting CTLs suppress neovascularization (8,9), we

aim to establish immunotherapy targeting VEGFR-2 for prevention from pathological angiogenesis in the eye.

## Materials and Methods

*Induction of CNV.*

Laser-induced CNV is widely used as an animal model for neovascular AMD and regarded to reflect the pathogenesis of inflammation-related CNV seen in AMD. In this animal model, new vessels from the choroid invade the subretinal space through Bruch's membrane after photocoagulation. Laser photocoagulation was performed with the wavelength of 532 nm, the power of 200 mW, the duration of 100 ms and the spot size of 75 $\mu$m by a single individual. Laser spots were applied in a standardized fashion around the optic nerve, using a slit lamp delivery system (NOVUS spectra™; Japan Lumenis, Tokyo, Japan). The morphologic end point of the laser injury was the appearance of a cavitation bubble, a sign thought to correlate with the disruption of Bruch's membrane. Laser-induced CNV was formed between the retina and the choroid as fibrovascular proliferative tissue as is seen in human neovascular AMD, and the highly vascularized pathological structure was visualized by immunohitisochemistry for CD31/PECAM-1 (a marker for endothelial cells) (Fig. 1).

*Quantification of laser-induced CNV.*

One week after laser injury, eyes were enucleated and fixed with 4% paraformaldehyde (PFA) for 30 minutes. Eye cups obtained by removing anterior segments were pretreated with buffer [PBS containing 1% bovine serum albumin (BSA; Sigma) and 0.5% Triton X-100 (Sigma)] for 30 minutes at room temperature, and then incubated overnight at 4ºC with 0.5% FITC-isolectin B4 (Vector Laboratories, Burlingame, CA). After two washes with PBS containing 0.1% Triton X-100, the neurosensory retina was detached and the choroid-sclera complex was flatmounted.

Flatmounts were evaluated with a scanning laser confocal microscope (FV1000; Olympus, Tokyo, Japan) and choroidal neovascularization was visualized with blue argon laser (wavelength 488 nm). Horizontal optical sections (1 $\mu$m step) of choroidal neovascularization were obtained from the surface to the deepest focal plane in which the surrounding choroidal vascular network connecting to the lesion could be identified. The area of choroidal neovascularization-related fluorescence was measured by NIH image. The summation of whole fluorescent area was used as the volume of choroidal neovascularization.

*RT-PCR for VEGFR-2.*

Three days after laser photocoagulation, total RNA was isolated from the choroid of CNV and nor-

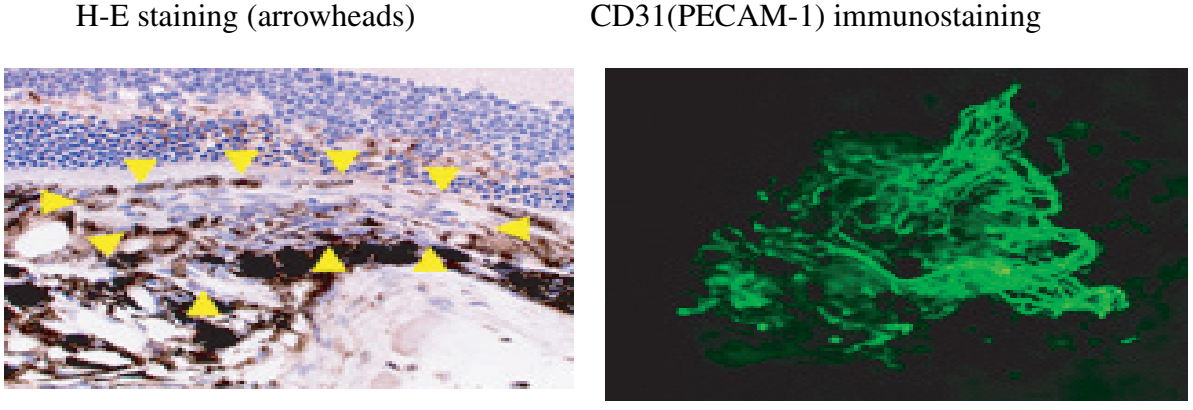


**Fig. 1.** Histopathological and immunohistochemical stainings of the laser-induced CNV in murine model.

mal mice using an extraction reagent (TRIzol; Invitrogen, Carlsbad, CA) and reverse-transcribed with a cDNA synthesis kit (First-Strand; Amersham Biosciences, Piscataway, NJ) according to the manufacturer's protocols. PCR was performed using *Taq* DNA polymerase (Toyobo, Tokyo, Japan) in a thermal controller (Gene Amp™ PCR system; Applied Biosystems, Foster, CA). Human/mouse VEGF R2 PCR Primer Pair™ (R&D Systems, Minneapolis, MN, USA) (569 bp) was utilized for RT-PCR of VEGFR-2. The primer sequences and the expected size of amplified cDNA fragments for $\beta$-actin are 5'-ATG TGG CAC CAC ACC TTC TAC AAT GAG CTG CG-3' (sense), 5'-CGT CAT ACT CCT GCT TGC TGA TCC ACA TCT GC-3' (antisense), and 837 bp.

*Analyses for CD4 and CD8 positive cells in CNV tissues.*

Six days after laser photocoagulation, CNV tissues were extracted from the choroid and analyzed lymphocyte subsets therein by using fluorescence-labeled anti-CD3, -CD4 or -CD8 monoclonal antibody, and fluorescence activated cell sorter (FACS). Immunohistochemisty for CD4 and CD8 were performed on frozen sections of CNV tissues separated at six and eight days after laser photocoagulation.

*Induction of cellular immunity by using Helios™ Gene Gun.*

Full-length VEGFR-2 cDNA was cloned and inserted to the expression vector pcDNA3.1. The cDNA inserted plasmid was coated with gold particles and administered intradermally to mice by the particle delivery technique (Helios™ Gene Gun, Bio-Rad) for gene transfection. The aim of this technique was to induce CTL-mediated cellular immunity since VEGFR-2 was expressed in and presented to T cells by the professional antigen-presenting cells, Langerhans cells. This VEGFR-2 immunization was performed twice at a two-week interval and CNV was induced with laser photocoagulation at the same time with the second immunization. One week after the CNV induction, eyes were enucleated and the inhibitory effect of the immunization on CNV volume was evaluated.

*Induction of peptide-specific cellular immunity.*

To show that the CNV inhibition was mediated via antigen-specific reaction to VEGFR-2, cellular immunity was induced in HLA-A24 transgenic mice using epitope candidates for human VEGFR-2 peptide described previously (10)(Fig. 2). Peptides with epitope of which amino-acid sequence was consistent with murine homologue (i.e., peptides 3 and 4 in Fig. 2) were selected. Two weeks and three days prior to laser photocoagulation, 100 $\mu$g of VEGFR-2 peptide 3 or 4 was intradermally administered with 100 $\mu$l of IFA (incomplete Freund's adjuvant) and 100 $\mu$g of tetanus toxoid as adjuvants. One week after CNV induction, CNV volume was measured.

*Elispot assay.*

To examine whether antigen-specific immunity against these VEGFR-2 peptides was induced, Elispot assay for IFN-$\gamma$ was performed. Three weeks after immunization with the peptide 3 or 4 in Fig. 2, spleen cells were harvested from the immunized A24 transgenic mice, and cultured with the VEGFR-2 peptide used for immunization (10, 1 or 0.1 $\mu$g/ml) as the specific stimulant or control peptide (myelov) and Jarkat cells as the antigen-presenting cells. Twenty-four hours after the stimulation, the number of IFN-$\gamma$-positive CTLs was evaluated by ELISA for IFN-$\gamma$.

| | human | | murine homologue |
|---|---|---|---|
| ① | VYSSEEAEL | — | VYSS**D**EA**G**L |
| ② | GYRIYDVVL | — | GYRIYDV**I**L |
| ③ | SYMISYAGM | — | SYMISYAGM |
| ④ | KWEFPRDRL | — | KWEFPRDRL |

**Fig. 2.** Amino acid sequences of the candidates for the homologous epitopes between human and murine VEGFR-2.

## Results

*VEGFR-2 expression following CNV induction.*

RT-PCR for VEGFR-2 showed marked upregulation of VEGFR-2 mRNA expression in the choroid extrated from mice with CNV at day 3 after laser photocoagulation, compared with that from mormal mice (Fig. 3).

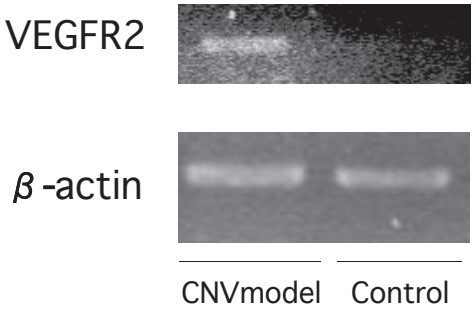


**Fig. 3.** Markedly upregulated VEGFR-2 mRNA expression in murine CNV tissue.

*Time course of changes in CNV volume after laser photocoagulation.*

As compared to CNV volume at week 1 after laser photocoagulation, CNV volumes at weeks 2 and 3 significantly decreased. Although no statistically significant difference was detected between the volumes at weeks 2 and 3, a tendency of spontaneously regressive change in CNV volume was noted in the time course after week 1 (Fig. 4).

*Infiltration of CD4 and CD8 positive cells in CNV tissues.*

FACS analyses revealed that the ratios of CD4 to CD3 and CD8 to CD3 positive cells in CNV tissues at day 6 after laser photocoagulation are 18.5% and 11.0%, respectively (Fig. 5). Immunohistochemistry demonstrated the infiltration of CD4 positive cells and CD8 positive cells in the CNV tissues at day 6 and a substantial increase in the number of these infiltrating $CD4^+$ cells and $CD8^+$ cells in the CNV tissues at day 8 (Fig. 6).

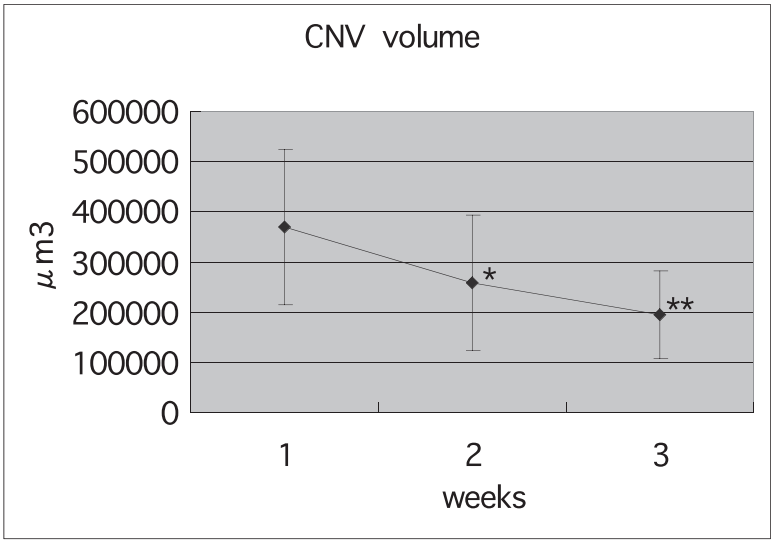


*(P<0.05)

**(P<0.05)

**Fig. 4.** Time course of changes in CNV volume after laser photocoagulation.

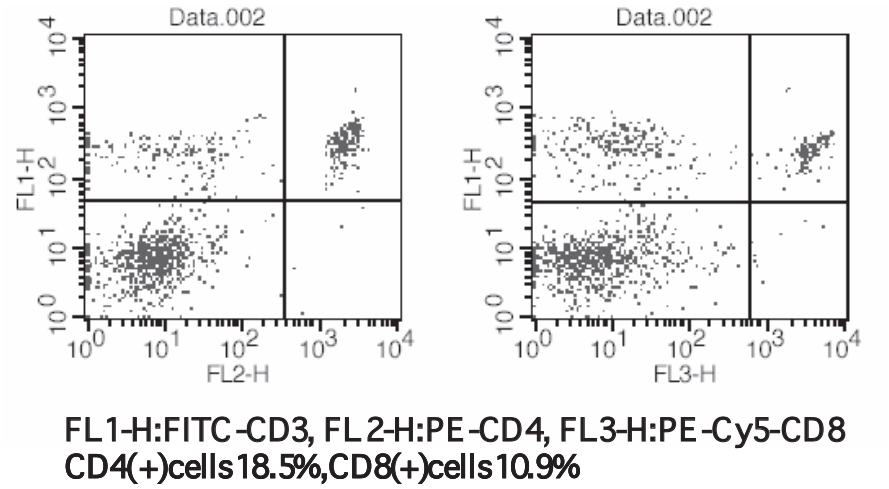


**Fig. 5.** FACS analyses of infiltration of CD4 T cells and CD8 T cells in the CNV tissues induced by laser photocoagulation.

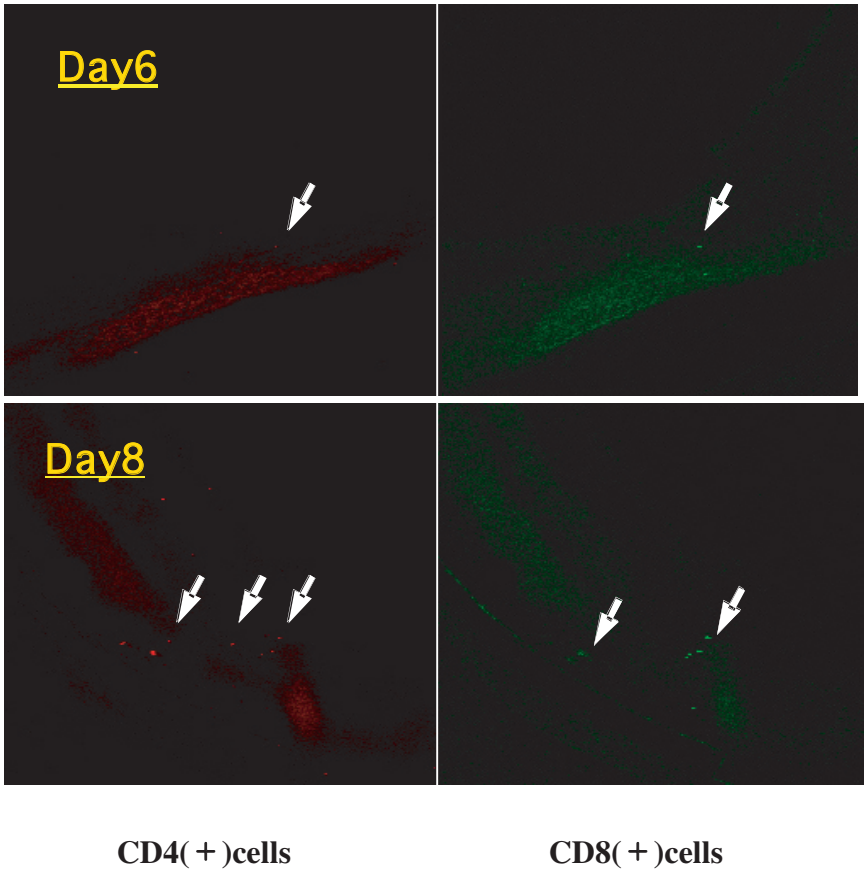


**Fig. 6.** Increase in the number of infiltrating CD4-positive cells and CD8-positive cells in the CNV tissue during the course after the laser photocoagulation.

*Generation of CNV after inoculation of full-length VEGFR-2 cDNA via Gene Gun.*

Mice were inoculated intradermally with VEGFR-2 full-length cDNA inserted plasmid or not inserted plasmid (control) via Gene Gun. Volume of the CNV generating after laser photocoagulation tended to become smaller in the VEGFR-2-cDNA inoculated group than the control group (Fig. 7).

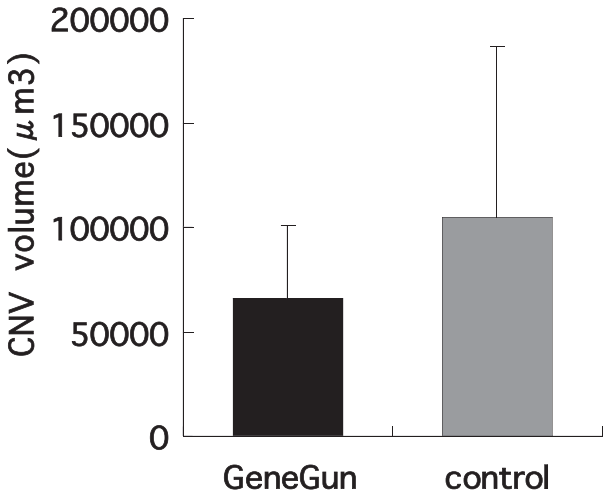


**Fig. 7.** Effect of VEGFR-2 gene inoculation via the "Gene Gun" on generation of the CNV after the laser photocoagulation.

*Examination of antigen-specific cellular immunity after VEGFR-2 peptide inoculation.*

To confirm that the peptide-specific cellular immunity was induced by inoculation of VEGFR-2 peptides, spleen cells of the peptide 3 or 4 (in Fig. 2) inoculated A24-transgenic mice were cultured with the inoculated peptide or non-rlated peptide (control), and IFN-$\gamma$ production in the culture was evaluated by Elispot Assay. As compared with the control peptide-applied group, the number of IFN-$\gamma$-producing cells increased mildly but significantly in the VEGFR-2 peptide-inoculated groups (both peptides 3 and 4) in the dose-dependent manner (Fig. 8).

Thus, it was confirmed that peptide-specific cellular immunity was induced by inoculation of VEGFR-2 peptides.

*Generation of CNV in A4 mice immunized with VEGFR-2 peptide.*

Volume of the CNV induced by laser photocoagulation was compared between the mice immunized with VEGFR-2 peptide 3 or 4 in Fig. 2 and the animals received the control peptide (myelov). There was no statistically significant difference in CNV volume between theVEGFR-2-immunized mice and the control group (Fig 9).

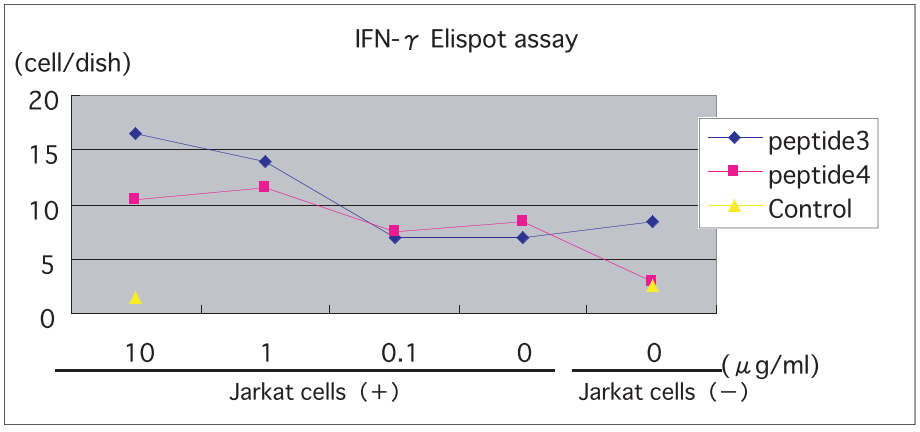


**Fig. 8.** Antigen-specific cellular immunity after VEGFR-2 peptide inoculation examined by Elispot assay for IFN$\gamma$.

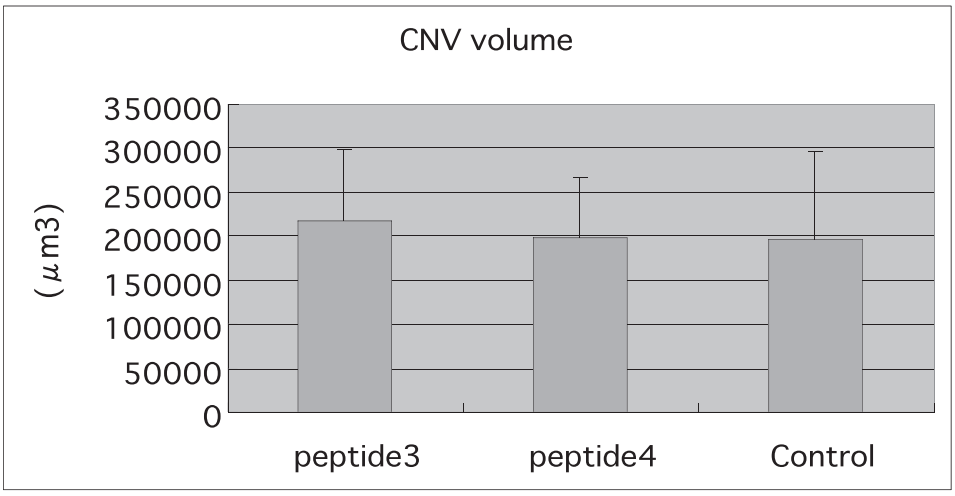


**Fig. 9.** Volume of the CNV after laser photocoagulation in the mice immunized with VEGFR-2 peptide.

## Discussion

The present study shows that, unlike VEGFR-2 full-length cDNA inoculated via Gene Gun which induced cellular immunity to prevent CNV generation, VEGFR-2 peptide 3 or 4 failed to induce cellular immunity potent enough to suppress the CNV generation. Considering future plans for clinical application, it is necessary to first establish peptide immunization in the animal model, since peptide immunization is simple and far from ethical problems as compared to other methods. In these experiments so far, there has been much room for improvement including the inoculation with other epitopes, the combined application of other adjuvants and the additive injection of IL-2 and -12 for enhancement of induced immunity. Future and further investigation is required for the more effective induction of cellular immunity against VEGFR-2, a key target molecule in retinal neovascular diseases.

## References

(1) Ishida S, Shinoda K, Kawashima S, Oguchi Y, Okada Y, Ikeda E. Coexpression of VEGF receptors VEGF-R2 and neuropilin-1 in proliferative diabetic retinopathy. ***Invest Ophthalmol Vis Sci***. 2000; **41**: 1649−1656.

(2) Gragoudas ES, Adamis AP, Cunningham ET Jr, Feinsod M, Guyer DR; VEGF Inhibition Study in Ocular Neovascularization Clinical Trial Group. Pegaptanib for neovascular age-related macular degeneration. ***N Engl J Med***. 2004; **351**: 2805−2816.

(3) Adamis AP, Altaweel M, Bressler NM, Cunningham ET Jr, Davis MD, Goldbaum M, Gonzales C, Guyer DR, Barrett K, Patel M; Macugen Diabetic Retinopathy Study Group. Changes in retinal neovascularization after pegaptanib (Macugen) therapy in diabetic individuals. ***Ophthalmology***. 2006; **113**: 23−28.

(4) Usui T, Ishida S, Yamashiro K, Kaji Y, Poulaki V, Moore JE, Moore TC, Amano S, Horikawa Y, Dartt D, Golding M, Shima DT, Adamis AP. VEGF164(165) as the pathological isoform: Differential leukocyte and endothelial responses through VEGFR-1 and VEGFR-2. ***Invest Ophthalmol Vis Sci***. 2004; **45**: 368−374.

(5) Ishida S, Usui T, Yamashiro K, Kaji Y, Amano S, Ogura Y, Hida T, Oguchi Y, Ambati J, Miller JW, Gragoudas ES, Ng YS, D'Amore PA, Shima DT, Adamis AP. VEGF164-mediated inflammation is required for pathological, but not physiological, ischemia-induced retinal neovascularization. ***J Exp Med***. 2003; **198**: 483−489.

(6) Ishida S, Yamashiro K, Usui T, Kaji Y, Ogura Y, Hida T, Honda Y, Oguchi Y, Adamis AP. Leukocytes mediate retinal vascular remodeling during

development and vaso-obliteration in disease. ***Nat Med***. 2003; **9**: 781−788.

(7) Ishida S, Usui T, Yamashiro K, Kaji Y, Ahmed E, Carrasquillo KG, Amano S, Hida T, Oguchi Y, Adamis AP. VEGF164 is proinflammatory in the diabetic retina. ***Invest Ophthalmol Vis Sci***. 2003; **44**: 2155−2162.

(8) Niethammer AG, Xiang R, Becker JC, Wodrich H, Pertl U, Karsten G, Eliceiri BP, Reisfeld RA. A DNA vaccine against VEGF receptor 2 prevents effective angiogenesis and inhibits tumor growth. ***Nat Med***. 2002; **8**: 1369−1375.

(9) Li Y, Wang MN, Li H, King KD, Bassi R, Sun H, Santiago A, Hooper AT, Bohlen P, Hicklin DJ. Active immunization against the vascular endothelial growth factor receptor flk1 inhibits tumor angiogenesis and metastasis. ***J Exp Med***. 2002; **195**: 1575−1584.

(10) Wada S, Tsunoda T, Baba T, Primus FJ, Kuwano H, Shibuya M, Tahara H. Rationale for antiangiogenic cancer therapy with vaccination using epitope peptides derived from human vascular endothelial growth factor receptor 2. ***Cancer Res***. 2005; **65**: 4939−4946.